Benemérita Universidad Autónoma de Puebla

Facultad de Ciencias Físico Matemáticas

"Self-consistent generalized Langevin equation theory for liquids of non-spherical brownian particles."

Thesis submitted to the

Postgraduate in Sciences (Applied Physics)

In Partial Fulfillment of the Requirements for the Degree of

DOCTOR IN SCIENCES (APPLIED PHYSICS)

Author:

Luis Fernando Elizondo Aguilera

Under the Supervision of

Dr. Olegario Alarcón Waess
Dra. Honorina Ruiz Estrada

Puebla Pue.

January 2015

Title: *"Self-consistent generalized Langevin equation theory for liquids of non-spherical brownian particles."*
Student:LUIS FERNANDO ELIZONDO AGUILERA

COMMITTEE

Dr. Gilberto Silva Ortigoza
FCFM-BUAP
President

Dr. Magdaleno Medina Noyola
IFUASLP
External Vocal

Dra. Minerva González Melchor
IFUAP
Secretary

Dr. Jose Luis Carrillo Estrada
IFUAP
External Vocal

Dr. Eladio Flores Mena
FCE-BUAP
Vocal

Dr. Ramón Castañeda Priego
DCI-UG
External Vocal

THESIS ADVISORS

Dr. Olegario Alarcón Waess
UDLAP

Dra. Honorina Ruiz Estrada
FCFM-BUAP

Acknowledgments

This work is the result of several years of effort, discipline and perseverance and it is dedicated with all my love to my family: my mother Teresa, my brother Iván, my father Luis Fernando, my beloved Berenice and to the memory of my grandfather Ramón. To reconcile a family life with a scientific career, has not been easy, and I thank to them for all their support, trust, solidarity and love which has always accompanied me, especially in the most difficult and adverse moments.

I would like to express my sincere gratitude to my advisors, Dr. Olegario Alarcón-Waess and Dr. Honorina-Ruiz Estrada, for all the help, patience and guideness that they provide me during these years to successfully complete this research work. Undoubtedly, their expertise in the field of colloids, anisotropic systems (specially in the case of dipolar systems), along with their comprehensive management of Legendre polynomials, spherical harmonics and other customary and useful techniques in the field of molecular liquids were decisive during the course and conclusion of this work. I will always remember this time during which, our friendship and our academic relationship became increasingly stronger.

Very specially, I need to manifest a great admiration and an enormous gratitude to my mentor, Professor Dr. Magdaleno Medina-Noyola. Through his sincere, warm and invaluable friendship, his endless and unconditional support and solidarity, his charismatic personality, but above all, his undeniable devotion to science, has been (and always will) the motor of my development and a huge inspiration to work as a scientist with perseverance and determination. To him I owe everything that has been achieved so far in my short career, and I will always cherish the wonderful moments that I had oportunity to shared with him during the course of my PhD work. I do not posess sufficient literary skills to express all the gratitude, admiration and affection that I feel for him and his family. This work is also dedicated to them.

Also, I would like to express my sincere gratitude to my dear friend, Professor Dr. Ramón Castañ̃eda Priego, for his tremendous support during my PhD work, his unlimited patience as well as his inspiring, exemplary, and outstanding performance as a young researcher. I really appreciate all the help and guideness that I received from him during these years, together with those fruitful discussions and raised comments which constantly contribute to improve the quality of my work. I have high hopes in starting a long and productive scientific collaboration with him and his research group. I would like take this opportunity to extend my gratitude to its warm and friendly family.

I thank to all my dear friends, professors and colleagues for all their support during the last years: professors Dr. José Luis Arauz, Dr. Mariana Kirchbach and Dr. Tanja Schilling. Also to my friends: Claudio Fabián Narambuena, Jorge Adrián Perera, Patricia Mendoza, Edilio Lázaro, Ernesto Cortés, Pablo Zubieta, Felipe Pacheco, Lorena Velázquez, Estela Ramos, Arlette Méndez, Erick Sarmiento, Leticia López, Francisco Alarcón, Alfredo Duarte, Javiera Palma, Pável

Mayorga, Melisa Mendez, Sebastian Salinas, Belinka González, Chacho González, and many others which are not mentioned here for brevity. I thank to all of them for the beautiful momments that we had during these years. Without their friendship, patience, solidarity and help, this work would have been, literaly, impossible.

Finally, I would like to thank to the Mexican working class, to whom I owe mi entire academic education. I thank the financial support granted by CONACYT (Consejo Nacional de Ciencia y Tecnología) through the doctoral fellowship 316765 and through grants No.132540 and No. 182132. I also thank for the financial support granted by Secretaria de Educación Pública (SEP) trough the grant No. PROMEP/103.5/13/5261.

Abstract

A theoretical approach is proposed in order to describe, in the absence of hydrodynamic interactions, the *equilibrium* self and collective dynamics of brownian liquids conformed by non-spherical interacting particles. As an extension of the *so-called* self-consistent generalized Langevin equation formalism (SCGLE), we derive equations of motion for the spherical harmonics projections of the collective and self intermediate scattering functions, $F_{lm,lm}(\mathbf{k},t)$ and $F^{S}_{lm,lm}(\mathbf{k},t)$. In the long-time asymptotic limit, these equations become the so-called bifurcation equations, whose solutions (the nonergodicity parameters) can be written, extending the spherical case, in terms of one translational and one orientational scalar dynamic order parameters, γ_T and γ_R, which characterize the possible dynamical arrest transitions of a given system. As concrete and ilustrative applications of our derivations we consider two model systems, namely, a dipolar hard sphere fluid, for which we determine the arrested phases diagram; and a classical Heisenberg dipolar system with positional disorder, for which we solve the full rotational dynamics to characterize spin glass transitions.

Contents

Abstract **v**

Introduction **ix**

1 General Concepts. **1**
- 1.1 Soft Matter and Colloids. . . . 1
- 1.2 Brownian Motion of non spherical particles. . . . 3
  - 1.2.1 Langevin Equation for a non-spherical interacting particle 3
  - 1.2.2 Homogeneity approximation 5
  - 1.2.3 Decoupling approximation 6
- 1.3 Collective dynamics of non spherical systems 6

2 SCGLE theory for the dynamics of Brownian liquids of non-spherically interacting particles **9**
- 2.1 State of the Art 9
- 2.2 Generalized Langevin Equation Formalism 11
  - 2.2.1 Self consistent scheme 15
- 2.3 Dynamical arrest theory 17
  - 2.3.1 Long-time asymptotic stationary solutions 17

3 Applications I: The Dipolar Hard Sphere Fluid **19**
- 3.1 The Dipolar Hard Sphere Fluid 19
- 3.2 Static structure factor 20
- 3.3 Dynamical arrest diagram 20

4 Applications II: Spin Glass transitions in a classical and disordered Heisenberg system. **27**
- 4.1 Disordered dipolar materials and Spin Glass transitions. 27
- 4.2 Slow Dynamics and Spin Glass transitions of a classical and disordered Heisenberg system. . . 30
  - 4.2.1 Slow dynamics 31
  - 4.2.2 Arrested Phases Diagram 34

5 Conclusions. **39**

6 Publications and other works. **41**

A Brownian motion of spherical particles **43**
- A.1 Langevin equation for a Brownian spherical tracer particle 43
- A.2 Langevin equation for a brownian spherical tracer particle in the presence of other interacting particles 44
- A.3 Generalized Langevin Equation Formalism and $\Delta\zeta(t)$ 45

A.4 Collective Dynamics 46
  A.4.1 Correlation Functions 46
  A.4.2 Correlation Functions in Fourier Space 47

B SCGLE theory of the dynamics of simple brownian liquids **49**
B.1 Long-time asymptotic stationary solutions: dynamical arrest theory 50

C Mean Spherical Approximation for the dipolar hard sphere fluid **51**

Introduction

One of the most challenging and relevant problems in statistical physics refers to the study of the dynamical properties of the *so-called* colloidal suspensions [1, 2]. Their science and technology is truly interdisciplinary, combining basic aspects of physics as well as chemistry, biology and engineering. Colloids possess the ability to display complex states of matter with a profound impact on modern technology as well as many other applications, and hence, have raised much interest in recent years in materials science. A particular aspect of the general problem of determining the dynamic properties of a colloidal suspension involves the description of the translational and rotational diffusion processes in suspensions of colloidal particles interacting through non-spherical pair potentials [3, 4, 5, 6]. In addition, the fundamental understanding of dynamically arrested states, which are commonly observed in a significant number of colloidal systems as well as many other relevant materials, is a major subject in the field of condensed matter physics [9, 10, 11]. The first principles description of dynamically arrested states represents a crucial step towards understanding the properties of an enormous amount of rather common materials, such as glasses and gels [12, 13], with which humans have an intimate daily contact.

Thus, a major challenge for statistical physics is to develop a fundamental theory that predicts the properties of these materials in terms of the intermolecular forces, applied external fields and, desirably, the protocol of fabrication. Truly first-principles theoretical frameworks leading to quantitative predictions of the dynamic properties of Brownian liquids near their dynamical arrest transitions are the conventional mode coupling theory (MCT) [14, 15] and the more recently proposed self-consistent generalized Langevin equation (SCGLE) theory of dynamic arrest [16, 17, 18, 19]. In the context of model liquid systems involving only spherically symmetric interparticle interactions both theories have demonstrated the ability to describe the collective and self dynamics and to predict the existence of dynamical arrest transitions, given the equilibrium structural properties of the system.

In systems that involve non-spherical interactions, the complex intrinsic coupling between orientational degrees of freedom and translational degrees of freedom leads to a variety of different dynamic phenomena [3, 4, 5, 6]. This opens the opportunity to study a wider range of new and fascinating properties, including a richer dynamical arrest scenario, not observed in liquids involving only radially symmetric interactions [6, 7, 8]. As a concrete example of these features, let us refer first to the recent experimental work carried out by Kazem V. Edmond and co-workers [3]. Using high-speed confocal microscopy to directly visualize the 3D translational and rotational motion of tracer tetrahedral colloidal clusters in a dense amorphous suspension of colloidal spheres, Edmond *et al.* showed how the translational and rotational diffusion of the tracers decouple from each other as the colloidal *environment* is brought to the *so-called* glass transition. Specifically, as this glass transition is approached, the long-time rotational diffusion of the tracers decreases proportionally with the bulk viscosity η whereas long-time translational diffusion decreases by a much lesser extent [see Fig. 1].

As showed in Fig. 1, near to the glass transition point of the colloidal environment, the mean square displacement of the tetrahedral clusters displays a plateau (blue circles, corresponding to a volume fraction $\phi = 0.5$) while the corresponding orientational mean square angular displacement remains in the diffusive

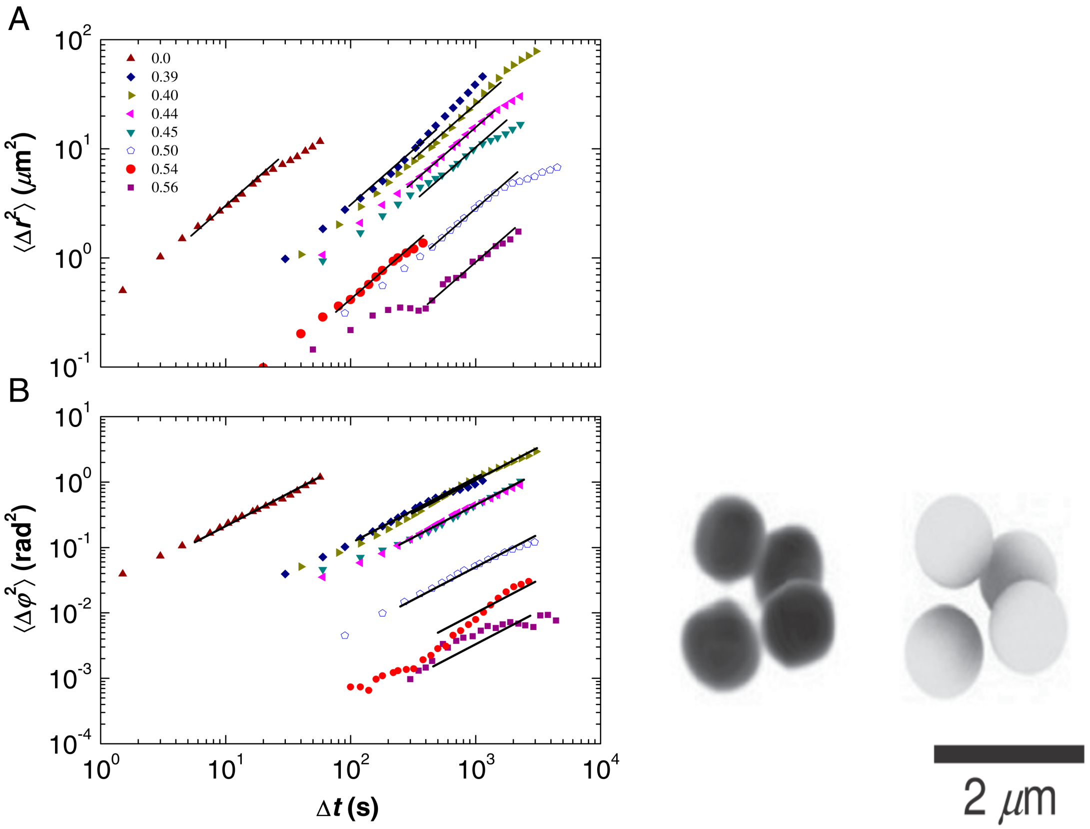

Figure 1: Translational and rotational mobility of tetrahedral colloidal clusters embedded in a dense hard sphere colloidal fluid. The upper panel (A) displays the mean square displacement, $< [\Delta \mathbf{r}(t)]^2 >$, measured using high-speed confocal microscopy, for a range of volume fractions of the hard sphere fluid. The lower pannel (B) shows the corresponding mean square angular displacement, $< (\Delta \boldsymbol{\phi})^2(t) >$. The solid circles and squares correspond to pentagonal clusters and the solid straight lines show a slope of 1 indicating the measured value of D_T and D_R. This plot was extracted from Ref. [3].

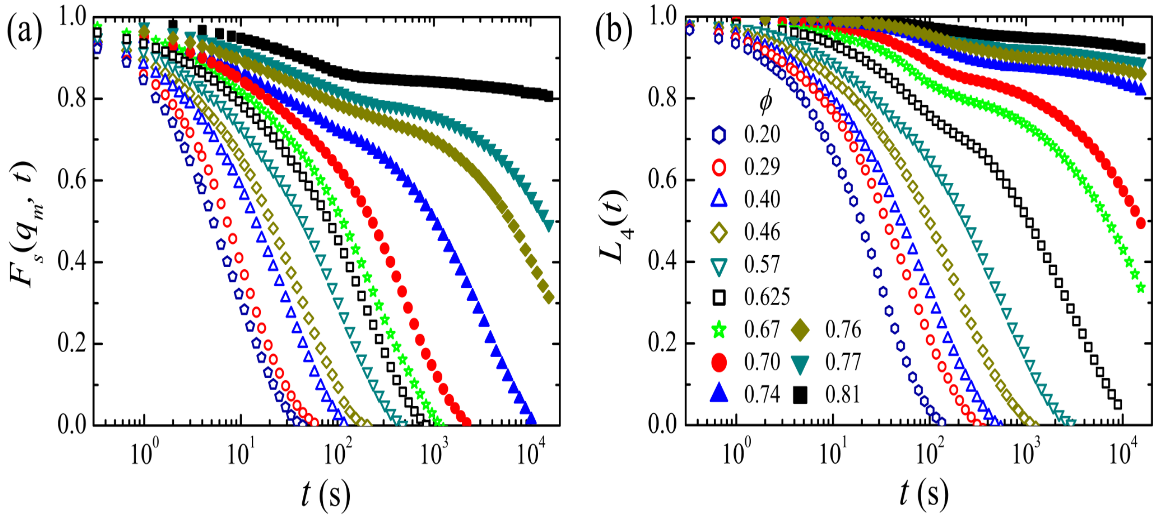

Figure 2: (a) The self-intermediate scattering function $F^S(k,t)$ evaluated at $k = 2.3\mu m^{-1}$ (the first peak position in the structure factor at high density). (b) Orientational correlation function $L_4(t)$, for different area fractions ocupied by the hard ellipsoids. This plot was extracted from Ref. [5].

regime, indicating the occurence of the referred decoupling. The solid circles and solid squares in Fig. 1 correspond to pentagonal clusters. As argued by the authors of this work, the decoupling of traslational and rotational diffusion seems to be a generic feature of glass forming molecular liquids that results from crowding.

In addition, let us consider as a second example the experimental work carried out by Zhongyu Zheng and co-workers [5], in which, video microscopy techniques were employed to study the slow dynamics and glass transitions in monolayers of colloidal hard ellipsoids strongly confined between two glass walls. The hard ellipsoids system is one of the most representative models of liquids with non-spherical interactions. As discused by Z. Zheng *et al.*, and in clear contrast with the glassy dynamics found by Edmond *et al.* for the tetrahedral clusters, a glass transition in the rotational degrees of freedom was observed to occur at a lower density than that in the translational degree of freedom. Specifically, the self-intermediate scattering function, $F^S(k,t) \equiv < \sum_{j=1}^{N} e^{i\mathbf{k}\cdot[\mathbf{r}_j(t)-\mathbf{r}_j(0)]}/N >$ (describing the translational degrees of freedom), and the orientational correlation function $L_4(t)$ (where $L_n(t) \equiv < \sum_{j=1}^{N} \cos n[\theta_j(t) - \theta_j(t=0)] >$), were measured for a range of area fractions, $\phi = \pi abn$, with a and b denoting, respectively, the semilong and semishort axes of the ellipsoids and n the number density [see Fig.2].

As shown in Figs. 2(a) and 2(b), the glass transitions of rotational and translational motions occur in two different area fractions, defining an intermediate orientational glass phase. At high concentrations both, $F^S(k,t)$ and $L_4(t)$, develop two-step relaxations and displays an increase of the relaxation time, which are well known characteristics upon approaching the glass transition. The *so-called* short-time β relaxation corresponds to motion within cages of neighboring particles, whereas the long-time α relaxation reflects structural rearrangement involving a series of cage breakings.

In a further attempt to study and characterize the referred decoupling of the orientational and translational

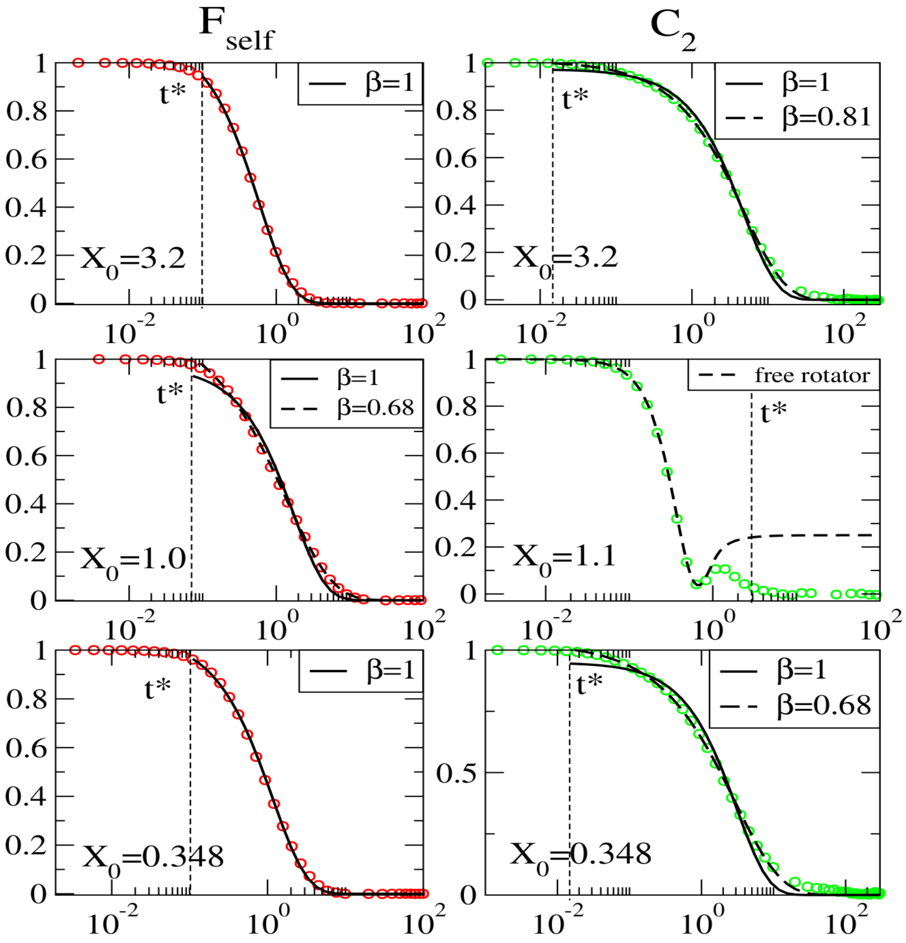

Figure 3: Behavior of $F^S(k,t)$ evaluated at $k = k_{max}$, where k_{max} is the wave vector corresponding to the first maximum of the center-of-mass static structure factor; and $C_2(t)$ for a fixed volume fraction, $\phi = 0.50$, and different values of X_0. Symbols are data from MD simulations. Solid lines are fits to exponential functions, while long-dashed lines are fits to stretched exponentials (β is the stretching parameter). Top: Prolate ellipsoids with $X_0 = 3.2$, C_2 shows a significant stretching while F^S decays exponentially. Middle: $X_0 = 1.0$ for F^S and $X_0 = 1.1$ forC_2. Bottom: Oblate ellipsoids with $X_0 = 0.348$. Plot extracted from Ref. [8]

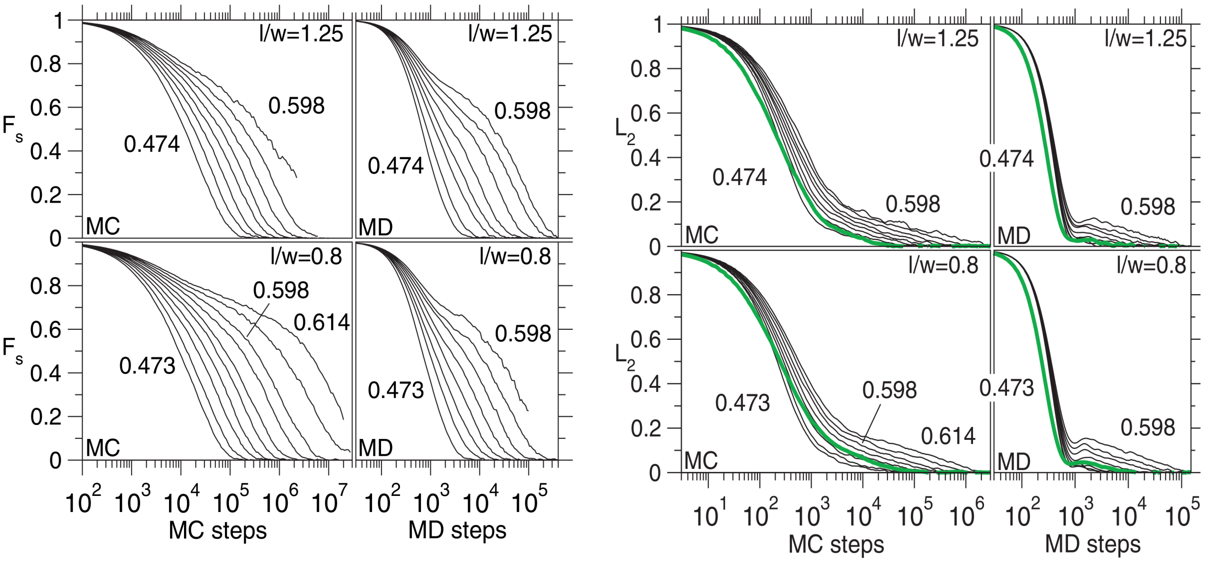

Figure 4: Upper left panel: Self-intermediate scattering functions for hard ellipsoids at several volume fractions ϕ (prolate: 0.474, 0.511, 0.533, 0.551, 0.565, 0.578, 0.588, 0.598; oblate: 0.473, 0.504, 0.533, 0.550, 0.565, 0.578, 0.589, 0.598, 0.606, 0.614). At high volume fractions there is a plateau on intermediate time scales. The final relaxation is slowed down strongly with increasing volume fraction, indicative of glassy dynamics. Upper right panel: Second-order orientational correlators, $L_2(t)$ at the same volume fractions. Again a plateau develops with increasing ϕ. Hence, orientational degrees of freedom are coupled to the positional ones. Also shown are the third-order correlators at the highest density (bold green lines). They do not slow down, indicating that flipping modes are not affected. This plot was extracted from Ref. [6]

degrees of freedom upon the corresponding glass transitions, Cristiano De Michelle and co-workers performed computational simulations for hard ellipsoids in three dimensions [8]. In such work, the *self*-intermediate scattering function, $F^S(k,t)$, was found to exhibit stretched relaxation (*i.e.*, glassy dynamics) only for large volume fraction, ϕ, and aspect ratio $X_0 \approx 1$; whereas the second order orientational correlator $C_2(t) \equiv < P_2(\cos\theta(t)) >$ only shown stretching for large and small X_0 values [see Fig. 3], indicating thus that the referred decoupling depends, not only on the volume fraction occupied by the hard ellipsoids, but also on the specific aspect ratio. Clear indicators of glassy dynamics, however, would include a strong increase of relaxation times with volume fraction, even pointing towards dynamical arrest. Typically, correlators then develop a two-step decay, whose second step is affected by this slowing-down. Such phenomena which has not explicity exhibit in [8] was observed in the independent simulation work carried out by P. Pfleiderer and co-workers [6]. Again, a slowing down of the diffusion and relaxation procces, accompanied by two-step relaxation in positional and orientational correlators were observed [see Fig. 4]. In this work however, the decoupling of both degrees of freedom was put into question.

From a theoretical point of view, the extension of MCT to non-spherical systems was an important step in understanding relaxation procces [20, 21] and slow dynamics in glass-forming molecular liquids [22, 23]. In this regard, the pioneering work carried out by Schilling and co-workers [7, 24, 25, 26], applied to study the idealized glass transition in liquids conformed by linear molecules, should be highlighted. In fact, when applied to hard ellipsoids in three dimensions, the MCT formalism was able to predict a very similar dynamical arrest scenario observed by Z. Zheng *et al.* [see Fig 5(a) and the discussion in Ref. [25] for the details]: one corresponding to the conventional glass transition for spherical particles, driven by the cage effect; a second transition with a glassy phase, consisting of domains within which there exist *nematic* order and where the center of mass motion is quasiergodic whereas the interdomain orientations build an orientational glass; and finally, a third kind of transition for nearly spherical ellipsoids where the orientational degrees of freedom with odd parity (e.g., 180° flips), freeze independently from the positions.

Another important and interesting application of the MCT formalism (closely related to the referred decoupling of the orientational and translational degrees of freedom) refers to the description of the slow dynamics and the dynamical arrest transitions of a dipolar hard sphere fluid [7, 26] which constitute another classical reference model for systems with non-spherical interactions. For this case, MCT also predicts the existence of three different phases depending on the control parameters which define the macroscopical state of the system: a fully ergodic liquid phase, where translational and orientational degrees of freedom are ergodic, a "mixed" phase where the former are frozen into a nonergodic glassy state, whereas the latter remain ergodic, and, finally, a fully non-ergodic or glassy phase where both degrees of freedom freezes [see Fig. 5(b)].

In contrast with the extensive MCT developments for non spherical systems, the SCGLE theory has only been applied so far to the simpler case of liquids involving only spherically-symmetric interactions. A first step in building the non-spherical version of the SCGLE formalism has its foundations on the work performed by Martín Hernández-Contreras and co-workers [27, 28, 29, 30, 31], where the generalized Langevin Equation (GLE) formalism [32, 33, 34] was employed in order to determine the memory kernels associated to the diffusion processes of non-spherical interacting tracer particles. As it will be shown later on this thesis, these results will provide some of the elements needed to perform the formal extension of the SCGLE for Brownian liquids constituted by non-spherical particles. Furthermore, a second step in the development of such extension was recently carried out by Pablo Zubieta-Rico [35], as the first concrete attempt to construct the referred non-spherical version of the full SCGLE formalism. While this attempt was a necessary and illustra-

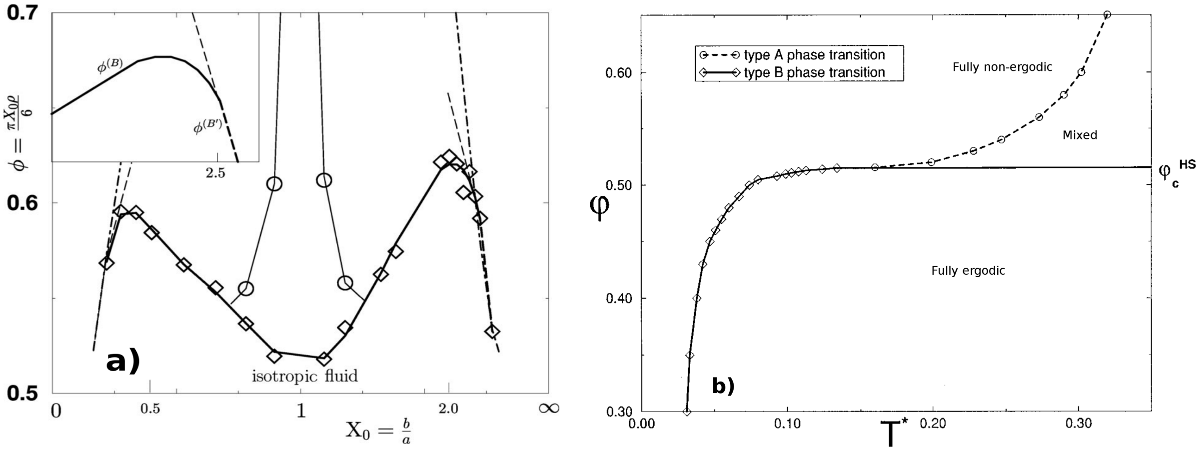

Figure 5: Left panel: arrested phases diagram predicted by MCT in Ref. [25] for the hard ellipsoids system in 3D (see text above). Right panel: arrested phases diagram predicted by MCT in Ref. [7] for the dipolar hard sphere fluid (see text above).

tive excersice, many questions and issues remain to be understood. For example in the work of Zubieta-Rico, it remain unclear what is the proper way to approximate the memory kernels associated to the transaltional and orientational degrees of freedom. Also, the explicit form of the equations describing the corresponding nonergodicity parameters lead to non expected results (compared with previous MCT predictions in Refs. [7, 26]) when applied to specific systems.

Thus, the main goal of the present work, is to stablish the final steps in the formal derivation of the non-spherical *equilibrium* version of the SCGLE theory, and to test its predictions for simple models. This expectation was nicely performed, and the main contribution of this thesis is contained in a recent manuscript publicated in the Physycal Review E [36], where such extension of the theory is proposed and applied to characterize the dynamical arrest scenario for the dipolar hard sphere fluid. Our expectative is that the alternative theoretical framework proposed in this work will join other approaches, (most notably MCT, and not many more), in the effort to improve our understanding and our predictive capability regarding dynamic arrest phenomena. Although the extension of the SCGLE theory to this richer class of systems is important by itself, a relevant additional motivation to develop such an extension is provided by the recent emergence [37] of the non-equilibrium generalization of the SCGLE theory (denoted as NE- SCGLE), which allows, for example, the description of aging phenomena [38, 39]. Extending this non-equilibrium theory to systems involving non-spherically symmetric interactions will thus allow the description of the aging processes of the rotational degrees of freedom in structural glasses, a highly desirable complement of the study of aging in simpler non-structural spin glasses [40]. Thus, an aditional fundamental basis of the SCGLE extension to non-spherical systems proposed in this work, is that it lends itself to the development of a promising approach to the description of irreversible non-stationary procces, which are the genuine fingerprint of glassy matter. The non-equilibrium extension of the theory mentioned here is in fact the subject of work in progress in colaboration with the group of professor Magdaleno Medina-Noyola [41]. The development of the rotational version of such non-equilibrium theory requires, however, the previous development of the corresponding equilibrium SCGLE theory, and this is, as we have already stablished, the main aim of the present thesis. For this, as in the spherical case, here we apply the generalized Langevin equation (GLE) formalism [42] and the concept of contraction of the description [32] to derive exact memory function equations for the spherical harmonics projections $F_{lm,lm}(k,t)$ and $F^S_{lm,lm}(k,t)$ of the collective and self intermediate scattering functions $F(k,\mathbf{\Omega},\mathbf{\Omega}',t)$ and $F^S(k,\mathbf{\Omega},\mathbf{\Omega},t)$. These dynamic equations only involve the corresponding projections $S_{lm,lm}(k)$ of the equilibrium static structure factor $S(k,\mathbf{\Omega},\mathbf{\Omega}')$. The exact equations thus derived require the independent determination of the corresponding self and collective memory functions. In a manner similar to the spherical case, here we propose simple Vineyard-like approximate closure relations for these memory functions, which convert the originally exact equations into a closed self-consistent system of equations for the dynamic properties involved.

One important application of the resulting theory is the description of dynamical arrest transitions in liquids with orientational degrees of freedom. Just like its MCT analog, the present theory only describes the dynamics of equilibrium states, and hence, cannot describe non-stationary non-equilibrium phenomena such as aging. Nevertheless, the dynamical arrest diagrams predicted by these equilibrium theories have a deep physical significance for the description of those non-equilibrium phenomena, as explained in Refs. [38, 39] in the context of liquids formed by spherical particles. Thus, as a concrete illustrative application of the general theory developed in this work we determine the dynamical arrest diagram of a simple model system, namely, the dipolar hard-sphere liquid, previously studied with MCT [7]. In adition, we also use the SCGLE formalism to describe the full rotational dynamics of a classical Heisenberg dipolar system with frozen positional disorder, for which we describe the occurence the *so-called* spin glas transitions.

This thesis is organized as follows: In chapter 1, for the benefit of the reader, we recall several well known results, and introduce the appropriate notation and many conceptual framework needed to construct our theoretical approach. In chapter 2 we formally derive the non spherical SCGLE formalism in order to obtain the exact equations of motion for the generalized dynamical properties, $F_{lm,lm}(k,t)$ and $F^S_{lm,lm}(k,t)$ which, upon the introduction of a few simple approximations, turn into the desired self-consistent closed system of equations. Then, by taking the long-time asymptotic limit of these self-consistent equations, we derive the equations for the stationary solutions (referred to as the bifurcation equations for the nonergodicity parameters, in the MCT language). This is the main contribution of the present work. In chapter 3 we apply these bifurcation equations to the dipolar hard-sphere liquid in order to exhibit the ability of these equations to identify dynamical arrest transitions and to obtain the corresponding arrested phases diagram. We contrast the predictions of our theory with previous results derived within the MCT formalism. In chapter 4, we adapt the full SCGLE equations in order to characterize the slow dynamics near the spin glass transition of a disordered Heisenberg-dipolar system, for which we describe dynamical properties and determine the corresponding phase diagram. Finally, we summarize the main conclusions of this thesis.

Chapter 1

General Concepts.

As we have already established, the main purpose of this work is to derive a theoretical approach able to describe the collective and self dynamics of colloidal suspensions conformed by particles interacting through non-spherical potentials. For this purpose, we need to describe the time evolution of a specific set of physical observables characterizing the dynamical state of a given system. As it will be shown, we will rely on the Generalized Langevin Equation formalism and the concept of contraction of the description [42, 32] to derive the corresponding equations of motion for the referred observables. In the process, many other conceptual objects and physical quantities will emerge and previous knowledge in the field of colloids, and in general in the theory of complex fluids, will be needed to follow our derivations.

Thus, let us start by briefly reviewing the most general aspects concerning to these objects and defining the relevant physical properties to be considered within our approach, as well as to introduce the appropriate language which is customary employed in the description and characterization of the structural and dynamical properties of non-spherical colloidal fluids. Rather than provide a detailed discussion for each of these objects, we will refer to the reader to appropriate original references and we will assume a minimun basic background in molecular-liquids theory. For the benefit of the reader, however, in appendix A we include a summary of the important results involved in the characterization of Brownian motion and the collective and self dynamics for spherical systems, in order to facilitate (some times by direct comparison) the comprehension of the discussion presented in what follows.

1.1 Soft Matter and Colloids.

The study of soft matter physics involves the understanding of the properties of materials which possess structural length scales in the range of a few nanometers ($\sim 10^{-9}m$) to several micrometers ($\sim 10^{-3}m$), and which are significantly affected by thermal fluctuations [1, 2]. A particularly important example of soft-matter materials are the *so-called* colloidal suspensions. To a large extent, colloids may be referred as complex systems constituted of "large molecules" ($\sim 10^{-6}m$) in solutions, where by large, we mean compared to the length scale associated to the constitutive molecules of the solvent (commonly $\sim 10^{-9}m$). As a consequence of this separation in lenght scales, a noticeable difference in the time scales associated to each component in the systems also appears. Because of the direct interactions between these particles and due to the interactions of the particles with the solvent constituents, colloids behave as Brownian particles. Colloids are considered large with respect to the solvent particles, but still "small" enough to exhibit thermal motion. A minimum size of a colloidal particle is set by the requirement that "*the structure of the solvent on the molecular (or atomic) length scale enters the interaction of the colloidal particles with the solvent only in an averaged way*" [1].

There are many reasons why physicist are interested in the study of colloids. They have proven to be nobel experimental reference systems to study simple fluids, mostly due to the fact that, with the sufficiently careful preparation, colloids approximate to hard particles [2, 43]. From a practical point of view, there are several examples, raging from biomedical applications [44, 45], the modelling of biological materials and processes [46], or even technological developments [47] which demands a thorough understanding of the dynamics and self assembly properties of coloidal fluids [48, 49]. The outstanding abundance in nature of these fascinating systems, as well as the promising future applications of these materials, placed them as one of the most relevant topics in the soft matter community [50]. Furthermore, as indicated on the introduction, the first principles description of the relaxation processes in colloidal systems pose one of the most important problems of statistical mechanics [12].

A particular, very relevant and forefront topic in this context, concerns to the understanding of the occurence of dynamically arrested states, in which, a given system (not necessarily colloidal) might suffer a kinetic transition and remain "*traped*" in a non-ergodic state, exhibting thus its inability to reach thermodynamic equilibrium within experimental times. Hence, their properties depend on the protocol of preparation, in obvious contrast with materials that have reached equilibrium. The theoretical description of such arrested states constitute one of the most outstanding problems in condensed matter physics, and the main purpose of this work is to address this fundamental problem, specially in what concerns to systems with both, translational and orientational degrees of freedom. As it will be shown latter, in this work we will derive a theoretical approach able to deal with these issues. Nevertheless, to construct such theory, we need to appeal to many known results in the context of the colloidal fluids, thus, in what follows we refer to this basic knowledge.

1.2 Brownian Motion of non spherical particles.

> *The very great theoretical importance presented by the phenomena of Brownian motion has been brought to our attention by M. Gouy. We are indebted to this physicist for having clearly formulated the hypothesis which sees in this continual movement of particles for suspended in a fluid an echo of molecular-thermal agitation, and having demonstrated this experimentally, at least in a qualitative manner, by showing the perfect permanence of Brownian motion, and its indifference to external forces when the latter do not modify the temperature of the environment.*
>
> P. Langevin

We have repeatedly pointed out that the main goal of the present thesis consist in deriving a theoretical approach able to describe the relevant dynamical properties of Brownian liquids constituted by particles interacting through non-spherical pair potentials. As argued above, in deriving such theory, many concepts and physical quantities will appear. While in the spherical case, the characterization of Brownian motion is a well known and classical problem in statistical mechanics (whose most important results can be found extensively discussed elswhere in the literature [1, 55, 51, 52, 53, 54], see also apendix A), the extension of this generic problem to the case of particles interacting through non-spherical potentials entails a set of new considerations with a considerable degree of complexity.

1.2.1 Langevin Equation for a non-spherical interacting particle

Let us consider the translational and rotational Brownian motion of a non-spherical colloidal tracer particle, in the absence of hydrodynamic interactions, but in the presence of other colloidal particles exerting direct forces and torques on it. For simplicity, we will assume that the other particles are identical to the tracer, that is, we will restrict to the monodisperse case. In order to further simplify the present discussion, we will also consider the particular case of linear particles, that is, particles which possess a symmetry axis. Ellipsoids, cylinders, hard spheres with a linear dipole in the center, and many other geometrical bodys belong to this class.

As it was nicely discussed by M.Hernández-Contreras in Ref. [27], the translational and orientational degrees of freedom of the tracer particle may be described by the following linearized Langevin equations describing the Brownian motion of the non-spherical colloidal tracer [see also Ref. [28, 29, 30]]

$$m\frac{d\mathbf{v}_t(t)}{dt} = -\overleftrightarrow{\zeta}^{0}_{T}\cdot\mathbf{v}_t(t) - \overleftrightarrow{\zeta}^{0}_{TR}\cdot\boldsymbol{\omega}_t(t) + \mathbf{f}^0(t) + \int d\mathbf{r}d\boldsymbol{\Omega}[\nabla\psi(\mathbf{r},\boldsymbol{\Omega})]n(\mathbf{r},\boldsymbol{\Omega};t) \tag{1.1}$$

$$\mathbf{I}\frac{d\boldsymbol{\omega}_t(t)}{dt} = -\overleftrightarrow{\zeta}^{0}_{RT}\cdot\mathbf{v}_t(t) - \overleftrightarrow{\zeta}^{0}_{R}\cdot\boldsymbol{\omega}_t(t) + \mathbf{t}^0(t) + \int d\mathbf{r}d\boldsymbol{\Omega}[\nabla_{ROT}\psi(\mathbf{r},\boldsymbol{\Omega})]n(\mathbf{r},\boldsymbol{\Omega};t) \tag{1.2}$$

with $\mathbf{v}_t(t)$ and $\boldsymbol{\omega}_t(t)$ denoting, respectively, the linear (center of mass) and angular velocity of the tracer, whose components are referred to a coordinate system with origin fixed in the laboratory frame but with orientation changing in time to coincide with the principal axis of the tracer. Also, $\nabla_{ROT} \equiv \mathbf{r}\times\nabla + \nabla_{\Omega}$, where ∇_{Ω} is the angular gradient operator [57], and $\psi(\mathbf{r},\boldsymbol{\Omega})$ denote the potential energy of the direct interactions between the tracer and anyone of the particles, located at position $\mathbf{r}$ relative to the tracer's center of mass and with principal axis rotated by a rotation $\mathbf{\Omega}$ with respect to the orientation of the tracer particle. In addition, the friction tensors $\overleftrightarrow{\zeta}^{0}_{T}$, $\overleftrightarrow{\zeta}^{0}_{TR}$, $\overleftrightarrow{\zeta}^{0}_{RT}$, $\overleftrightarrow{\zeta}^{0}_{R}$ are assumed to produce hydrodynamic drag forces and torques, linear on the velocities, that couple to the thermally driven solvent random forces $\mathbf{f}^0$ and torques $\mathbf{t}^0$ and are related by a fluctuation-dissipation theorem in the sense of Eq. (9) of Ref. [30]. Finally, the last terms in the right hand side of both equations describe the total force and torque on the tracer produced by the direct interactions with the instantaneous local concentration $n(\mathbf{r},\mathbf{\Omega};t)$ of the *host* suspension. Both Langevin equations may be written compactly as [1] [31]

$$\overleftrightarrow{M}\cdot\frac{d\overleftrightarrow{\mathbf{V}}(t)}{dt}=-\overleftrightarrow{\boldsymbol{\zeta}}^{0}\cdot\overleftrightarrow{\mathbf{V}}(t)+\overleftrightarrow{\mathbf{f}^{0}}(t)+[\overleftrightarrow{\nabla}\,\underline{\psi}(t)]\circ\delta\underline{n}(t),\tag{1.3}$$

where $\overleftrightarrow{\mathbf{V}}(t)\equiv[\mathbf{v}_t(t),\boldsymbol{\omega}_t(t)]$, $\overleftrightarrow{\nabla}\equiv[\nabla,\nabla_{ROT}]$, $\overleftrightarrow{\mathbf{f}^{0}}(t)\equiv[\mathbf{f}^{0}(t),\mathbf{t}^{0}(t)]$, $\overleftrightarrow{M}_{ij}=m\delta_{ij}$ for $i,j=1,2,3$ and $\overleftrightarrow{M}_{ij}=\delta_{ij}I_{i-3}$ for $i,j=4,5,6$; with m,I_1,I_2,I_3 being, respectively, the mass and principal moments of inertia of the tracer particle; also, the generalized tensor $\overleftrightarrow{\boldsymbol{\zeta}}^{0}$ clearly groups the friction tensors $\overleftrightarrow{\zeta}^{0}_{T}$, $\overleftrightarrow{\zeta}^{0}_{TR}$, $\overleftrightarrow{\zeta}^{0}_{RT}$, $\overleftrightarrow{\zeta}^{0}_{R}$. We have introduced the *inner product* operator "$\circ$" defined here as the convolution operator $\int d\mathbf{r}\int d\mathbf{\Omega}$ and also, for the sake of notation, we used *underlined* symbols to not write explicit the $(\mathbf{r},\mathbf{\Omega})$ dependence of ψ and $\delta n(t)$.

As argued in Ref. [27], in the particular case of linear molecules the coupling tensors $\overleftrightarrow{\zeta}^{0}_{TR}$ and $\overleftrightarrow{\zeta}^{0}_{RT}$ vanishes and therefore, the only nonzero components of $\overleftrightarrow{\boldsymbol{\zeta}}^{0}$ are $\zeta^0_{11}=\zeta^0_{22}=\zeta^0_{\perp}$, $\zeta^0_{33}=\zeta^0_{\parallel}$, $\zeta^0_{44}=\zeta^0_{55}=\zeta^0_{R}$ and $\zeta^0_{66}=0$. Thus, in Eq. (1.3), the force and the torque on the tracer due to *direct* interactions can be written *exactly* as linear functions of the instantaneous fluctuations $\delta n(\mathbf{r},\mathbf{\Omega};t)$ of the local concentration [see Eq.(1.11)], whereas the force and torque exerted by the solvent can be written as an ordinary Langevin equation, that is, a dissipative plus a random term; the latter assumed to have zero mean and time-correlation function given by the fluctuation-dissipation relation $\langle\overleftrightarrow{\mathbf{f}^{0}}(t)\overleftrightarrow{\mathbf{f}^{0}}^{\dagger}(0)\rangle=k_BT\overleftrightarrow{\boldsymbol{\zeta}}^{0}2\delta(t)$.

As discussed in Refs. [27] and [29], a time evolution equation for $\delta\underline{n}(t)$ can be obtained from general arguments of linear irreversible theory of fluctuations. Such equation together with (1.3) constitute a stationary procces that can be modeled using the theorems of stationarity and contraction of the description (see Ref. [33]) for the *stocastic vector* $\mathbf{a}(t)=[\overleftrightarrow{\mathbf{V}}(t),\delta\underline{n}(t)]^{\mathbf{t}}$. Thus, contracting the description to eliminate $\delta\underline{n}(t)$ one arrives to the following Langevin equation

$$\overleftrightarrow{M}\cdot\frac{d\overleftrightarrow{\mathbf{V}}(t)}{dt}=-\overleftrightarrow{\boldsymbol{\zeta}}^{0}\cdot\overleftrightarrow{\mathbf{V}}(t)+\overleftrightarrow{\mathbf{f}^{0}}(t)-\int_0^t dt'\Delta\overleftrightarrow{\boldsymbol{\zeta}}(t-t')\cdot\overleftrightarrow{\mathbf{V}}(t')+\overleftrightarrow{\mathbf{F}}(t),\tag{1.4}$$

with $\overleftrightarrow{\mathbf{F}}(t)$ grouping a random force and torque on the tracer which turns out to have zero mean, time-correlation function given by $\langle\overleftrightarrow{\mathbf{F}}(t)\overleftrightarrow{\mathbf{F}}^{\dagger}(0)\rangle=k_BT\Delta\overleftrightarrow{\boldsymbol{\zeta}}(t)$, and where the time-dependent friction function is given by

$$\Delta\overleftrightarrow{\boldsymbol{\zeta}}(t)=k_BT[\overleftrightarrow{\nabla}\,\underline{n}^{eq}]\circ\underline{\sigma}^{-1}\circ\underline{C}(t)\circ[\overleftrightarrow{\nabla}\,\underline{n}^{eq}]^{\dagger}.\tag{1.5}$$

---

[1] Compare equations 1.3 with the corresponding Langevin equation A.7 in appendix A for the spherical case. Clearly, both possess the same mathematical structure.

where $\underline{n}^{eq} \equiv < \underline{n}(t) >$, and $\underline{\sigma}^{-1}$ denotes the inverse function of the inhomogeneous static correlation function $\underline{\sigma}$, defined trough the relation

$$\int d\mathbf{r}'' d\mathbf{\Omega}'' \sigma(\mathbf{r},\mathbf{r}'',\mathbf{\Omega},\mathbf{\Omega}'')\sigma^{-1}(\mathbf{r}'',\mathbf{r}',\mathbf{\Omega}'',\mathbf{\Omega}') = \delta(\mathbf{r}-\mathbf{r}')\delta(\mathbf{\Omega}-\mathbf{\Omega}'). \tag{1.6}$$

Also $\underline{C}(t)$ denotes the collective-diffusion propagator $\underline{C}(t) = \underline{G}^*(t) \circ \sigma^{-1}$, with $\underline{G}^*(t)$ being the van Hove function $G^*(\mathbf{r},\mathbf{r}',\mathbf{\Omega},\mathbf{\Omega}';t) = n^{-1}\langle \delta n(\mathbf{r},\mathbf{\Omega};t)\delta n^\dagger(\mathbf{r}',\mathbf{\Omega}';0)\rangle$, referred to the tracer's position and orientation. That is, $\underline{G}^*(t)$ is the solution of the linearized diffusion equation that governs the diffusive relaxation of $\delta\underline{n}(t)$, as described from the tracer's reference frame, and whose initial condition is, the static correlation $\underline{G}^*(0) = \langle \delta\underline{n}(0)\delta\underline{n}^\dagger(0)\rangle \equiv \sigma/n$.

1.2.2 Homogeneity approximation

To evaluate $\Delta\overleftrightarrow{\zeta}(t)$ from Eq.(1.5) we need to determine first the two static structural properties $\underline{n}^{eq}$ and $\underline{\sigma}^{-1}$. In principle, these equilibrium properties should be obtained by means of the statistical thermodynamic theory of inhomogeneous fluids [55]. In fact, the determination of $n^{eq}(\mathbf{r},\mathbf{\Omega}_T,\mathbf{\Omega})$ involves only a pair correlation function (between the tracer and other particle with center of mass located at $\mathbf{r}$ as seen from the tracer's reference frame), whereas the determination of $\sigma(\mathbf{r},\mathbf{r}',\mathbf{\Omega},\mathbf{\Omega}')$ requires the determination of a three-particle distribution function (two particles in the presence of the tracer). This last calculation may constitute by itself a rather difficult task in practice. For this reason, it is useful to introduce a simplifying approximation which consists into approximate $\underline{\sigma}$ by its value in the absence of the tracer, *i.e.*, by its bulk value. This amounts to ignoring the inhomogeneity produced by the field generated by the tracer, and thus, $\underline{\sigma}$ reduces to a pair correlation function. Under such conditions, $\sigma(\mathbf{r},\mathbf{r}',\mathbf{\Omega},\mathbf{\Omega}')$ and $\sigma^{-1}(\mathbf{r},\mathbf{r}',\mathbf{\Omega},\mathbf{\Omega}')$ no longer depends separately on $\mathbf{r}$ and $\mathbf{r}'$, but only on the difference $\mathbf{r}-\mathbf{r}'$. This approximation can be expressed as

$$\begin{aligned}\sigma(\mathbf{r},\mathbf{r}',\mathbf{\Omega},\mathbf{\Omega}') &\approx \sigma(\mathbf{r}-\mathbf{r}',\mathbf{\Omega},\mathbf{\Omega}') \\ &= \frac{1}{(2\pi)^3}\int d^3k e^{-i\mathbf{k}\cdot(\mathbf{r}-\mathbf{r}')}\sigma(\mathbf{k},\mathbf{\Omega},\mathbf{\Omega}')\end{aligned} \tag{1.7}$$

Thus, $\sigma(\mathbf{k},\mathbf{\Omega},\mathbf{\Omega}')$ denotes the *spatial*-Fourier transform of the function $\sigma(\mathbf{r}-\mathbf{r}',\mathbf{\Omega},\mathbf{\Omega}')$, which is directly related to the static structure factor by $\sigma(\mathbf{k},\mathbf{\Omega},\mathbf{\Omega}') = nS(\mathbf{k},\mathbf{\Omega},\mathbf{\Omega}')$ [57, 55]. A similarly assumption may be proposed for the collective diffusion propagator $\underline{C}(t) = C(\mathbf{r},\mathbf{r}',\mathbf{\Omega},\mathbf{\Omega}';t)$. Thus, using this approximations together with the generalized Parseval's theorem we can approximate (1.5) by:

$$\begin{aligned}\Delta\overleftrightarrow{\zeta}(t) &= \frac{k_BT}{(2\pi)^3}n\int d\mathbf{k}\int d\mathbf{\Omega}d\mathbf{\Omega}'d\mathbf{\Omega}''d\mathbf{\Omega}'''[\overleftrightarrow{\nabla}_k h(\mathbf{k},\mathbf{\Omega}_T,\mathbf{\Omega})]S^{-1}(\mathbf{k},\mathbf{\Omega},\mathbf{\Omega}') \\ &\times \; F^*(\mathbf{k},\mathbf{\Omega}',\mathbf{\Omega}'';t)S^{-1}(\mathbf{k},\mathbf{\Omega}'',\mathbf{\Omega}''')\times[\overleftrightarrow{\nabla}_k[h(\mathbf{k},\mathbf{\Omega}_T,\mathbf{\Omega}''')]^\dagger\end{aligned} \tag{1.8}$$

where $h(\mathbf{k},\mathbf{\Omega},\mathbf{\Omega}')$ denotes the Fourier transform of the total correlation function, $\overleftrightarrow{\nabla}_k \equiv [\mathbf{k},\mathbf{k}\times\nabla_k+\mathbf{L}]^{\mathbf{t}}$, and with $\underline{F}^*(t)$ being the intermediate scattering function, $\langle n(\mathbf{k},\mathbf{\Omega};t)n^\dagger(\mathbf{k},\mathbf{\Omega}';0)\rangle$, where the superindex "*" indicates that the local concentration $\underline{n}(t)$ (and consequently $\underline{F}^*(t)$) is referred to the tracer's reference system.

1.2.3 Decoupling approximation

To obtain more explicit results for the sub-tensors $\Delta\overleftrightarrow{\zeta}_{\alpha}(t)$ $(\alpha = T, R)$ in Eq. (1.8) let us consider the Fourier representation of $\underline{C}(t)$ given by

$$C(\mathbf{k},\mathbf{\Omega},\mathbf{\Omega}';t) = \int d\mathbf{\Omega}'' F^{*}(\mathbf{k},\mathbf{\Omega},\mathbf{\Omega}'';t) S^{-1}(\mathbf{k},\mathbf{\Omega}'',\mathbf{\Omega}'), \tag{1.9}$$

As discussed by Medina-Noyola in [33], for the spherical case one can adopt a decoupling approximation (first suggested by Hess and Klein [58]) for the dynamic correlator $F^{*}(k,t)$ for the case where the tracer is one of the macrofluid particles. Such approximation reads $F^{*}(k,t) \approx F^{S}(k,t) \times F(k,t)$ where the collective propagator referred to the tracer coordinate system is substituted by the product of the *normal* (referred to a fixed laboratory frame) collective propagator times the tracer-diffusion propagator. Thus, in order to obtain the spherical SCGLE as the spherical limit of our derivations, we may propose the following approximation:

$$F^{*}(\mathbf{k},\mathbf{\Omega},\mathbf{\Omega}';t) \approx \int d\mathbf{\Omega}'' F^{S}(\mathbf{k},\mathbf{\Omega},\mathbf{\Omega}'';t) F(\mathbf{k},\mathbf{\Omega}'',\mathbf{\Omega}';t), \tag{1.10}$$

which represents the angular convolution of both propagators.

1.3 Collective dynamics of non spherical systems

In this section we present the correlation functions of our interest and introduce some features that will be considered in what follows in the construction of the non-spherical SCGLE formalism. Rather than provide a detailed discussion of the theoretical description of fluids with orientational degrees of freedom, we refer the reader to the classical textbook of C. Gray and K. Gubbins [57]. Thus, let us start by considering a colloidal system composed by N-linear and rigid identical particles, with mass m and inertia tensor $\mathbf{I}$ contained in a volume V. The translational degrees of freedom are described by the vectors $\mathbf{r}^N \equiv (\mathbf{r}_1,...,\mathbf{r}_N)$ and $\mathbf{p}^N \equiv (\mathbf{p}_1,...,\mathbf{p}_N)$, where $\mathbf{r}_n$ denotes the center-of-mass position vector of the nth-particle and $\mathbf{p}_n \equiv m d\mathbf{r}_n/dt = m\mathbf{v}_n(t)$ is the associated linear momentum. Also, the orientational degrees of freedom are described by the abstract vectors $\mathbf{\Omega}^N \equiv (\mathbf{\Omega}_1,...,\mathbf{\Omega}_N)$ and $\mathbf{L}^N \equiv (\mathbf{L}_1,...,\mathbf{L}_N)$, where $\mathbf{\Omega}_n$ denotes the Euler angles which specify the orientation of the nth molecule, and $\mathbf{L}_n = \mathbf{I}(\mathbf{\Omega}_n)\boldsymbol{\omega}_n$ is the corresponding angular momentum. In this last equation, $\boldsymbol{\omega}_n$ denotes the angular velocity. In the particular case of linear particles, the third Euler angle results redundant and thus $\mathbf{\Omega}_n = \mathbf{\Omega}_n(\theta_n,\phi_n)$. For our present purpose we will assume that, in the absence of hydrodynamic interactions, the microscopic translational and rotational dynamics of this system can be described by the Langevin equations (1.3)

As in the spherical case discussed in appendix A, the most basic quantity for the description of the dynamical properties of a non-spherical colloidal system is the time dependent microscopic one-particle density [see Eq. A.17] which, for this case, may be extended to

$$n(\mathbf{r},\mathbf{\Omega};t) \equiv (1/\sqrt{N}) \sum_{n=1}^{N} \delta(\mathbf{r}-\mathbf{r}_n(t))\delta(\mathbf{\Omega}-\mathbf{\Omega}_n(t)). \tag{1.11}$$

By using the fact that *any* function $f(\mathbf{r},\mathbf{\Omega})$ can be expanded with respect to plane waves and spherical harmonics as

$$f(\mathbf{r},\mathbf{\Omega}) = \frac{1}{V}\frac{1}{\sqrt{4\pi}}\int d\mathbf{k}\sum_{lm}(i)^l f_{lm}(\mathbf{k})e^{-i\mathbf{k}\cdot\mathbf{r}}Y^*_{lm}(\mathbf{\Omega}) \tag{1.12}$$

where

$$f_{lm}(\mathbf{k}) = \sqrt{4\pi}i^l\int_V d\mathbf{r}\int d\mathbf{\Omega} f(\mathbf{r},\mathbf{\Omega})e^{-i\mathbf{k}\cdot\mathbf{r}}Y_{lm}(\mathbf{\Omega}) \tag{1.13}$$

we obtain, from (1.11) the *so-called* tensorial density modes

$$n_{lm}(\mathbf{k},t) = \sqrt{\frac{4\pi}{N}}i^l\sum_{n=1}^{N}e^{i\mathbf{k}\cdot\mathbf{r}_n(t)}Y_{lm}(\mathbf{\Omega}_n(t)), \tag{1.14}$$

and thus, the following generalized correlators can be defined as

$$\begin{aligned} F_{lm;l'm'}(\mathbf{k},t) &\equiv \langle\delta n^*_{lm}(\mathbf{k},t)\delta n_{l'm'}(\mathbf{k},0)\rangle \qquad (1.15)\\ &= \frac{4\pi}{N}i^{l-l'}\sum_{n\neq n'}^{N}\left\langle e^{i\mathbf{k}\cdot[\mathbf{r}_n(t)-\mathbf{r}_{n'}(0)]}Y^*_{lm}(\mathbf{\Omega}_n(t))Y_{l'm'}(\mathbf{\Omega}_{n'}(0))\right\rangle, \end{aligned}$$

where $\delta n_{lm}(\mathbf{k},t) \equiv n_{lm}(\mathbf{k},t) - \langle n_{lm}(\mathbf{k},t)\rangle$. For $\mathbf{k} = \mathbf{0}$, $(l,m) = (l',m') = (0,0)$, $F_{lm,l'm'}(k,t)$ vanishes.

For completeness, we also define the self components

$$n^S_{lm}(\mathbf{k},t) \equiv \sqrt{4\pi}i^l e^{i\mathbf{k}\cdot\mathbf{r}_T(t)}Y_{lm}(\mathbf{\Omega}_T(t)), \tag{1.16}$$

and the corresponding self-correlator

$$\begin{aligned} F^S_{lm;l'm'}(\mathbf{k},t) &\equiv \langle n^{S*}_{lm}(\mathbf{k},t)n^S_{l'm'}(\mathbf{k},0)\rangle\\ &= 4\pi i^{l-l'}\left\langle e^{i\mathbf{k}\cdot[\mathbf{r}_T(t)-\mathbf{r}_T(0)]}Y_{lm}(\mathbf{\Omega}_T(t))Y_{l'm'}(\mathbf{\Omega}_T(0))\right\rangle, \qquad (1.17) \end{aligned}$$

where $\mathbf{r}_T(t)$ denotes the position of the center of mass of any of the particles at a given time, and $\mathbf{\Omega}_T(t)$ describes its orientation.

It is useful to introduce now the translational (T) and rotational (R) current densities, $\mathbf{j}^T_{lm}(\mathbf{k},t)$ and $\mathbf{j}^R_{lm}(\mathbf{k},t)$, respectively, as

$$\mathbf{j}^\alpha_{lm}(\mathbf{k},t) \equiv \sqrt{\frac{4\pi}{N}}i^l\sum_{n=1}^{N}\mathbf{v}^\alpha_n(t)e^{i\mathbf{k}\cdot\mathbf{r}_n(t)}Y_{lm}(\mathbf{\Omega}_n(t)), \tag{1.18}$$

where we are employing the convenient notation of reference [7], and thus

$$\mathbf{v}^\alpha_n(t) = \begin{cases}\mathbf{v}_n(t), & \alpha = T,\\ \boldsymbol{\omega}_n(t), & \alpha = R.\end{cases} \tag{1.19}$$

Note that equations (1.14) and (1.18) imply the following continuity equation:

$$\frac{\partial n_{lm}(\mathbf{k},t)}{\partial t} = i\sum_{\alpha} \mathbf{k}_{\alpha} \cdot \mathbf{j}^{\alpha}_{lm}(\mathbf{k},t), \tag{1.20}$$

where $\mathbf{k}_{\alpha}$ is an operator defined in terms of the $\mathbf{k}$-wave vector and the angular momentum operator $\mathbf{L}$ by:

$$\mathbf{k}_{\alpha} = \begin{cases} \mathbf{k}, & \alpha = T, \\ \mathbf{L}, & \alpha = R, \end{cases} \tag{1.21}$$

and whose action over a function f_{lm} is given by the following equations:

$$k^{\nu}_{\alpha} f_{lm}(\mathbf{k},t) = \begin{cases} k^{\nu} f_{lm}(\mathbf{k},t), & \alpha = T, \\ \sum_{m'=-l}^{l} L^{\nu}_{l,mm'} f_{lm'}(\mathbf{k},t), & \alpha = R, \end{cases} \tag{1.22}$$

where $\nu = x,y,z$ denotes cartesian components and

$$\begin{gathered} L^{x}_{l,mm'} \pm L^{y}_{l,mm} \equiv L^{\pm}_{l,mm'} = \sqrt{l(l+1) - m(m\pm 1)}\,\delta_{m',m\pm 1}, \\ L^{z}_{l,mm'} = m\delta_{m'm}. \end{gathered} \tag{1.23}$$

There are important symmetry properties for these correlators due to time translations, time reversal and/or rotations that we will not discuss here. Most of these properties are summarized, for example, in ref. [7], and are extensively discussed in [57]. Also, in the particular case of linear particles, it is usually more convenient to represent these correlators (as well as other properties) in the so-called *k-frame* [55, 57], i.e., we choose a reference frame such that $\mathbf{k} \equiv (0,0,k)$. Under such conditions, it can be show that $F_{lm,l'm'}(\mathbf{k},t)$ must be diagonal in m and m', that is

$$F_{lm;l'm'}(\mathbf{k},t) \rightarrow F_{ll';m}(k,t)\delta_{mm'} \tag{1.24}$$

Chapter 2

SCGLE theory for the dynamics of Brownian liquids of non-spherically interacting particles

> *Glasses are disordered materials that lack the periodicity of crystals but behave mechanically like solids. The most common way of making a glass is by cooling a viscous liquid fast enough to avoid crystallization. Although this route to the vitreous state −supercooling− has been known for millennia, the molecular processes by which liquids acquire amorphous rigidity upon cooling are not fully understood.*
>
> Pablo G. Debenedetti and Frank H. Stillinger

In this chapter we present the main contribution of this work, namely, the formal derivation of the SCGLE theory for colloidal system composed of linear interacting particles. We will show that, starting from a proper set of dynamical variables, the extension of the SCGLE approach can be done following a similar procedure of the the previous spherical case. For the benefit of the reader, the main feature of the spherical version of the SCGLE is considered in appendix B. Thus, using the GLE formalism and the concept of contraction of the description [32, 33] we will obtain exact memory function equations for the generalized dynamic correlators $F_{lm;lm}(k,t)$ and $F^{S}_{lm;lm}(k,t)$ in terms of the corresponding static correlation functions $S_{lm;lm}(k)$. These exact equations require the independent determination of the corresponding self and collective memory functions. To obtain a closed self-consistent system of equations for the dynamic properties involved we propose simple Vineyard-like approximate closure relations similar to the spherical case. In the long-time asymptotic limit, these equations leads to the so-called bifurcation equations, whose solutions can be written, extending the spherical case, in terms of one translational and one orientational scalar dynamic order parameters, γ_T and γ_R, which characterize the possible dynamical arrest transitions of a given system. The spherical limit of the SCGLE formalism is thus recovered for the particular case $l = m = 0$. The main features, possible applications and limitations of the present theory are discussed.

2.1 State of the Art

The most basic and fundamental information describing the thermodynamic properties of a given material is contained in its equilibrium phase diagram [59, 60]. The description of the gas-liquid transition using the *so-called* van der Waals state equation is one of the oldest and paradigmatic attempts to contruct such phase diagram starting from molecular arguments [61]. Furthermore, the microscopical description of the second law of thermodynamics [62] is perhaps the greatest achievement of statistical mechanics. Given an interaction potential, statistical thermodynamics allows to obtain the corresponding phase diagram by identifying each equilibrium state using the *so-called* minimum energy principle. During nearly a hundred years, this fundamental principle has been the basis for the study of the equilibrium properties as well as phase transitions of many relevant systems [63, 64].

Statistical thermodynamics is thus appropiate to study systems in equilibrium, leaving out of reach the characterization of the properties of all those systems which are not in thermodynamic equilibrium. Such is the case of glasses, gels, foams, spin glasses and many other materials with which we have daily contact and which possess a common feature, namely, a noticeable growth of their corresponding relaxation times, exhibiting thus their inability to reach equilibrium within experimental times. Understanding the origin of this behavior falls outside the realm of classical and statistical thermodynamics. In fact, as indicated on the introduction of this work, a major challenge for statistical physics is to develop a fundamental theory that predicts the properties of these materials in terms not only of the intermolecular forces and applied external fields, but also in terms of the protocol of preparation of the material [65, 66].

As we have already mentioned previously, both, the MCT and SCGLE formalisms, are first principles theoretical approaches leading to quantitative predictions for the dynamic properties of liquids near their dynamic arrest transition. Both formalisms allows to describe the collective and self dynamic properties of a given system and are able to predict the existence of dynamical arrest transitions, given the equilibrium structural properties. In systems involving non-spherical interactions, the degree of complexity increases given the emerging coupling between orientational degrees of freedom (ODF) and translational degrees of freedom (TDF). The main added complication is the fact that the phase-space probability density for particles with ODF is not immediately factorisable into kinetic and configurational parts. This leads to a variety of different dynamic phenomena and a richer dynamical arrest scenario (see for instance [3, 4, 5, 6]). The non spherical version of the MCT formalism has been carried out previously [7, 20, 21, 22, 23, 24, 25, 26] and it has been applied to several systems composed by linear particles. In contrast, the SCGLE approach has been limited so far to the study of systems with spherical symmetry. The development of the corresponding equilibrium non spherical SCGLE theory and its application to describe dynamical properties as well as dynamical arrested states in model systems is the main aim of this work.

Thus, in this chapter we will formaly derive the extension of the SCGLE theory to non spherical systems and show that a dynamical arrest theory can be derived, extending the previous spherical case. As a result, we will construct a practical tool able to sistematically obtain arrested phases diagrams and, in general, to predict the relevant dynamic properties of a given system using as an input the corresponding equilibrium structural properties. To simplify the discussion as much as possible, we will restrict here to the case of monodisperse systems conformed by linear molecules, however, the extension of our derivations to consider mixtures and/or particles of arbitrarily shape is straightforward. In what follows we will show that the generalization of the SCGLE approach for non-spherical systems whose configurational space state is extended from $\mathbf{r}^N$ to $(\mathbf{r}^N, \mathbf{\Omega}^N)$ may be proposed following a similar procedure of the spherical case. In the process we will arrive to a new set of coupled equations for generalized dynamical correlators and we will derive a simplified dynamical arrest theory able to describe the loose of ergodicity in both, translational and orientational degrees of freedom. The mathematical form of the equations for the corresponding nonergodicity parameters results very similar that of the SCGLE dynamical arrest theory for spherical colloidal mixtures [19].

2.2 Generalized Langevin Equation Formalism

In this section, we introduce our theoretical approach for the description of the dynamics of nonspherical colloids. Our procedure will lead us to exact equations for the time evolution of the spherical harmonic projections of the self- and collective intermediate scattering functions defined in eqs. (1.15) and (1.17) in terms of the corresponding unknown memory functions and of the static properties. These exact expressions must be complemented with a number of approximations, leading to a closed system of equations that has to be solved self-consistently.

The basis of this approach are thus the general mathematical conditions that the dynamical variable $\delta n(\mathbf{r},\mathbf{\Omega};t)$, defined in eq. (1.11), must satisfy. These general conditions are stated by the theorem of stationarity [32], according to which, the most general linear stochastic differential equation that describes a (multi-variable) stationary stochastic process, denoted by the abstract vector $\mathbf{a}(t) = [a_1(t), a_2(t)..., a_\nu(t)]$, must have the following structure

$$\frac{d\mathbf{a}(t)}{dt} = -\omega\chi^{-1}\mathbf{a}(t) - \int_0^t dt L(t-t')\chi^{-1}\mathbf{a}(t') + \mathbf{f}(t), \tag{2.1}$$

where χ is the matrix of static correlations, $\chi_{ij} \equiv \langle a_i(0)a_j^*(0)\rangle$, ω is an anti-Hermitian matrix $[\omega_{ij} = -\omega_{ji}^*]$ and the memory matrix $L(t)$ is determined by the fluctuation-dissipation relation $L_{ij}(t) = \langle f_i(t)f_j(t)\rangle$, where $f_i(t)$ is the ith-component of the vector of random *forces* $\mathbf{f}(t)$.

The application of this general formalism starts with the concrete identification of the variables $a_1(t), a_2(t)..., a_\nu(t)$ that describe the state of the system. The selection of these variables depends of the actual physical system and process we wish to describe, and of the specific questions we want to answer. For example, to derive a time-evolution equation for the dynamical variable $\delta n(\mathbf{r},\mathbf{\Omega};t)$ we must include this variable as one of the components of the state vector $\mathbf{a}(t) = [a_1(t), a_2(t)..., a_\nu(t)]$. Thus, for $a_1(t)$ we may choose either $a_1(t) = \delta n(\mathbf{r},\mathbf{\Omega};t)$ or $a_1(t) = \delta n_{lm}(\mathbf{k},t)$. The rest of the variables, $a_2(t)..., a_\nu(t)$, are chosen according to the degree of detail of the description from which we wish to derive the desired time-evolution equation for $\delta n(\mathbf{r},\mathbf{\Omega};t)$ or for its components $\delta n_{lm}(\mathbf{k},t)$. Our choice for the present derivation is defined by the stochastic vector

$$\mathbf{a}(t) = [\delta n_{lm}(\mathbf{k},t), \delta \underline{j}^{T}_{lm}(\mathbf{k},t), \delta \underline{j}^{R}_{lm}(\mathbf{k},t)]^{\mathbf{t}}, \tag{2.2}$$

where the super index $\mathbf{t}$ indicates transpose, and where we have defined the normalized fluctuations on the *longitudinal* current densities as

$$\delta \underline{j}^{\alpha}_{lm}(\mathbf{k},t) \equiv \frac{1}{k_l^{\alpha}(k)}\mathbf{k}_{\alpha}\cdot\mathbf{j}^{\alpha}_{lm}(\mathbf{k},t), \tag{2.3}$$

with

$$k_l^{\alpha}(k) = \begin{cases} k, & \alpha = T \\ \sqrt{l(l+1)}, & \alpha = R. \end{cases} \tag{2.4}$$

Notice that the choice of the stochastic variables in $\mathbf{a}(t)$ implies that the static correlation matrix χ of Eq. (2.1) possesses the following structure (see Eq. (40) of Ref. [7]),

$$\chi = \begin{bmatrix} S_{lm;lm}(\mathbf{k}) & 0 & 0 \\ 0 & (k_BT/m) & 0 \\ 0 & 0 & (k_BT/I) \end{bmatrix}. \tag{2.5}$$

The hermiticity of $L(t)$ and the anti-hermeticity of ω, along with the time-reversal symmetry properties of the stochastic components of the vector $\mathbf{a}(t)$, define selection rules [32] that determine the vanishing of some of the elements of ω and $L(t)$. This leads immediately to [35]

$$\omega = \begin{bmatrix} 0 & \omega_{nT} & \omega_{nR} \\ -\omega^*_{nT} & 0 & 0 \\ -\omega^*_{nR} & 0 & 0 \end{bmatrix}, \tag{2.6}$$

and

$$L(t) = \begin{bmatrix} L_n^{(lm)}(t) & 0 & 0 \\ 0 & L_T^{(lm)}(t) & L_{TR}^{(lm)}(t) \\ 0 & L_{RT}^{(lm)}(t) & L_R^{(lm)}(t) \end{bmatrix}. \tag{2.7}$$

In addition, some of the non-zero elements of the matrices $L(t)$ and ω can be determined as follows. Using Eqs. (2.5)-(2.7) in Eq. (2.1) leads to the time evolution equation of the components of the state vector $\mathbf{a}(t)$. The resulting equation for $\delta n_{lm}(\mathbf{k},t)$, however, must coincide with the continuity equation (1.20), and this determines $\omega_{nT} = -\omega^*_{Tn} = -(k_BT/M)ik$, $\omega_{nR} = -\omega^*_{Rn} = -(k_BT/I)i\sqrt{l(l+1)}$, and $L_n^{(lm)}(t)$=0. As a result, we can rewrite Eq. (2.1) as three time-evolution equations (for $\delta n_{lm}(\mathbf{k},t), \delta \underline{j}^T_{lm}(\mathbf{k},t)$, and $\delta \underline{j}^R_{lm}(\mathbf{k},t)$), namely,

$$\frac{\partial \delta n_{lm}(\mathbf{k},t)}{\partial t} = i[k\delta \underline{j}^T_{lm}(\mathbf{k},t) + \sqrt{l(l+1)}\delta \underline{j}^R_{lm}(\mathbf{k},t)], \tag{2.8}$$

$$\begin{aligned} \frac{\partial \delta \underline{j}^T_{lm}(\mathbf{k},t)}{\partial t} &= -\omega_{Tn} S^{-1}_{lm;lm}(\mathbf{k})\delta n_{lm}(\mathbf{k},t) \\ &- \int_0^t dt' L_T^{(lm)}(t-t')\chi_T^{-1}\delta \underline{j}^T_{lm}(\mathbf{k},t') \\ &- \int_0^t dt' L_{TR}^{(lm)}(t-t')\chi_R^{-1}\delta \underline{j}^R_{lm}(\mathbf{k},t') + \mathbf{f}_T(t), \end{aligned} \tag{2.9}$$

$$\begin{aligned} \frac{\partial \delta \underline{j}^R_{lm}(\mathbf{k},t)}{\partial t} &= -\omega_{Rn} S^{-1}_{lm;lm}(\mathbf{k})\delta n_{lm}(\mathbf{k},t) \\ &- \int_0^t dt' L_R^{(lm)}(t-t')\chi_R^{-1}\delta \underline{j}^R_{lm}(\mathbf{k},t') \\ &- \int_0^t dt' L_{RT}^{(lm)}(t-t')\chi_T^{-1}\delta \underline{j}^T_{lm}(\mathbf{k},t') + \mathbf{f}_R(t), \end{aligned} \tag{2.10}$$

where $\chi_T \equiv k_BT/m$, $\chi_R \equiv k_BT/I$.

The next step in our derivation is to contract the description, *i.e.*, to eliminate $\delta \underline{j}^T_{lm}(\mathbf{k},t)$ and $\delta \underline{j}^R_{lm}(\mathbf{k},t)$ from this set of equations. This can be done by solving Eqs. (2.9) and (2.10) and then substituting the solution in Eq. (2.8), a process referred to as a contraction of the description [32, 33], leading to the desired time-evolution equation for $\delta n_{lm}(\mathbf{k},t)$ alone. This equation, multiplied by the initial value $\delta n_{lm}(\mathbf{k},0)$, becomes an equation for the time correlation function $F_{lm;lm}(\mathbf{k},t) \equiv \langle \delta n^*_{lm}(\mathbf{k},t)\delta n_{lm}(\mathbf{k},0)\rangle$ which, in Laplace space, reads [35]

$$F_{lm;lm}(\mathbf{k},z) = \frac{S_{lm;lm}(\mathbf{k})}{z+\Gamma^{(lm)}(\mathbf{k},z)S^{-1}_{lm;lm}(\mathbf{k})}, \tag{2.11}$$

where

$$\begin{aligned}\Gamma^{(lm)}(\mathbf{k},z) \; = \; & \frac{k^2\chi_T}{z+\chi_T^{-1}L_T^{(lm)}(z)-\dfrac{\chi_T^{-1}\chi_R^{-1}L_{TR}^{(lm)}(z)L_{RT}^{(lm)}(z)}{z+\chi_R^{-1}L_R^{(lm)}(z)}} \\ + \; & \frac{l(l+1)\chi_R}{z+\chi_R^{-1}L_R^{(lm)}(z)-\dfrac{\chi_T^{-1}\chi_R^{-1}L_{TR}^{(lm)}(z)L_{RT}^{(lm)}(z)}{z+\chi_T^{-1}L_T^{(lm)}(z)}} \\ - \; & \frac{k\sqrt{l(l+1)}[L_{TR}^{(lm)}(z)+L_{RT}^{(lm)}(z)]}{[z+\chi_T^{-1}L_T^{(lm)}(z)][z+\chi_R^{-1}L_R^{(lm)}(z)]-\chi_T^{-1}\chi_R^{-1}L_{TR}^{(lm)}(z)L_{RT}^{(lm)}(z)}.\end{aligned} \tag{2.12}$$

Notice that the use of the parenthesis in the super index symbol (lm) of Γ is intended to emphasize the fact that these quantities are not spherical harmonic projections of certain memory functions. Instead, $\Gamma^{(lm)}$ represents the memory function associated to the projection δn_{lm} considered in $\mathbf{a}(t)$.

It is worth stressing that equations (2.11) and (2.12) are exact and general results, whose usefulness only appears when they refer to particular classes of systems and after introducing simplifying approximations. In this regard, from now on let us only consider the particular case of orthotropic particles, *i.e.*, geometric bodies with three pairwise orthogonal planes of symmetry. Spheres, spheroids (ellipsoid of revolution), biaxial (or triaxial) ellipsoids and cylinders belong to this class. Orthotropic particles have no short-time translational-rotational coupling [67], i.e., the translational-rotational subtensors $[\overleftrightarrow{\zeta}^0]_{TR}$ and $[\overleftrightarrow{\zeta}^0]_{RT}$ of the short-time (or “free-diffusion”) friction tensor $\overleftrightarrow{\zeta}^0$ (appearing, for example, in the first term of the right side of the Langevin equation in Eq. (1.3)) vanishes. In addition, let us assume for simplicity that, for orthotropic particles, this translational-rotational decoupling also holds at the level of the corresponding memory functions, so that in a first approximation the memory functions $L_{TR}^{(lm)}(z)$ and $L_{RT}^{(lm)}(z)$ vanish. This clearly simplifies the expression for $\Gamma^{(lm)}(\mathbf{k},z)$ in Eq (2.12).

An additional simplification appears when one considers the overdamped limit of this equation. This limit refers to long times compared with the velocity relaxation times $\tau_T \equiv M/\zeta_0^T$ or $\tau_R \equiv I/\zeta_0^R$, where ζ_0^α are the corresponding orientationally-averaged free diffusion friction coefficients. To introduce these time scales, let us first take the time-derivative of the $\alpha = T$ component of Eq. (2.3) (together with the microscopic expression for $\mathbf{j}^\alpha_{lm}(\mathbf{k},t)$ in Eq. (1.18)). To evaluate $d\mathbf{v}^\alpha_n(t)/dt$ of the right side of the resulting equation, we use now the N-particle Langevin equation, i.e., one equation like Eq. (1.3) for each particle. Approximating the translational-translational diagonal component $[\overleftrightarrow{\zeta^0}]_T$ as $[\overleftrightarrow{\zeta^0}]_T = \zeta^0_T \overleftrightarrow{\mathbf{I}}$, with $\overleftrightarrow{\mathbf{I}}$ being the 3×3 identity tensor, the resulting equation reads

$$\begin{aligned} \frac{\partial \delta j^T_{lm}}{\partial t}(\mathbf{k},t) &= -\frac{\zeta^0_T}{m}\delta j^T_{lm}(\mathbf{k},t) + \sqrt{\frac{4\pi}{N}}\, i^l \sum_{n=1}^{N} \hat{\mathbf{k}} \cdot \mathbf{b}_n(t) e^{i\mathbf{k}\cdot\mathbf{r}_n(t)} Y_{lm}(\mathbf{\Omega}(t)) \\ &+ \sqrt{\frac{4\pi}{N}}\, i^l \sum_{n=1}^{N} \hat{\mathbf{k}} \cdot \mathbf{v}_n(t) \frac{\partial}{\partial t}\{e^{i\mathbf{k}\cdot\mathbf{r}_n(t)} Y_{lm}(\mathbf{\Omega}(t))\}, \end{aligned} \tag{2.13}$$

where $\mathbf{b}(t) = \frac{1}{m}\{\mathbf{f}^0(t) + \mathbf{F}_n(t)\}$. The first two terms in the right-hand side of this equation clearly derive from the first two terms of the $\alpha = T$ *component* of the referred N-particle Langevin equation. They describe the effect of the solvent friction on each colloidal particle due to spatial translations. Although it is not possible to establish a detailed correspondence of the other terms with those of Eq. (2.9) the above results suggests that the memory function $L_T(t)$ could be written as

$$L^{(lm)}_T(\mathbf{k},z) = \frac{\zeta^0_T}{m}\chi_T + \Delta L^{(lm)}_T(\mathbf{k},z). \tag{2.14}$$

An analogous argumentation for the $\alpha = R$ *components* leads to

$$L^{(lm)}_R(\mathbf{k},z) = \frac{\zeta^0_R}{m}\chi_R + \Delta L^{(lm)}_R(\mathbf{k},z). \tag{2.15}$$

Introducing these considerations in Eq. (2.12), the expression for $\Gamma^{(lm)}(\mathbf{k},z)$ simplifies to

$$\Gamma^{(lm)}(\mathbf{k},z) = \frac{k^2 D^0_T}{1 + \frac{z}{z_T} + m^2\beta^2 D^0_T \Delta L^{(lm)}_T} + \frac{l(l+1)D^0_R}{1 + \frac{z}{z_R} + I^2\beta^2 D^0_R \Delta L^{(lm)}_R}, \tag{2.16}$$

where $\beta^{-1} = k_B T$, $D^0_\alpha \equiv k_B T/\zeta^0_\alpha$ being the free particle diffusion coefficients, and with $z_T \equiv \zeta^0_T/m$ and $z_R \equiv \zeta^0_R/I$ being the corresponding Brownian frequencies τ_T^{-1}, τ_R^{-1}. At this point we can take the overdamped limit, defined as $t \gg max[\tau_T, \tau_R]$ (or, alternatively, by $z/z_T \ll 1$ and $z/z_R \ll 1$), which transforms eqs.(2.11) and (2.16) in the following expression for $F_{lm;lm}(\mathbf{k},z)$,

$$F_{lm}(\mathbf{k},z) = \frac{S_{lm}(\mathbf{k})}{z + \frac{k^2 D^0_T S^{-1}_{lm}(\mathbf{k})}{1 + C^{(lm)}_T(\mathbf{k},z)} + \frac{l(l+1)D^0_R S^{-1}_{lm}(\mathbf{k})}{1 + C^{(lm)}_R(\mathbf{k},z)}}, \tag{2.17}$$

with $C^{(lm)}_\alpha(\mathbf{k},z) = m^2_\alpha \beta^2 D^0_\alpha \Delta L^{(lm)}_\alpha(\mathbf{k},z)$, and where for the sake of notation, we have omitted the second lm subindex in the collective dynamic and the static correlators. A similar argumentation for the *self*-components (see Eq. (1.17)) leads to

$$F_{lm}^{(S)}(\mathbf{k},z)=\frac{1}{z+\frac{k^2D_T^0}{1+C_T^{S(lm)}(\mathbf{k},z)}+\frac{l(l+1)D_R^0}{1+C_R^{S(lm)}(\mathbf{k},z)}}. \tag{2.18}$$

Eqs. (2.17) and (2.18) constitutes then the first element of the SCGLE theory for orthotropic-linear molecules. Notice that for $l=0$, these equations clearly reduce to the spherical case in eqs. (B.1) and (B.2).

2.2.1 Self consistent scheme

Given the choice of the stochastic variables in $\mathbf{a}(t)$ (Eq. (2.2)) it is not possible to determine in more detail the structure of the translational and rotational memory functions $C_\alpha^{(lm)}(\mathbf{k},z)$ and $C_\alpha^{S(lm)}(\mathbf{k},z)$ in eqs.(2.17) and (2.18). In the present work we are primarily interested in developing a simplified version of the non-spherical *equilibrium* SCGLE theory which allow us to qualitatively test its predictive ability when applied to simple systems but also that can be easily implemented from a technical point of view. Also, this theory should be such that, in the appropriate limit, reproduce the spherical equations discussed in appendix B. Thus, similar to the spherical case, we expect to introduce again the intuitive notion that collective and *self*-dynamics may be connected at the level of memory functions (see Eq.(B.3)). For that purposes, let us introduce now the following simple first order Vineyard-like approximations

$$C_\alpha^{(lm)}(\mathbf{k},z)=C_\alpha^{S(lm)}(\mathbf{k},z). \tag{2.19}$$

which will be regarded as the second element in our self consistent scheme.

Let us recall that the basic idea behind these Vineyard's approximations is that the collective motion must be indeed some form of superposition of the individual motion of the particles, however the detailed manner in which are realted is not known exactly. This physical expectation, together with the aim of simplify as much as possible our derivations, clearly inspires this proposal. where we are neglecting coupling effects between them. We could stablish these relations at the level of still higher order memory functions, however, from the previous experience in the spherical case (see, for instance, refs. [17, 18]) we would expect that this will only lead to quantitative improvements relevant only at short times. Since the main purpose of the present extension of the SCGLE theory is to study the long-time features of the slow dynamics of glassy systems, we prefer to leave this topic out of the scope of the present work.

At this stage, a model for the *self*-memory functions $C_\alpha^{S(lm)}(\mathbf{k},t)$ must be suggested. By considering the spherical SCGLE theory, eqs.(B.1-B.6), discussed previously as a *reference* case (the particular condition $l=m=0$ in our equations), we choose to connect these self memory functions to those properties describing the individual coupled motion of non-spherical Brownian interacting particles. As discussed in the previous chapter, translational and rotational memory kernels for the tracer diffusion can also be obtained within the EGL formalism [29, 27]. Thus, using eqs. (1.8) and (1.10) we may propose the following factorization approximations

$$C_T^{S(lm)}(\mathbf{k},t)=\Delta\zeta_T^*(t)\lambda_T^{(lm)}(|\mathbf{k}|)\equiv\frac{1}{3}Tr\left[\Delta\overleftrightarrow{\zeta}^*_T(t)\right]\lambda_T^{(lm)}(|\mathbf{k}|) \tag{2.20}$$

$$C_R^{S(lm)}(\mathbf{k},t)=\Delta\zeta_R^*(t)\lambda_R^{(lm)}(|\mathbf{k}|)\equiv\frac{1}{2}Tr\left[\Delta\overleftrightarrow{\zeta}^*_R(t)\right]\lambda_R^{(lm)}(|\mathbf{k}|) \tag{2.21}$$

where the function $\lambda_T^{(lm)}(|\mathbf{k}|)$ coincides, for $l = m = 0$, with the phenomenological interpolating function introduced in the spherical version of SCGLE (see Eq. (B.5)), namely,

$$\lambda_T^{(00)}(k) = [1 + (k/k_c)^2]^{-1}, \tag{2.22}$$

where $k_c = \alpha \times k_{max}$, with k_{max} denoting the position of the principal peak of $S_{00}(k)$ and where α is an arbitrarily chosen parameter. In general, the SCGLE formalism allows flexibility in the election of α. To fix a specific value of this adjustable parameter, we must use certain criterium. For example, α may be adjusted to fine-tune a comparison between the SCGLE results and simulation data [90]. For concrete applications, in this work we may *calibrate* $\alpha = 1.941$ for reasons that will be explained later in chapter 3.

The diagonal components of the tensors $\Delta \overleftrightarrow{\zeta}^*_\alpha(t)$ are defined as $\left[\Delta \overleftrightarrow{\zeta}^*_\alpha(t)\right]_{ii} \equiv \left[\Delta \overleftrightarrow{\zeta}_\alpha(t)\right]_{ii} / \left[\zeta^0_\alpha\right]_i$, $(i = x, y, z)$. For further specific purposes, we may simplify these approximations by considering $\lambda_R^{(lm)}(|\mathbf{k}|) = 1$. Eqs. (2.20)-(2.21) together with (1.8) constitutes, respectively, the third and fourth elements of the present theory.

Let us finally summarize the main results and approximations that will constitute, thus, our simplified version of the SCGLE for non spherical liquids. For simplicity and technical convenience we will consider hereafter the k-frame reference system [57]. Also, in order to simplify our approach as much as possible we will restrict our equations to the case where all the static and dynamic correlators involved become diagonal in l and m (see, for instance, eqs. (36) and (37) of Ref. [26] and recall that this condition is satisfied exactly in the particular case of the Mean Spherical Approximation (MSA) for the dipolar hard sphere system for $h_{lm;l'm'}(k)$ and $S_{lm;l'm'}(k)$) [68]. First, from eqs. (2.17)-(2.21) we obtain

$$F_{lm}(k,z) = \cfrac{S_{lm}(k)}{z + \cfrac{k^2 D_T^0 S_{lm}^{-1}(k)}{1 + \Delta\zeta_T^*(z)\lambda_T^{(lm)}(k)} + \cfrac{l(l+1) D_R^0 S_{lm}^{-1}(k)}{1 + \Delta\zeta_R^*(z)\lambda_R^{(lm)}(k)}}, \tag{2.23}$$

$$F^S_{lm}(k,z) = \cfrac{1}{z + \cfrac{k^2 D_T^0}{1 + \Delta\zeta_T^*(z)\lambda_T^{(lm)}(k)} + \cfrac{l(l+1) D_R^0}{1 + \Delta\zeta_R^*(z)\lambda_R^{(lm)}(k)}}. \tag{2.24}$$

On the other hand, within well defined approximations discussed in appendix A of reference [36] it is straightforward to obtain a spherical harmonic expansion of the diagonal elements of eqs.(1.8) which leads to

$$\Delta\zeta_T^*(t) = \frac{1}{3}\frac{D_T^0}{(2\pi)^3 n}\int d\mathbf{k} k^2 \sum_l [2l+1]\left[1 - S_{l0}^{-1}(k)\right]^2 F^S_{l0}(k;t) F_{l0}(k;t) \tag{2.25}$$

with $D_T^0 \equiv 2D_\perp^0 + D_\parallel^0$, and

$$\Delta\zeta_R^*(t) = \frac{1}{2}\frac{D_R^0}{(2\pi)^3}\frac{n}{4}\frac{1}{(4\pi)^2}\int d\mathbf{k} \sum_{l,m} [2l+1]\, h_{l0}^2(k)\, [A_{l;0m}]^2 \left[S_{lm}^{-1}(k)\right]^2 F^S_{lm}(k;t) F_{lm}(k;t) \tag{2.26}$$

where, in general, $h_{lm}(k)$ denotes the diagonal k-frame projections of the total correlation function $h(\mathbf{k},\mathbf{\Omega},\mathbf{\Omega}')$, *i.e.*, $h_{lm}(k)$ are defined as $h_{lm}(k) = (4\pi/n)\left[S_{lm}(k)-1\right]$. Also $A_{l;mm'} \equiv \left[C^{+}_{lm}\delta_{m+1,m'} + C^{-}_{lm}\delta_{m-1,m'}\right]$ and $C^{\pm}_{lm} \equiv \sqrt{(l \mp m)(l \pm m+1)}$.

Thus eqs. (2.23)-(2.26) will form a self-consistent and closed set of coupled equation of motion whose solution provide the full time evolution of the dynamic correlators $F_{lm}(k;t)$ and $F^{S}_{lm}(k;t)$ and the memory functions $\Delta\zeta^{*}_{\alpha}(t)$. These equations, which constitutes the main result of the present work, may be numerically solved using standard methods once the projections $S_{lm}(k)$ of the static structure factor are provided.

2.3 Dynamical arrest theory

The complete solution of the self-consistent system of equations discussed above provides the full wave-vector and time dependence of the generalized correlators $F_{lm}(k;t)$ and $F^{S}_{lm}(k;t)$. Thus, a detailed description of the slow dynamics of a given system may be realized by solving Eqs. (2.23)-(2.26) for every relevant value of l and m (in many cases, as in the example described below, these values for l and m are restricted due to symmetry considerations imposed by the system itself). Under some circumstances, however, one may only be interested in identifying and locating the regions of the different ergodic or non ergodic phases involving the translational and orientational degrees of freedom of our system in its state space. For this purpose it is possible to derive from the full SCGLE equations the so-called bifurcation equations which allow us to obtain the dynamical arrest diagram in a similar fashion as in the spherical case. In this section we first derive these bifurcation equations and latter, in the following chapters, we will apply them to particular systems, namely, a dipolar hard sphere fluid and a classical Heisenberg system with positional disorder for which we will also solve the full rotational dynamics to characterize spin glass transitions.

2.3.1 Long-time asymptotic stationary solutions

One important aspect of the SCGLE theory refers to the long-time stationary solutions of equations (2.23)-(2.26). These are referred to as the nonergodicity parameters, defined as

$$f_{lm}(k) \equiv \lim_{t\to\infty} \frac{F_{lm}(k;t)}{S_{lm}(k)}, \tag{2.27}$$

$$f^{S}_{lm}(k) \equiv \lim_{t\to\infty} F^{S}_{lm}(k;t), \tag{2.28}$$

and

$$\Delta\zeta^{*(\infty)}_{\alpha} \equiv \lim_{t\to\infty} \Delta\zeta^{*}_{\alpha}(t), \tag{2.29}$$

with $\alpha = T$ (translational) and R (rotational). The simplest manner to determine these asymptotic solutions is to take the long-time limit of Eqs. (2.23)-(2.26), leading to a system of coupled equations for the nonergodicity parameters $f_{lm}(k)$, $f^{S}_{lm}(k)$, and $\Delta\zeta^{*(\infty)}_{\alpha}$.

It is not difficult to show that the resulting equations (referred to as bifurcation equations in the context of MCT) can be written as

$$f_{lm}(k) = \frac{\left[S_{lm}(k)\right]\lambda^{(lm)}_{T}(k)\lambda^{(lm)}_{R}(k)}{S_{lm}(k)\lambda^{(lm)}_{T}(k)\lambda^{(lm)}_{R}(k) + k^{2}\gamma_{T}\lambda^{(lm)}_{R}(k) + l(l+1)\gamma_{R}\lambda^{(lm)}_{T}(k)} \tag{2.30}$$

and

$$f^S_{lm}(k) = \frac{\lambda_T^{(lm)}(k)\lambda_R^{(lm)}(k)}{\lambda_T^{(lm)}(k)\lambda_R^{(lm)}(k) + k^2\gamma_T\lambda_R^{(lm)}(k) + l(l+1)\gamma_R\lambda_T^{(lm)}(k)}, \tag{2.31}$$

with the dynamic order parameters γ_T and γ_R, defined as

$$\gamma_\alpha \equiv \frac{D^0_\alpha}{\Delta\zeta^{*(\infty)}_\alpha}, \tag{2.32}$$

given by

$$\frac{1}{\gamma_T} = \frac{1}{6\pi^2 n}\int_0^\infty dk\, k^4 \sum_l [2l+1]\left[1 - S^{-1}_{l0}(k)\right]^2 S_{l0}(k) f^S_{l0}(k) f_{l0}(k), \tag{2.33}$$

and

$$\frac{1}{\gamma_R} = \frac{1}{16\pi^2 n}\int_0^\infty dk k^2 \sum_{lm} [2l+1][S_{l0}(k) - 1]^2 S^{-1}_{lm}(k) f^S_{lm}(k) f_{lm}(k) A^2_{l;0m}. \tag{2.34}$$

Fully ergodic states are described by the condition that the nonergodicity parameters (i.e., $f_{lm}(k)$, $f^S_{lm}(k)$, and $\Delta\zeta^{*(\infty)}_\alpha$) are all zero, and hence, the dynamic order parameters γ_T and γ_R are both infinite. Any other possible solution of these bifurcation equations indicate total or partial loss of ergodicity. Thus, γ_T and γ_R finite indicate full dynamical arrest whereas γ_T finite and $\gamma_R = \infty$ corresponds to the mixed state in which the translational degrees of freedom are dynamically arrested but not the orientational ones. Notice, however, that according to Eqs. (2.30)-(2.34), the opposite mixed state, in which the orientational degrees of freedom are dynamically arrested but not the translational ones ($\gamma_T = \infty$ and γ_R finite), is not a mathematically allowed possibility. To see this, let us consider first the state defined by the equations γ_T finite and $\gamma_R = \infty$. From eqs. (2.30)-(2.34), we observe that γ_T (which explicitly depends on γ_R) may be finite for $\gamma_R = \infty$ due to the contribution of the $l = 0 = m$ summand in the right hand side of eq. (2.33) which contains products of the form $l(l+1)\gamma_R$ on the denominator. On the other hand, the opposite state demands $\gamma_T = \infty$ which now, by virtue of eq. (2.34), automatically implies $\gamma_R = \infty$. Nevertheless, it is worth to stress that this mathematical restriction might be the result of all the approximations and assumptions performed to arrive to these bifurcation equations and therefore, this feature should not be considered as a general result applicable to any arbitrary system.

The application of this set of equations for a given system -*i.e.*, for a given pair potential- requires the determination of the the k-frame projections $S_{lm}(k)$ of the static structure factor at every point in state space. This is the only external input needed to solve Eqs. (2.33) and (2.34) for γ_T and γ_R simultaneously using, for example, iterative methods. Then, analyzing the resulting numerical values of these coupled parameters, one can determine the dynamical arrest diagram of the system, i.e., one can identify the regions of fully ergodic, fully arrested, and possible mixed states, and the different transition lines which separates these regions.

Chapter 3

Applications I: The Dipolar Hard Sphere Fluid

In this chapter we apply the dynamical arrest theory derived from the non spherical SCGLE formalism in order to determine the arrested phases diagram of a model system, namely, a dipolar hard sphere (DHS) fluid . As discussed in the previous chapter, to solve the bifurcation equations for the dynamic order parameters γ_T and γ_R, we need to determine previously the spherical harmonics projections, $S_{lm}(k)$, of the static structure factor of the system. For this, we will rely on the mean spherical approximation (MSA) for the DHS fluid [68] and the Ornstein-Zernike integral equation formalism extended to systems with orientational degrees of freedom [69, 70]. For the benefit of the reader, the main details in the determination of the non-zero projections, $S_{00}(k), S_{10}(k)$ and $S_{11}(k)$ are summarized in appendix C. For completeness, we also determine the behavior of the ergodicity parameters, $f_{lm}(k)$, in the vicinity of the glass transition lines and show how our theory is able to predict dynamically arrested states in a similar fashion of the MCT formalism. From the comparison of the results of both theories we contrast the main diferences as well as the relevant similarities between these two approaches. As an additional bonus, however, the behavior of the localization length along the different transition line is annalized and discussed in order to describe the different glass transitions occuring in the system.

3.1 The Dipolar Hard Sphere Fluid

The description of the structural and dynamical properties of homogeneous molecular fluids is of paramount importance in the physics of complex fluids, specially in the context of soft matter and disordered systems [72, 73, 74]. As discussed in the first Chapter of this thesis, the corresponding particle densities, distribution functions and relevant dynamic properties can be developed along lines similar to those followed in the atomic case [55, 57]. As we have mentioned previously, there exist an emerging complexity caused by the inclusion of the orientational degrees of freedom, and this entails fascinating dynamic phenomena not observed in the spherical case, for example, the occurence of exotic mixed dynamically arrested (glassy) states [3, 7, 5, 4]. Within a wide range of systems with orientational degrees of freedom, the dipolar hard sphere fluid (DHS) emerges as one of the most representative reference models with anisotropic interactions which has been subject of many studies and characterizations ranging from its structural [68, 69, 70, 72, 73, 74] to their dynamical properties [7, 71]. Because of the long-range nature of the dipolar interactions, $\sim 1/r^3$, the orientational motion of different molecules are correlated over long distances.

In the context of systems exhibiting dynamically arrested states, the remarkable work of W. Götze and co-workers [20, 21, 22, 23], as well as the work of R. Schilling and co-workers [7, 24, 25, 26], extending and applying the MCT approach to characterize fluids consituted by linear molecules, should be referred as one of the most outstanding theoretical efforts in understanding glass transitions in system with anisotropic interactions. One important prediction of the MCT approach for the DHS fluid is the existence of two different dynamically arrested states for the system [7, 26]: one in which the traslational degrees of freedom freezes whereas the orientational degrees of freedom remain ergodic, and a fully dynamically arrested state in which both degrees of freedom freezes in a random configuration of positions and orientations [see Fig. 5 b) on the Introduction]. As we will show latter in this chapter, the nonspherical SCGLE theory predicts essentially the same physical scenario, providing mutual support to both approaches and their predictions. Before considering this dynamical characterization, however, let us recall the main details involved in the determination of the static structural properties of the DHS system, which are needed in our dynamical arrest theory to sketch the corresponding arrested phases diagram.

3.2 Static structure factor

Let us consider a model system consisting of N-identical hard spheres with diameter d and dipolar momentum $\boldsymbol{\mu}_n$, where $|\boldsymbol{\mu}_n| = \mu$ for all n. Besides the hardcore interaction, the *pairwise* potential also includes a dipolar term given by

$$\begin{aligned} U_{dip}(\mathbf{r}^N, \boldsymbol{\Omega}^N) = \mu^2 \sum_{n \neq n'} |\mathbf{r}_n - \mathbf{r}_{n'}|^{-5}[(\mathbf{r}_n - \mathbf{r}_{n'})^2(\mathbf{e}_n \cdot \mathbf{e}_{n'}) \\ -3((\mathbf{r}_n - \mathbf{r}_{n'}) \cdot \mathbf{e}_n)((\mathbf{r}_n - \mathbf{r}_{n'}) \cdot \mathbf{e}_{n'})], \end{aligned} \tag{3.1}$$

where the unit vector $\mathbf{e}_n \equiv \boldsymbol{\mu}_n/\mu$ pointing in the direction of the dipole $\boldsymbol{\mu}_n$ describes the orientation of the nth particle, also denoted previously as $\boldsymbol{\Omega}_n$.

For this system, approximated analytical results for the pair direct correlation function $c(\mathbf{r}, \boldsymbol{\mu}, \boldsymbol{\mu}')$ exist. As showed by M. S. Wertheim [68], within the MSA approximation, which consist in approximate $c(\mathbf{r}, \boldsymbol{\mu}, \boldsymbol{\mu}')$ by:

$$c(\mathbf{r}, \boldsymbol{\mu}, \boldsymbol{\mu}') = -\beta U(\mathbf{r}, \boldsymbol{\mu}, \boldsymbol{\mu}'); \quad r = |\mathbf{r}| > d) \tag{3.2}$$

the calculation of $c(\mathbf{r}, \boldsymbol{\mu}, \boldsymbol{\mu}')$ may be *reduced* to the case of simple hard spheres, for which $c(r)$ is known, e.g., in the Percus-Yevick approximation. The main details in the determination of the spherical harmonics projections, $S_{lm}(k)$, of the corresponding static structure factor, $S(\mathbf{k}, \boldsymbol{\mu}, \boldsymbol{\mu}')$, can be found elsewhere, however, we summarize them in appendix C.

The typical behavior of the only non zero projections, $S_{00}(k), S_{10}(k)$ and $S_{11}(k)$, of $S(\mathbf{k}, , \boldsymbol{\mu}, \boldsymbol{\mu}')$ within this approximation is displayed on Figs. 3.1(a), 3.1(b) and 3.1(c). The "*hard sphere*" correlator, $S_{00}(k)$, describes TDF, that is, the center of mass distribution of the system. The coupling between the TDF and ODF is described by the correlator $S_{10}(k)$ which resembles as an "*effective hard sphere*". Finally, the correlator $S_{11}(k)$ describes the long range correlations induced by the dipolar contribution to the potential energy.

3.3 Dynamical arrest diagram

We now illustrate the use of the bifurcation equations derived in Chapter 2 to determine the dynamical arrest diagram of the DHS. The only external input needed to solve Eqs. (2.33) - (2.34) can be obtained using the equations of appendix E of Ref. [7] together with eq. (C.20). Recall we need to solve, simultaneously, Eqs. (2.33) - (2.34) in every point in the state space spaned by the two control parameters of the system,

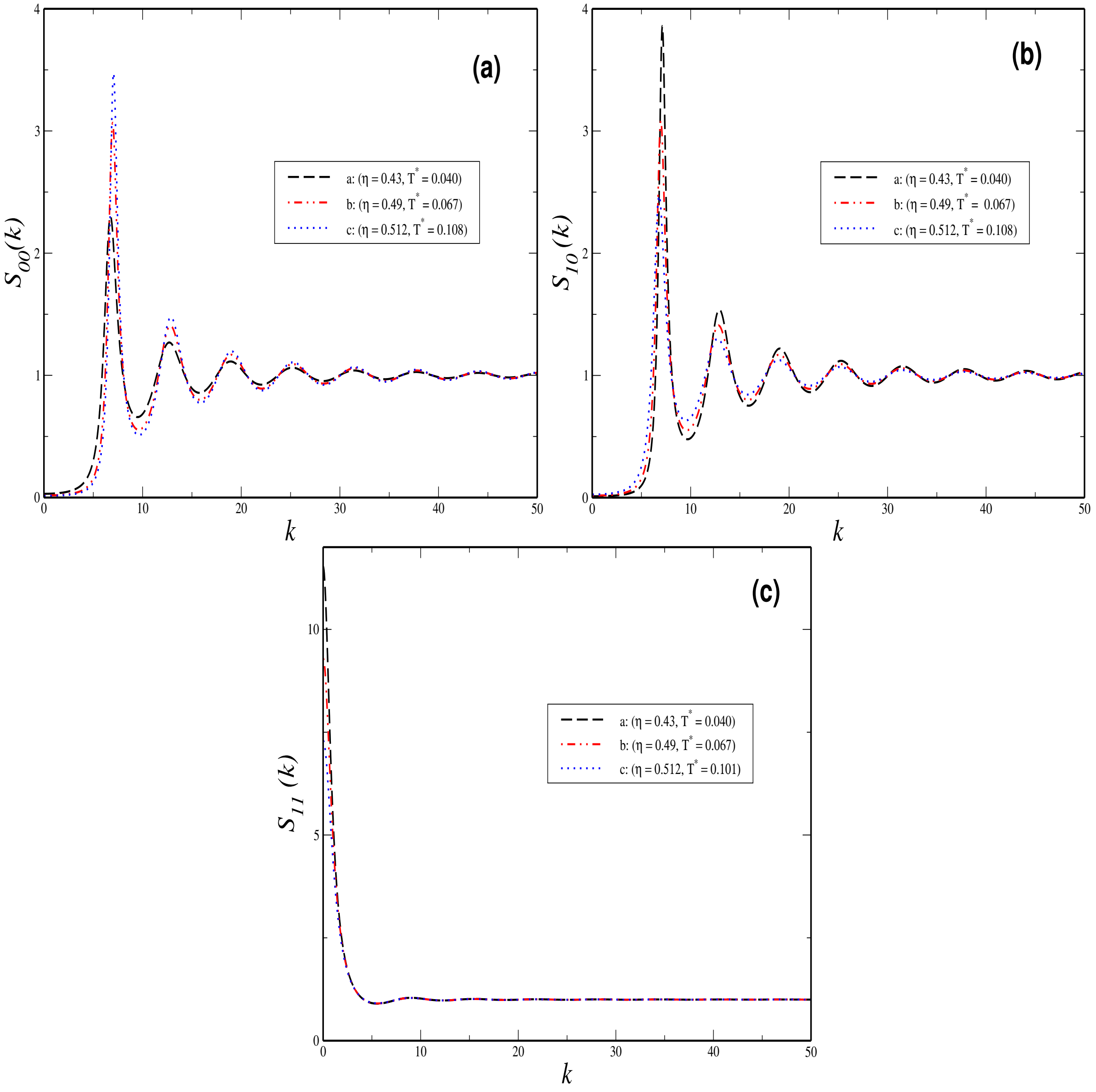

Figure 3.1: Behavior of the spherical harmonics prohections of the static structure factor within the mean spherical approximation (a) $S_{00}(k)$, (b) $S_{10}(k)$ and (c) $S_{11}(k)$, for three different points (T_i^*, η_i), $i = A$ (black dashed lines), B (red dashed-pointed) and C (blue pointed).

(η, T^*) , whose solutions are the values $\gamma_T(\eta, T^*)$ and $\gamma_R(\eta, T^*)$ of the dynamic order parameters at that state point. This determine the expected dynamic state of the system at that particular point. Thus, scanning in this manner the full state space, we may determine the regions of fully ergodic, fully arrested, and dynamically mixed states.

The result of these calculations is summarized in the dynamic arrest diagram of Fig. 3.2, where the state space (η, T^*) is partitioned into three distinct regions. A fully-ergodic fluid region (**I**) is delimited by two different boundaries. Thus, starting from a point in this region, the control parameters may be varied to induce two types of transitions. One of these transitions, occurring at the (blue) vertical dashed line, drives the system into a mixed state (**II**) where the translational degrees of freedom freeze, whereas the orientational degrees of freedom remain ergodic. Notice that this transition occurs at a virtually T^* independent critical volume fraction, $\eta \cong 0.51$, which coincides with the MCT prediction for the glass transition of the hard sphere fluid using the Percus Yevick approximation. Let us recall, however, that we have *calibrated* the parameter α in Eq. (2.22) to the value $\alpha = 1.941$ to match this transition line to the corresponding MCT predicted line in [7], in order to contrast the results of both formalisms for the same system.

The second transition, occuring at the (black) solid line of Fig. 3.2, may be observed starting from the same initial point as before and isochorically lowering the temperature. This process drives the system into a fully non-ergodic phase (**III**), where both, translational and orientational degrees of freedom freeze simultaneously in a glassy state. Finally, another type of transition (*spin-glass* like), occuring at the (red) dashed-pointed line, is observed by starting from a point in the mixed region (**II**), where the orientational degrees of freedom can also be freezed lowering the temperature.

In the inset of this figure we also display a comparison between our results and the corresponding MCT phase diagram for the DHS fluid . From this comparison we may infer that, within our approach, the general physical scenario for the dynamical arrest transitions is essentially the same predicted by MCT in ref. [7]. The localization of the two transition lines enclosing region **III** clearly differs, as well as the position of the corresponding bifurcation point (white square for SCGLE and black square for MCT). In particular, our predicted transition line separating region **I** from region **III** (solid black) is located above the corresponding line predicted by MCT (black dots). In other words, we observe this transition under less structured conditions for the system. In contrast, the line which separates regions **II** and **III** (red dashed-pointed) is predicted to lie below the corresponding MCT line (red diamonds). Also, the bending of the latter is more pronounced than the former.

To complement these results, we may consider the critical nonergodicty parameters, $f_{lm}^{(c)}(k)$, defined as the solution of Eq. (2.30) evaluated at the transition line separating regions **I** and **III** (solid-black). We specifically evaluate these parameters in the three points A,B and C (white circles) in Fig. 3.2. The values of the packing fractions, η_A, η_B and η_C, were chosen to coincide with the three values used in the upper panels in Figs. 2, 3 and 4 of ref. [7], two of which correspond to the black circles in the inset of Fig. 3.2.

The k-dependence of $f_{00}^{(c)}(k), f_{10}^{(c)}(k)$ and $f_{11}^{(c)}(k)$ is displayed, respectively, in Figs. 3.3(a), 3.3(b), and 3.3(c). This dependence is *in phase* with the k dependence of $S_{lm}(k)$. From Fig. 3.3a we observe a similar behavior for $f_{00}^{(c)}(k)$ as already found in the spherical SCGLE theory. The meaning of $f_{00}^{c}(k) \to 1$ when $k \to 0$ has been discussed in ref. [18]. Also, in agreement with the MCT results of ref. [7], a strong m dependence for $f_{1m}^{c}(k)$ is observed. The same qualitative behavior for $f_{10}^{c}(k=0)$ and $f_{11}^{c}(k=0)$ going from point A to C is obtained.

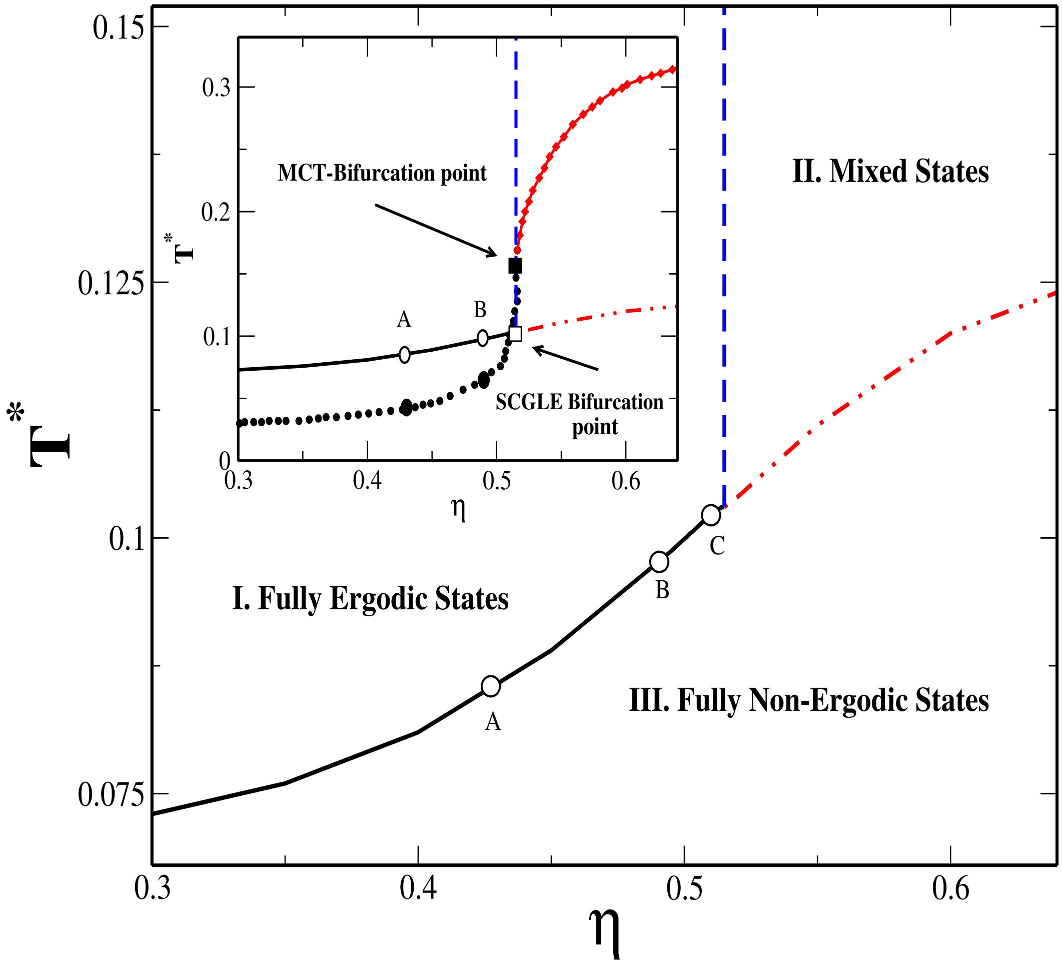

Figure 3.2: Phase diagram for the liquid and glassy states of the dipolar hard spheres system. Inset shows a comparison between this diagram and the MCT phase diagram (black circles and red diamonds) in reference. [7]. The corresponding translational arrest lines (dashed vertical blue) match at a volume fraction $\eta \cong 0.51$ *calibrating* the parameter α in Eq. (2.22) to the value $\alpha = 1.941$.

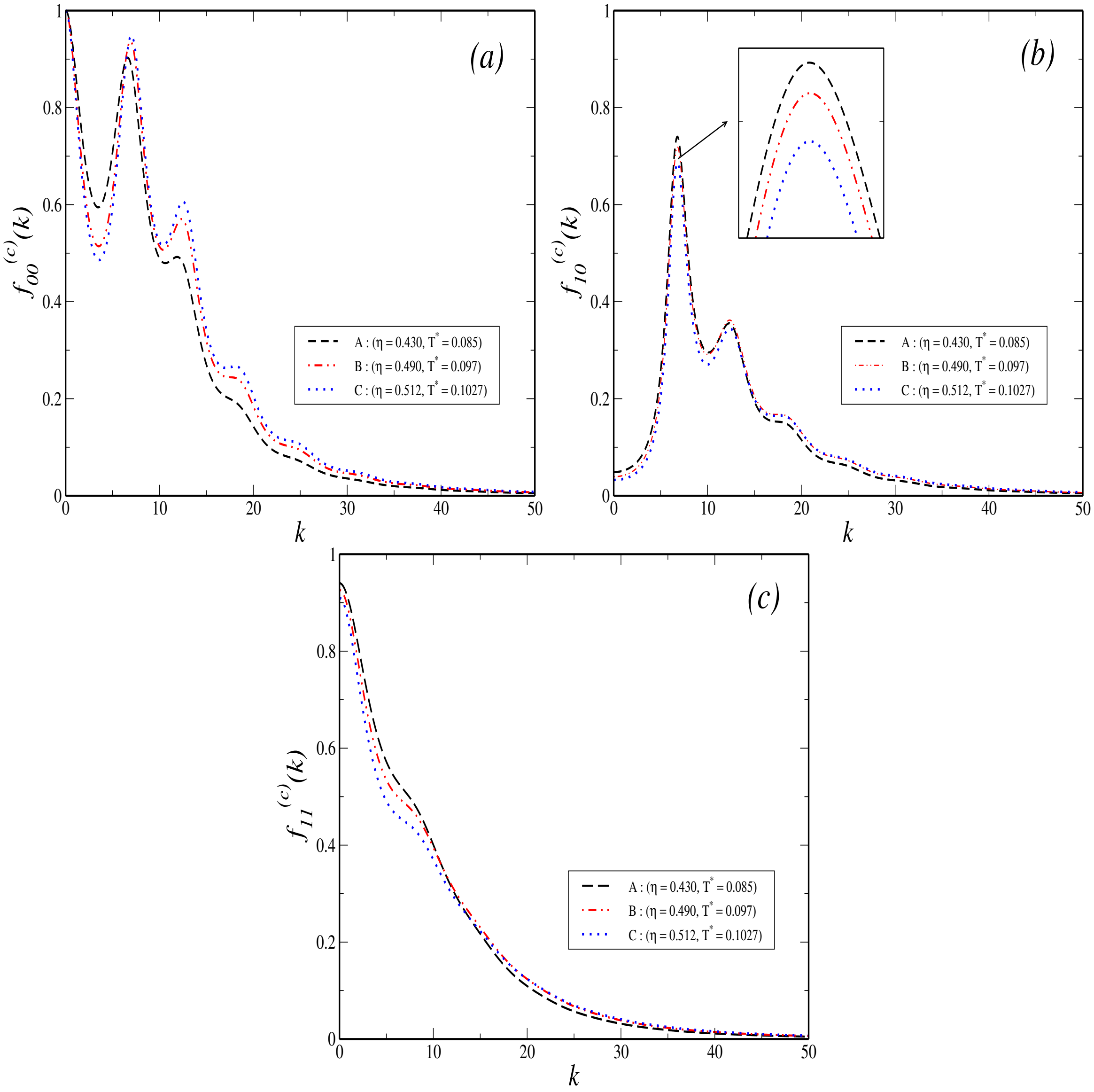

Figure 3.3: (Color online) The critical nonergodicty parameters, (a) $f_{00}^{(c)}(k)$, (b) $f_{10}^{(c)}(k)$ and (c) $f_{11}^{(c)}(k)$, for three different points (T_i^*, η_i), $i = A$ (black dashed lines), B (red dashed-pointed) and C (blue pointed), on the critical line which separate fully ergodic states from fully nonergodic states.

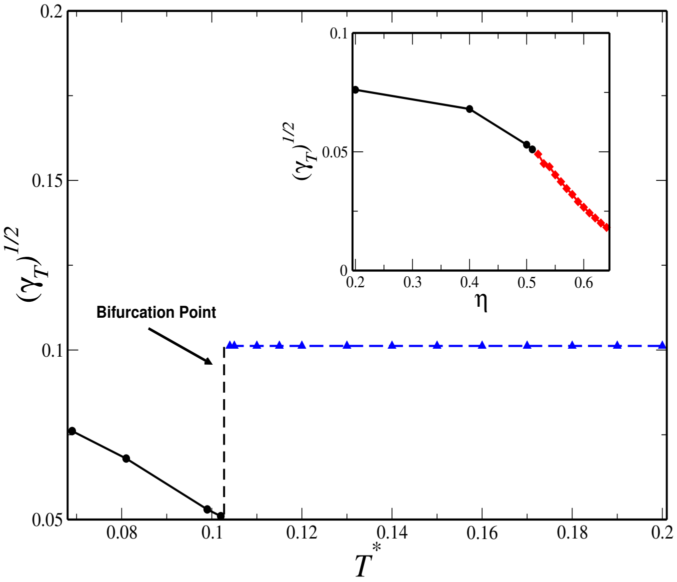

Figure 3.4: (Color online) Localization length, ${\gamma_T}^{1/2}$, along the glass line which separates region **I** from regions **II** (blue triangles) and **III** (black dots). In the inset of this figure, we also display this localization length along the line which separates region **II** from region **III** (red diamonds).

Finally, we also calculate the localization length, $(\gamma_T)^{1/2}$, along the glass line which separate regions **I** and **III** (solid black in Fig. 3.2), up to the bifurcation point and then going through the other two different transition lines. As shown in Fig. 3.4, for $T^* \lesssim 0.103$, and going from point A to point C in Fig. 3.2, $(\gamma_T)^{1/2}$ behaves as a decreasing function of T^*. For this temperature regime, the influence of the dipolar interactions become important, even for a dense fluid, where one observes that both ergodicity parameters, γ_T and γ_R, become finite simultaneously. At the bifurcation, however, the localization length display a discontinuous "*jump*" to a constant value ($\sim 0.1d$) observed at the purely translational arrest line (dashed blue in Fig. 3.2). This feature is characteristic of the hard sphere system and may be interpreted as a dense fluid forming an amporphous solid. Also, in the inset of this figure we show the behavior of $(\gamma_T)^{1/2}$ as a function of η calculated at the two transition lines enclosing the region of totally arrested states **III**.

Thus, both approaches predict the occurence of three different dynamic phases depending on T^* and η and the same mechanisms to trigger the dynamical transitions between each phase. Also, both theories suggest a hierarchy for freezing: the orientational degrees of freedom can never be frozen before the translational degrees of freedom. To decide which of these results are more accurate, we should compare them in the light of experimental or computational simulation data.

Chapter 4

Applications II: Spin Glass transitions in a classical and disordered Heisenberg system.

As a second application of the nonspherical SCGLE formalism, we now discuss the slow dynamics near to the spin glass (SG) transition [75] of a Heisenberg system consisting of a set of linear interacting classical dipoles with random positional disorder. Starting from the dipolar fluid reference model discussed in the last Chapter, we artificially introduce quenched positional disorder in the system to annalize the rotational dynamics near the SG transition in terms of the correlation functions, $F^S_{10}(k,t) = \langle e^{i\mathbf{k}\cdot\mathbf{r}}\cos(\theta(t))\cos(\theta(t=0))\rangle$ and $F^S_{11}(k,t) = \langle e^{i\mathbf{k}\cdot\mathbf{r}}\sin(\theta(t))\sin(\theta(t=0))e^{i\Delta\phi(t)}\rangle$, where $\theta(t)$ and $\phi(t)$ denote, respectively, *the spherical coordinates describing the orientation of any dipole at time t*. Our findings suggest a progresive increase of the *equilibrium* relaxation time as the *effective* temperature, T^*, decreases; and its eventual divergence at a critical temperature, T_c, suggesting the loss of ergodicity in the system. Using the bifurcation equations (2.27), (2.28) and (2.29), the corresponding state space can be partitioned in two regions: a) an ergodic isotropic phase above T_c, where the spatially fixed dipole moments explore all its orientational configuration space; and b) a *spin-glass* phase, below T_c, where the orientational degrees of freedom freezes in a configuration of random orientations. Regardless the simplicity of the model proposed here, our results are in qualitative agreement with recent experiments for disordered magnetic materials, and with more sophisticated simulation results.

4.1 Disordered dipolar materials and Spin Glass transitions.

One of the most intriguing and fundamental problems in condensed matter physics refers to the study of the combined effects of disorder and frustration in magnetic materials, both of which may cause the individual magnetic moments (or spins) to *freeze* into disordered states [75, 76, 77]. Disordered-magnetic systems possess different and richer properties than those of their “*pure*" (ordered) counterparts, and these properties may modify dramatically the thermodynamic behavior of the system [78] (mostly because of the greater difficulty to find *equilibrium* configurations). In addition, within the mean field models of magnetic materials using “Ising-*like*" Hamiltonians, it is a well known fact that disorder and frustration are factors which may suppress the expected ferromagnetic transition, leading to the possibility of the occurrence of exotic dynamically arrested states, such as it occurs in the spin-glass (SG) phase observed in certain magnetic materials [75, 79, 80, 81]. From the experimental point of view, there are well-defined criteria to determine if a given magnetic material behaves as a SG. For instance, the slow decay of the correlation function $C(t) \equiv \langle M(t)M(t=0)\rangle$, where $M(t)$ denotes the time-dependent magnetization of the system, or the emergence of a sharp cusp in the nonlinear susceptibility $\chi"(f,T)$, where T denotes the temperature and f the frequency of an applied external field, may be considered as concrete phenomenology associated to the SG transition [78] [see Fig. 4.1].

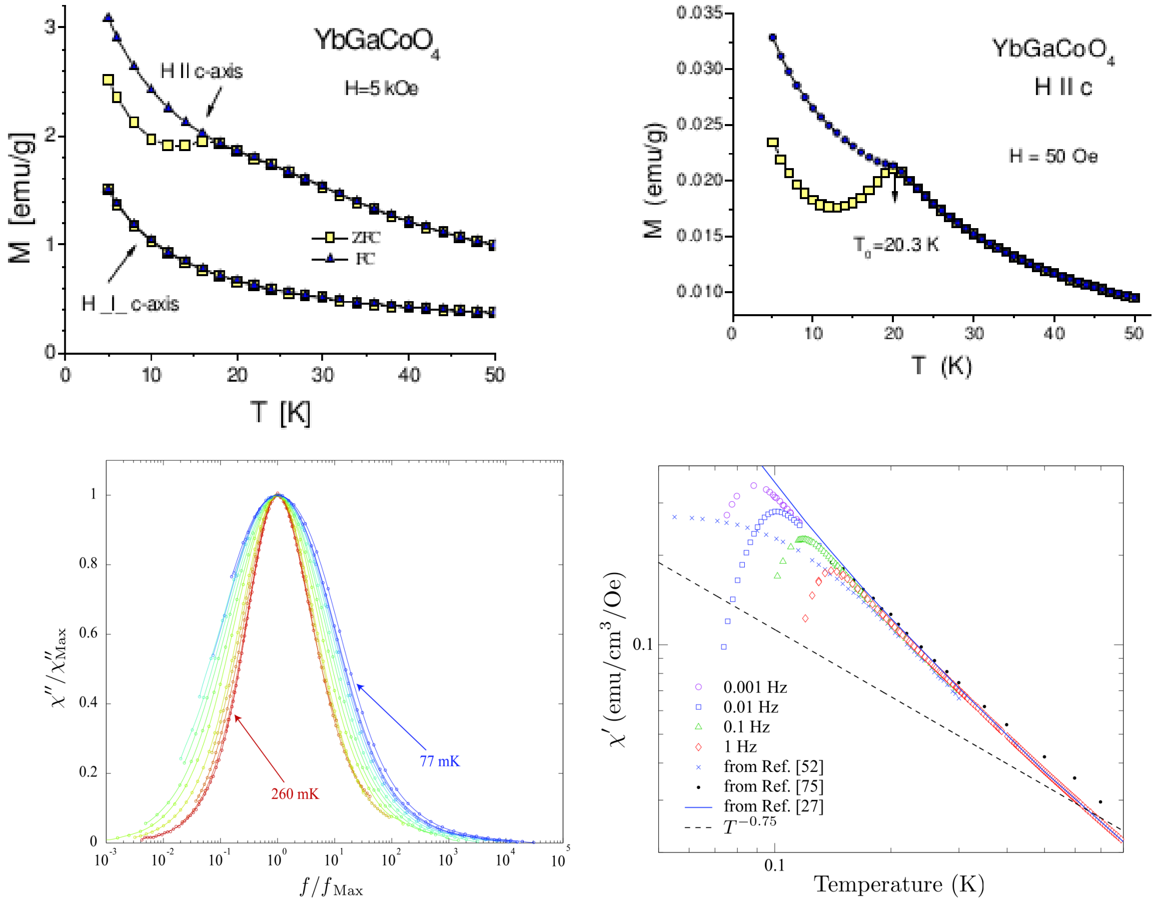

Figure 4.1: Experimental characterization of a Spin Glass material. Upper left panel: temperature dependence of the zero-field cooled (squares) and fiel cooled (triangles) magnetization recorded in $H = 5kOe$ applied along the c axis, and perpendicularly to this axis, to a YbCoGaO$_4$ sobgle crystal. Upper right panel: temperature dependence of the zero field cooled magnetization recorded in $H = 50Oe$ applied along the c axis. Lower left panel: imaginary part of the AC susceptibility, χ'', as a function of frequency, f , normalized to its maximum value χ_{max} at frequency f_max, and for temperatures between 77 mK and 260 mK. Right lower panel: real part of the AC susceptibility, $\chi'(f,T)$, as a function of temperature. All the plots where extracted from *Journal of Physics: Conference Series* **303**, (2011) 012064.

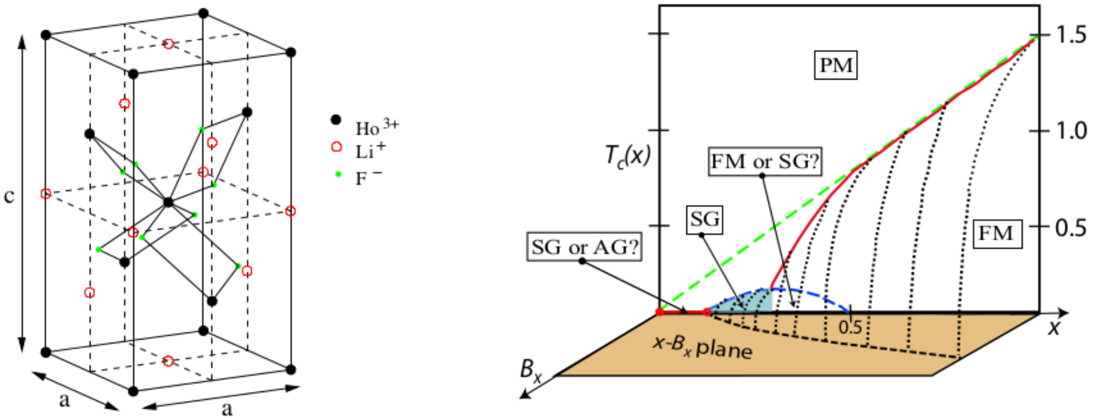

Figure 4.2: The left panel shows the crystalline tetragonal structure of LiHoF$_4$ with lattice spacing $a = 5.175$ and $c = 10.75$. The thin solid lines illustrate the superexchange pathways between magnetic Ho^{+3} ions (black circles) mediated via fluorine F$^-$ ions (green circles). In LiHo$_x$Y$_{1-x}$F$_4$, the magnetic Ho^{+3} ions are substituted randomly by non-magnetic Y^{+3} ions, with the lattice structure remaining the same for all x. The global Ising direction is along the c axis and a magnetic field B_x is applied perpendicular to that axis in transverse field experiments. The right panel shows a schematic temperature $(T)-$dilution $(x)-$transverse field (B_x) phase diagram of LiHo$_x$Y$_{1-x}$F$_4$. At high temperature T or large B_x , the system is in a paramagnetic (PM) phase. For $x = 1$, LiHoF$_4$ is an Ising dipolar ferromagnet (FM) below $T_c = 1.53K$. Upon the substitution of Ho^{+3} by Y^{+3} , the FM phase persists down to $x \sim 0.25$. Upon cooling the diluted FM for $0.25 \lesssim x \lesssim 0.5$, magnetic susceptibility measurements find the development of a “ferroglass” regime (FM or SG?). As x decreases, random frustration builds in and, for $x \lesssim 0.25$, a dipolar Ising spin glass (SG) phase develops (shaded blue region). Whether the dipolar SG exists down to $x = 0^+$ or an exotic quantum disordered “antiglass” (AG) phase occurs at $x > 0$ (red line segment) is not yet resolved and is the subject of much controversy. The application of a transverse field B_x introduces quantum fluctuations causing a reduction of $T_c(x)$ (surface delineated by dotted lines) which, ultimately, drives a zero temperature quantum phase transition at zero temperature (dash-line curve in the x-B_x plane). Both curves where extracted from Ref. [83].

As a particular and relevant example of a magnetic material displaying this phenomena let us mention the rare earth compound LiHo$_x$Y$_{1-x}$F$_4$ [80, 81, 82, 83]. The parent compound LiHoF$_4$, which is one of the best realizations of the Ising model, is a well known ferromagnet with a transition temperature $T_c = 1.53K$ [80, 84] [see the left panel of Fig. 4.2]. The main interactions between the Ho^{+3} ions are magnetostatic dipole-dipole interactions [83]. Random disorder may be induced by randomly replacing magnetic holmium atoms by non-magnetic yttrium atoms, yielding the compound LiHo$_x$Y$_{1-x}$F$_4$. Recently, the slow dynamics of this material has been the subject of experimental characterizations [85] and of computer simulation modelling [81], and evidence of the SG behavior has been found in terms of $\chi^{''}(f)$ [85] as well as the magnetization-correlation function $C(t)$ [see Fig. 4.3].

In this Chapter, a simplified (yet physically sound), model to describe the SG transition in a classical Heisenberg dipolar system with frozen positional disorder is proposed and discussed within the SCGLE approach. After solving our corresponding dynamic equations for the correlators $F^S_{lm}(k,t)$, we contrast our

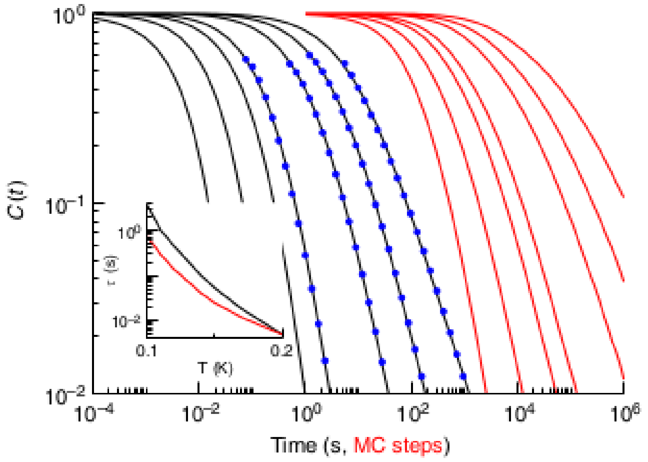

Figure 4.3: Dynamic correlation function, $C(t)$, maesured in experiments (black curves) for the $LiHo_{0.045}Y_{0.955}F_4$ compound compared with Monte Carlo simulations results (red curves), including dipolar, hyperfine and exchange interactions. The temperatures considered in the experiments are $0.10, 0.11, 0.12, 0.14, 0.15, 0.17$ and $0.20K$, from right to left. This plot was extracted from Ref. [80].

results with experimental data to show that the SCGLE theory predicts a similar physical scenario. Although this topic constitutes by itself a relevant motivation in the context of SG phases in magnetic materials, the recent emergence [37, 38, 39] of the *non-equilibrium* generalization of the SCGLE theory (refered to as NE-SCGLE), and its further extension proposed to describe systems with orientational degrees of freedom (ODF) [41], suggest that this work may be extended to describe aging phenomena in non-structural spin glasses [40].

4.2 Slow Dynamics and Spin Glass transitions of a classical and disordered Heisenberg system.

As already mentioned, the physics of the SG transition may be described in terms of both, the temperature and frequency dependence of the ac susceptibility $\chi(t)$ as well as the slow decay of the correlation function $C(t) = \langle M(t)M(0)\rangle$. Within the experimental work for the $LiHo_{0.045}Y_{0.955}F_4$ compound, an increase of the relaxation time of $C(t)$ of the order of three decades has been observed for temperatures varying from 0.2K to 0.12K [85]. Further work on simulations for the system corroborates these results [80, 81]. In what follows we show how our theoretical approach can be employed to describe these observed SG transitions in dipolar disordered systems. Regardless the simplicity of our model or the fact that the SCGLE formalism is, in principle, a theory developed to describe dynamics in brownian liquids (instead of a formal theory of magnetic disordered systems) it is remarkable that we may reproduce, to a large extent, the same physical behavior upon the SG transition.

4.2.1 Slow dynamics

Let us explain how to use the SCGLE equations together with the MSA approximation to describe the rotational dynamics of a classical Heisenberg system with positional disorder. We start by considering the DHS fluid of the previous chapter. From section 3.2 and appendix C, we know that the MSA allows to calculate the static correlators $S_{lm}(k), (l = 0,1, m = -1,0,1)$, which are needed to solve the equations of motion for $F_{lm}(k,t)$ and $F_{lm}^S(k,t)$. In figure 4.4 we display again the behavior of these projections for fixed T^* and for three different concentrations: $\eta \equiv (\pi/6)\rho d^3 = 0.1, 0.01$, and 0.001.

For $\eta \gtrsim 0.01$ the k variations of $S_{00}(k)$ and $S_{10}(k)$ are rather similar to each other and resemble that of a simple liquid with a well pronounced main peak at $k = 2\pi/d$. In contrast, the dipolar correlator $S_{11}(k)$ behaves quite differently. It exhibits only one well defined peak at $k = 0$, and it becomes almost structureless for $k > \Delta k$, with Δk being the peak width at half maximum. Thus, the distribution of centers of mass (or, equivalently, the spatial distribution of the dipoles) is very similar to that of a Hard Sphere (HS) fluid , that is, with no long range order. However, as showed in fig. 4.4, the hard core interactions become neligible in the dilute regime, and the short range order is supressed, *i.e.,* a random distribution of linear dipoles is obtained.

Besides the structural information contained in the projections $S_{lm}(k)$, let us recall that another important input of the SCGLE equations are the short-time self-diffusion coefficients, $D_\alpha^0, (\alpha = T,R)$. These are the diffusion coefficients that describes the translational and rotational motion of the particles between collisions, so that, if we arbitrarily set $D_T^0 = 0$ in Eqs. 2.23, 2.24, 2.25 and 2.26, it means that the particles are assumed not to diffuse in any time scale, i.e., to remain fixed in space. Hence, we may consider the particular application of the SCGLE equations in which $D_R^0 \neq 0$ whereas $D_T^0 = 0$. Notice that this implies that $\gamma_T = 0$, so that, in the assymptotic long time regime, we only need to solve Eq. 2.34 for the dynamic order parameter γ_R to characterize the dynamic state of the system.

Thus, we proceed as follows: first, we obtain the static structure factor within the MSA approximation for the DHS fluid; once the static correlators $S_{00}(k)$, $S_{10}(k)$ and $S_{11}(k)$ are determined, we arbitrarily set the translational difussion coefficient, D_T^0, equal to zero and solve the resulting dynamic equations, which now reads

$$F_{lm}(k,z) = \frac{S_{lm}(k)}{z + \frac{l(l+1)D_R^0 S_{lm}^{-1}(k)}{1+\Delta\zeta_R^*(z)\lambda_R^{(lm)}(k)}}, \tag{4.1}$$

$$F_{lm}^S(k,z) = \frac{1}{z + \frac{l(l+1)D_R^0}{1+\Delta\zeta_R^*(z)\lambda_R^{(lm)}(k)}}. \tag{4.2}$$

and

$$\Delta\zeta_R^*(t) = \frac{1}{2}\frac{D_R^0}{(2\pi)^3}\frac{n}{4}\frac{1}{(4\pi)^2}\int d\mathbf{k}\sum_{l,m}[2l+1]\,h_{l0}^2(k)\,[A_{l;0m}]^2\left[S_{lm}^{-1}(k)\right]^2 F_{lm}^S(k;t)F_{lm}(k;t) \tag{4.3}$$

Hence, within this simplified model, the orientational dynamics of the system is described by the correlators $F_{10}(k;t), F_{10}^S(k;t), F_{11}(k;t)$ and $F_{11}^S(k;t)$, for which we solve eqs. (4.1), (4.2) and (4.3). In Fig. 4.5(a)

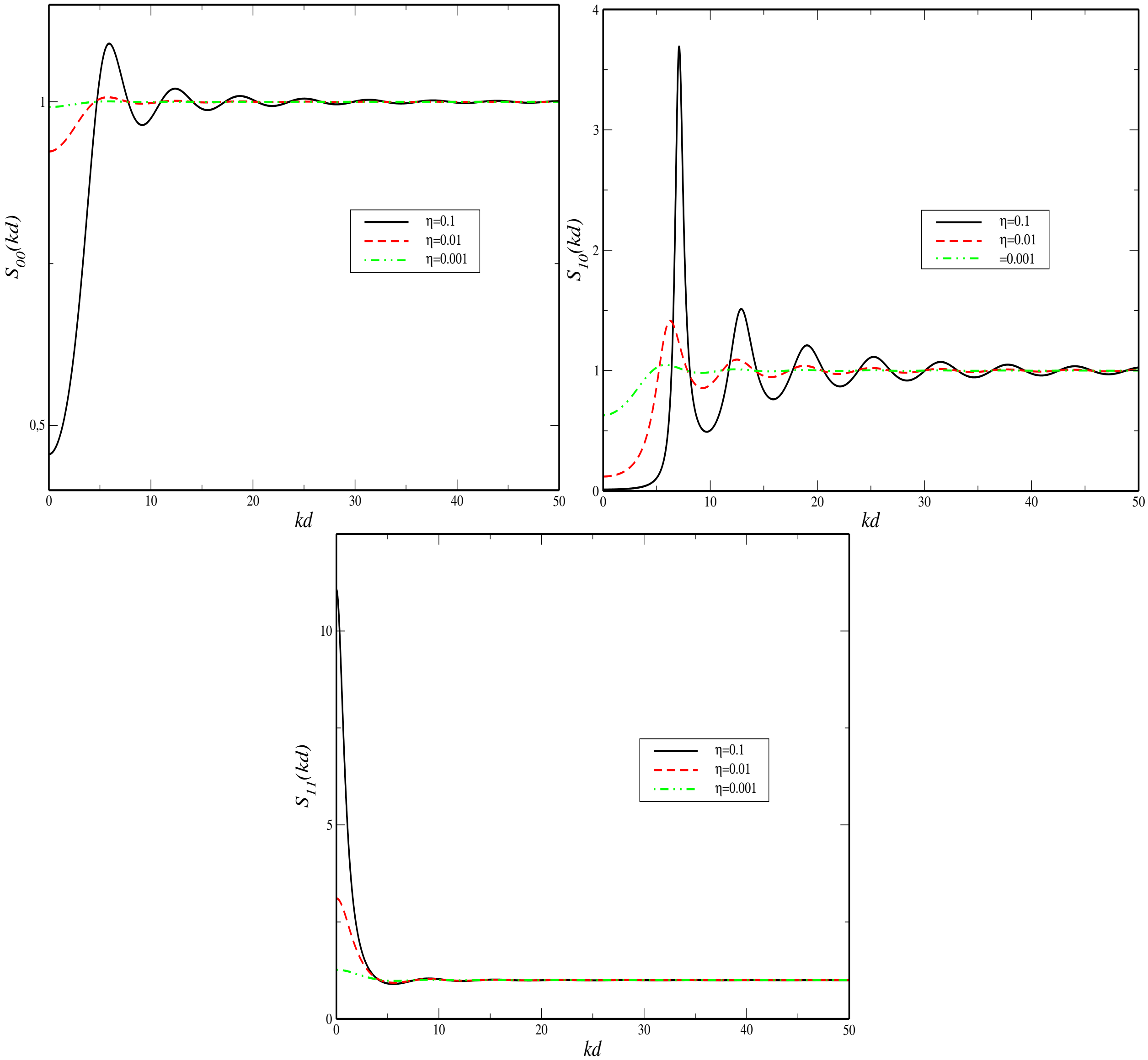

Figure 4.4: Characteristic behavior of the $S_{00}(k), S_{10}(k)$ and $S_{10}(k)$ spherical harmonic projections of the static structure factor, $S(\mathbf{k},\mathbf{\Omega},\mathbf{\Omega'})$, in the MSA approximation for a fixed effective temperature $T^* \equiv \beta\mu^2/d^3 = 0.1$ and packing fractions $\eta = 0.1, 0.01, 0.001$.

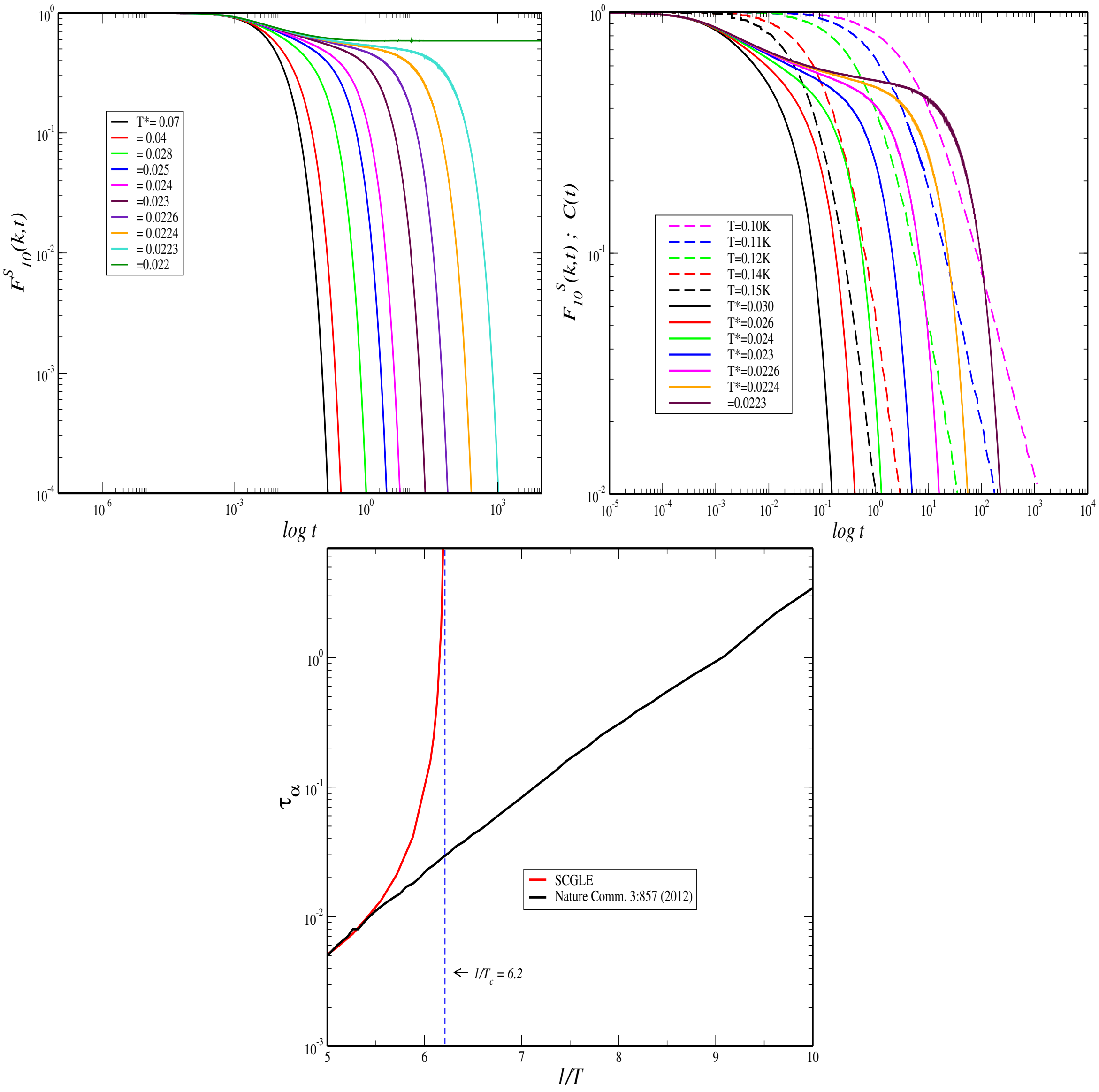

Figure 4.5: a) Time dependence of the self correlator $F^S_{10}(k=1;t)$ predicted by the SCGLE equations for fixed packing fraction $\eta = 0.001$. From left to right, the scaled temperature decreases from $T^* = 0.007$ to $T^*_g = .022$. b) A qualitative comparison of our results with the experimental data of reference [81] showed in Fig. 4.3. c) Relaxation times, τ_α, as function of the inverse temperature; the SCGLE formalism predicts a divergence of τ_α at $T_g = 0.22$

we display representative results for $F^S_{10}(k=0.1;t) \propto \langle e^{i\mathbf{k}\cdot\mathbf{r}} \cos(\theta_{tr}(t))\cos(\theta_{tr}(0))\rangle$ for fixed concentration ($\eta = 0.001$) and for a set of scaled temperatures near the SG transition.

The relaxation time, τ_α, defined by the relation $F^S_{10}(k,\tau_\alpha) = 1/e$, is predicted to increase by almost four decades within a temperature range $T^*_g = 0.0223 < T^* < T^*_1 = 0.03$. Below T^*_g, the correlator $F^S_{10}(k=1,t)$ reaches a *plateau* suggesting the loose of ergodicity in the system, that is, its inability to find a minimal energy configuration. In figures 4.5(b) and 4.5(c), we contrast the results of our simplfied model with the experimental data of reference [81] for the compound $\mathrm{LiHo}_{0.045}\mathrm{Y}_{0.955}\mathrm{F}_4$ in a range of temperatures from $T = 0.1K$ to $T = 0.2K$. We use the rotational difussion coefficient as an “adjustable” time parameter to fit the curves. Clearly, a divergence of the relaxation time is predicted by our theory for $T = T_g$.

This comparison with the experiments exhibit important differences of both, the short and long time regimes of $F^S_{10}(k,t)$ predicted by our theory. For example, a two steps relaxation not observed in the referred work (but characteristic of relaxation procces in brownian simple fluids), is predicted by the SCGLE solutions. From the previous experience in the spherical SCGLE theory, we already know that the short time regime (which is not relevant within our discussion of dynamically arrested states) may not be correctly described due to the simplicity imposed in the Vineyard approximation 2.19. In addition, the differences in the long time relaxation could be due to the hyperfine interactions which are not considered in our simple model. As discussed in [83], in many Ho-based materials there is a strong hyperfine coupling between the electronic ($J = 8$) and nuclear ($I = 7/2$) moments of Ho^{3+} in LiHoF_4. The hyperfine interaction also strongly influences the phase diagram of the dilute compound $\mathrm{LiHo}_x\mathrm{Y}_{1-x}\mathrm{F}_4$. Thus, the hyperfine interaction is extremely important, and should not be omitted in a proper quantitative description of the low-temperature properties of this material. Again, the results presented here, should be considered at the moment only to illustrate the abilty of our approach to predict dynamically arrested states for dipolar magnetic and disordered systems.

4.2.2 Arrested Phases Diagram

Finally, to complement our results, and in order to exhibit in more detail how our theory is also able to describe a more general scenario for dynamically arrested states, let us now make use of the bifurcation equations 2.23, 2.24, and 2.26 to scan state space of the system. From the previous Chapter, we know that considering the numerical value of the ergodicity parameter γ_R in all the state space, we may determine the corresponding arrested phases diagram. In the context of our actual discussion, this exercise allow us to consider also the effect of the excluded volume (hard core interactions) in our description. This incorporates short range correlations due to the referred hard core interactions which affects the critical temperature $T_g = T_g(\eta)$. In Figure 4.6 we display the resulting phase diagram.

The existence of a concentration-dependent critical temperature, $T_g = T_g(\eta)$, at which the SG occurs, is predicted to behave as an increasing function of the concentration. In the dilute limit, this temperature behaves as a *non-linear* funtion of the concentrarion of dipolar hard spheres. For $\eta \gtrsim 0.2$, a linear behavior is predicted. To describe separately the influence of both control parameters on the SG transition, we may fix for example the volume fraction to an arbitrary value and annalize the solutions of the full SCGLE equations for several values of temperature near the SG transition line. This is done for the trajectory described by the points *A,B,C,D,E* in our phase diagram, and the results for $F^S_{11}(k,t)$ are displayed in the left panel of Fig.4.7. The other possibility is to fix T and vary the value of η, for instance, by following the trajectory described by the points *a,b,c,d,e* in the phase diagram. This is done in the right panel of Fig. 4.7.

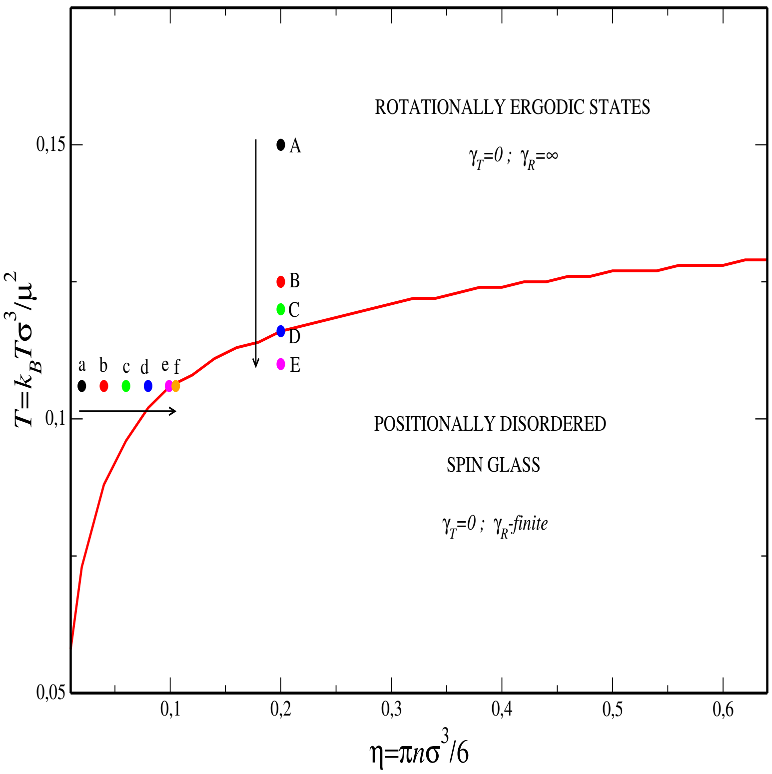

Figure 4.6: Arrested phases diagram of a classical and disordered Heisenberg system.

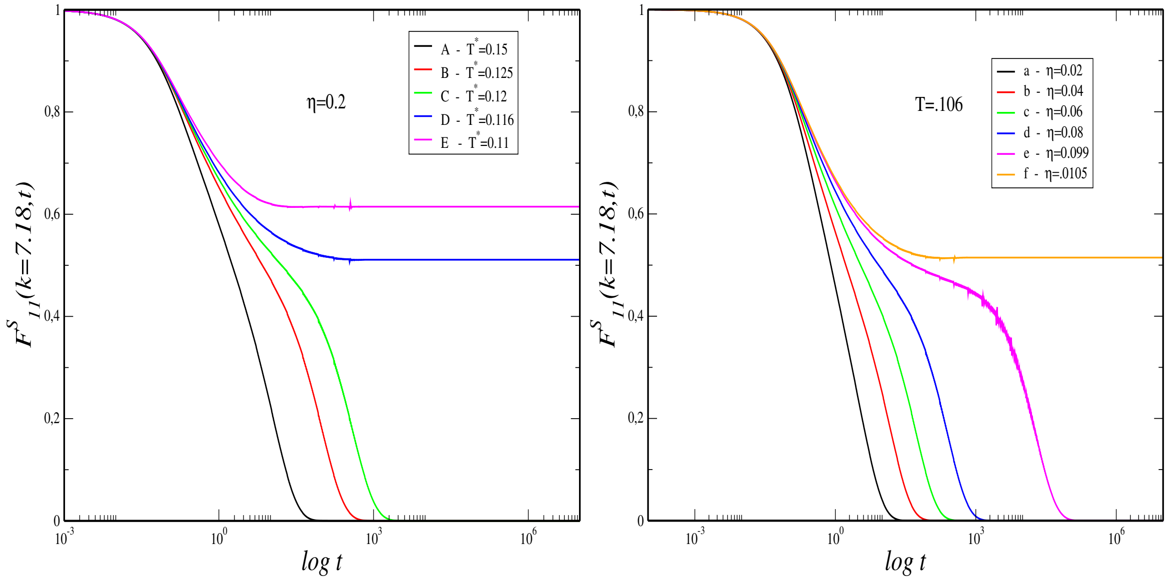

Figure 4.7: Left panel: behavior of the correlator $F^S_{11}(k = 7.18, t)$ for fixed volume fraction, $\eta = 0,2$, and for different temperatues in the vicinity of the SG transition predicted by the ergodicity parameter, γ_R. Right panel: behavior of $F^S_{11}(k = 7.18, t)$ for fixed temprature $T = 0.106$ and several volume fractions in the vicinity of the transition line shown in Fig. 4.6

At the present momment, we are working on the complementary simulation work to corroborate all these results and we expect to report soon all these calculations.

Chapter 5

Conclusions.

In this work we have developed the formal extension of the *equilibrium* SCGLE theory of colloid dynamics to describe the translational and rotational dynamics of Brownian liquids formed by particles that interact through non-spherically symmetric pairwise potentials. The main result of our formal derivations is a set of coupled equations describing the time-evolution of the spherical harmonics projections of the collective and self intermediate scattering functions, $F_{lm;lm}(\mathbf{k},t)$ and $F^{S}_{lm;lm}(\mathbf{k},t)$, whose respective memory functions are written approximately in terms of the translational and rotational time-dependent friction functions involving $\Delta\zeta^{*}_{T}(t)$ and $\Delta\zeta^{*}_{R}(t)$. Introducing approximate expressions for these friction functions in terms of the intermediate scattering functions themselves, leads to a self consistent scheme (Eqs. (2.23)-(2.26)), which only requires the projections $S_{lm;lm}(\mathbf{k})$ of the equilibrium static structure factor as an external input.

The resulting self-consistent theory is now ready to be applied to the description of the dynamic properties of specific model liquids. In this work, however, we did not attempt the solution of the full self-consistent scheme. Instead, here we discussed its use in the derivation of the bifurcation equations, Eqs. (2.33) - (2.34), whose solution allows us to determine the dynamical arrest diagram of the generic system studied in chapter 3, namely, the dipolar hard sphere liquid. This is an interesting exercise in terms of its prediction of the existence of two distinct dynamically arrested states, one in which both, the translational and the rotational degrees of freedom are arrested, and another involving mixed states, in which the translational degrees of freedom are arrested but not the rotational ones. The impossibility to arrest the orientational degrees of freedom with the translational ones not arrested, is probably originated by the decoupling of translational and orientational degrees of freedom imposed to the memory function. Let us stress, however, that these results are presented here only to illustrate the ability of the SCGLE theory to predict physically complex and fascinating dynamical arrest scenarios when the rotational degrees of freedom are included in the description.

In the present thesis we did not aim at achieving any specific progress in the description and understanding of the dynamic arrest phenomenology of the dipolar hard-sphere liquid, since that specific model system was thoroughly studied before with MCT by Schilling and Scheidsteger [7]. It is reassuring, however, that the main qualitative features of our results are fully consistent with the results of that pioneering study. This applies not only to the mere dynamical arrest diagram of the DHS fluid, but also to the additional information generated in our illustrative exercise such as the behavior of the relevant nonergodicity parameters $f^{S}_{lm}(k)$. Of course, it will be interesting to report and discuss more information, as well as the results of the actual solution of the complete self-consistent scheme in Eqs. (2.23)-(2.26) to exhibit the full time dependence of the dynamic properties involved.

We also employed the SCGLE approach in order to describe the spin glass transitions of a dipolar system with positional disorder. For this, we adapted our general equations and solve the rotational dynamics of a simplified model in which we artificially introduce quenched positional disorder by arbitrarily seting the translational diffusion coeficient, D_T^0, equal to zero. The behavior of the only dynamic order parameter, γ_R, was also studied in order to determine the corresponding arrested phases diagram. Our findings are in qualitative agreement with previous experimental and simulation characterizations of disordered magnetic systems suggesting that our approach might be able to predict and describe dynamically arrested states in disordered magnetic systems as well. In fact, we have started to develop this particular application of the non spherical SCGLE theory, but this has proved to possess by itself a very rich phenomenology which demands a more carefully and detailed characterization. We believe that such discussion is beyond the scope of the present work and should form part of a separate work. The theory presented and discussed here, also opens additional perspectives of research on the translational and rotational dynamics of liquids involving non-spherical interactions. For example, to simplify our derivations here we considered only the particular case of monocomponent systems conformed by orthotropic-linear particles. The extension of these derivations to the case of mixtures of particles of arbitrary shape may, however, be proposed following the canonical procedure employed in this work [see for instance Ref. [35]]. Similarly, although the conceptual framework that we employed here refers to colloidal systems [without hydrodynamic interactions], we expect that the essential ideas and results in this work will also be relevant to molecular liquids, very much in the same fashion as in the spherical case [86, 87, 88, 89]. Finally, as we stated in the introduction, we expect that this formalism may be generalized in order to describe aging phenomena on systems involving non-spherically symmetric interactions, as already done for liquids formed by spherical particles [37, 39].

Furthermore, the non-equilibrium extension of the theory presented here is in fact the subject of work in progress, carried out in collaboration between the author of this work and a PhD student (Ernesto Cortés-Morales) in the group of Professor M. Medina-Noyola. Due to the extension and the authorship of such work we have to keep these developments separate from the present discussion. The development of the rotational version of such non-equilibrium theory requires, however, the previous development of the corresponding equilibrium SCGLE theory, which is the main aim of the work presented in this thesis. We expect that the results of the present work will be the basis of a program of research dealing with these problems.

Chapter 6

Publications and other works.

Publications

1. L.F. Elizondo-Aguilera, P.F. Zubieta Rico, H. Ruiz-Estrada and O. Alarcón-Waess *Self-consistent generalized Langevin equation theory for liquids of non-spherical brownian particles.*, Physical Review E, **90**, 052301, (2014).

To be submited

2. L.F. Elizondo-Aguilera and M. Medina Noyola *Localization and dynamical arrest of colloidal fluids in a disordered matrix of polydisperse obstacles.*
3. L.F. Elizondo-Aguilera, E.C. Cortés-Morales, R. Castañeda-Priego and M. Medina-Noyola *Spin-Glass transition in a dipolar system with frozen positional disorder: a self-consistent generalized Langevin equation approach.*
4. E.C. Cortés-Morales, L.F. Elizondo-Aguilera and M. Medina-Noyola *Equilibration and aging of liquids of non-spherically interacting particles.*

National Invited Talks.

1. Universidad Autónoma de Zacatecas, Unidad Académica de Física. Title: *Dynamic Arrest in Porous Media.* February 17th, 2011.
2. Universidad Autónoma Metropolitana, Campus Iztapalapa, Departamento de Física. Title: *Dynamical arrest in porous media: generating protocols and polidispersity effects.*, June 9th, 2011.
3. Benemérita Universidad Autónoma de Puebla, Facultad de Ciencias Físico Matemáticas, Seminario de Materia Banda Condensada. Title: *Dynamical arrest in colloidal suspensions embedded in porous media: effects of polidispersity.*. February 24th, 2012.
4. Universidad de Guanajuato, División de Ciencias e Ingenierías-Campus León, Departamentos de Ingeniería Física e Ingenierías Química, Electrónica y Biomédica. Title: *Dynamical arrest in colloidal suspensions embedded in porous media: effects of polidispersity.*, March 7th, 2012.
5. Universidad Autónoma de Puebla, Facultad de Ciencias Físico Matemáticas, Seminario de Materia Banda Condensada. Title: *An extention of the Self-consistent generalized Langevin equation theory for anistropic systems.*, April 27th, 2012.
6. Universidad Autónoma de San Luis Potosí, Instituto de Física. Seminario de Física Estadística. Title: *Self-consistent generalized Langevin equation theory for non spherical systems: translational and rotational dynamic arrest criteria.*, August 30th, 2013.
7. Universidad de Guanajuato, División de Ciencias e Ingenierías-Campus León, Departamentos de Ingeniería Física e Ingenierías Química, Electrónica y Biomédica. Title: *Self consistent generalized Langevin equation theory for liquids of non-spherically interacting particles*. February 12th, 2014.
8. 3er Conreso Nacional de la Red Temática de la Materia Condensada Blanda. Title: *Spin-Glass transitions in a dipolar system with frozen positional disorder: a self-consistent generalized Langevin equation approach November 27th, 2014.*

International Invited Talks.

1. Physics Colloquium, Université Du Luxembourg, Campus Limperstsberg. Title: *Self consistent generalized Langevin equation theory for liquids of non-spherically interacting particles*. January 22th, 2014.
2. Seminari del Dep. Física Fonamental, Facultat de Física, Universitat de Barcelona. Title: *Self consistent generalized Langevin equation theory for liquids of non-spherically interacting particles.* January 29th, 2014.
3. 1st International Workshop on Matter Out of Equilibrium, Title *Equilibration and aging of dense non-spherical glasss forming liquids: Qualitative molecular theory of dynamical arrest in non-spherical Brownian fluids.* December 8-12th, 2014.

Meetings, Conferences and Workshops:

1. Tercer Taller de la Red-Promep de Física de la Materia Blanda. Oral presentation: *Dynamical arrest in porous media: polidispersity effects.*. April, 2011.
2. XXIV International Conference on Science and Technology of Complex Fluids, Instituto de Física, Universidad Autónoma de San Luis Potosí. San Luis Potosí, México. Poster participation. Title: *Effects of Polidispersity on the liquid-glass transition of colloidal fluids embedded in a disordered porous media*. August, 2011
3. XVI Encuentro regional de investigación y enseñanza de la Física, Instituto Nacional de Astrofísica Óptica y Electrónica (INAOE), Tonantzintla, Pue. México. Poster participation. Title: *Dynamical arrest in porous media: polidispersity effects.*. October, 2011.
4. LIV Congreso Nacional de Física, Mérida, Yuc. México. Poster participation. Title: *Dynamical arrest in porous media: polidispersity effects.*. October 2011.
5. Primera Reunión Nacional de la Red Temática de CONACYT *Materia Condensada Blanda*. Poster participation. Title: *Effects of polydispersity on the liquid-glass transition of colloidal fluids embedded in a disordered porous media*. January, 2012.
6. XLI Winter Statistical Physics Meeting, Xalapa, Ver. México. Poster participation. Title: *Effects of Polydispersity on the liquid-glass transition of colloidal fluids embedded in a disordered porous media*. January, 2012.
7. Primer Taller de estática y dinámica, Red PROMEP *Física de la Materia Blanda*, May, 2012. Taller Final de estática y dinámica de la Red PROMEP *Física de la Materia Blanda*, September, 2012.
8. XLII Winter Statistical Physics Meeting, Taxco, Gue. México. Poster participation. Title: *An extension of the self-consistent generalized Langevin equation theory for anisotropic colloids*. January 2013.
9. Segunda Reunión Nacional de la Red Temática de CONACYT *Materia Condensada Blanda*. Poster participation. Title: *An extension of the self-consistent generalized Langevin equation theory for anisotropic colloids*. January 2013.
10. XXV International Conference on Science and Technology of Complex Fluids, Puebla, Pue. México. Poster participation. Title: *Self-Consistent generalized Langevin equation theory for linear molecules: first principles glass transition predictors*. This poster was selected for oral presentation. July 2013.
11. XLIII Winter Meeting on Statistical Physics, Taxco, Gue. México. Poster participation. Title: *Self consistent generalized Langevin equation theory for liquids of non-spherically particles*. January 2014.
12. XXVI International Conference on Science and Technology of Complex Fluids, Puebla, Pue. México. Poster participation. Title: *Spin Glass transition in a dipolar system with frozen positional disorder*. This poster was selected for oral presentation. July 2014.
13. Primer Taller de Equilibración, Envejecimiento y Arresto Dinámico de la Red Temática Promep *Física de la Materia Blanda*. February-Mach, 2014.
14. Segundo Taller de Equilibración, Envejecimiento y Arresto Dinámico de la Red Temática Promep *Física de la Materia Blanda*. July, 2014.
15. XLIV Winter Meeting on Statistical Physics, México D.F.. Poster participation. Title: *Localization and dynamical arrest transitions in random porous media within the SCGLE theory: Quenched-Annealed and Equilibrated-Mixture Systems*. January 2015.

Appendix A

Brownian motion of spherical particles

A.1 Langevin equation for a Brownian spherical tracer particle

Let us consider the Brownian motion of a spherically symmetric colloidal particle in the absence of direct interactions with other particles and embedded in a solvent. The motion of this particle may be described using the *so-called* Langevin equation [51, 52]:

$$m\frac{d\mathbf{v}(t)}{dt} = -\zeta^0\mathbf{v}(t) + \mathbf{f}^0(t) \tag{A.1}$$

where $\mathbf{v}(t)$ denotes the instant velocity of the tracer, m its mass and ζ^0 is the hydrodynamic friction coefficient that we assume previously determined through some given experiment or a theoretical framework. As we know, in the spherical ζ^0 is determined by using the linearized Navier-Stokes equation. A well known result for spherically symmetric particles within this theory reads: $\zeta^0 = 6\pi\eta\sigma$, where η denotes the viscosity of the solvent and σ is the diameter of the particle.

In addition, $\mathbf{f}^0(t)$ represents a *random* force which characterizes the spontaneous fluctuations on the total force excerted by the solvent on the tracer particle. Customarily, this force is "*modeled*" as a stationary-gaussian-random stocastic procces [1] (white noise), with zero mean ($\langle\mathbf{f}(t)\rangle = 0$) and correlation function given by the following fluctuation disipation theorem [1, 42]

$$\langle\mathbf{f}(t)\mathbf{f}^{\dagger}(0)\rangle = 2k_BT\zeta^0\delta(t)\hat{\mathbf{I}} \tag{A.2}$$

where $\hat{\mathbf{I}}$ is the 3×3 identity matrix, $\delta(t)$ denotes the delta Dirac function, k_B is the Boltzman constant and T is the temperature. Thus, $\mathbf{v}(t)$ is also a stationary-gaussian-random stocastic proces with zero mean and self-correlation function given by [1]

$$\langle\mathbf{v}(t)\cdot\mathbf{v}^{\dagger}(0)\rangle = \frac{k_BT}{m}\hat{\mathbf{I}}\exp\left(\frac{\zeta^0 t}{m}\right) \tag{A.3}$$

Unlike the Newton's equation, where a given mechanical problem is considered "solved" once $\mathbf{v}(t)$ is determined at any time, the Brownian motion is fully characterized once Eq. (A.3) is used to determine physical observables like the difussion coeficient or the mean square displacement (MSD), $\langle(\Delta\mathbf{r}(t))^2\rangle$, where $\Delta\mathbf{r}(t) \equiv \mathbf{r}(t) - \mathbf{r}(0)$ denotes the displacement of the tracer after the time t, and the angular braquets $\langle\ldots\rangle$ denote ensemble averages. It is easy to show from Eq. (A.3) that, in the diffusive regime

---

[1] Eq. (A.3) defines the time scale $\tau_B = m/\zeta^0$ at which the average mommentum of a tracer particle relaxes to equilibrium. We will be interested in consider the diffusive regime, that is, the time scale defined by $t \gg \tau_B$ where inertial terms are negligible.

$$\langle(\Delta\mathbf{r}(t))^2\rangle = 6\frac{k_BT}{\zeta}t \tag{A.4}$$

The diffusion coefficient is defined as

$$D^0 = \lim_{t\to\infty}\frac{\langle(\Delta\mathbf{r}(t))^2\rangle}{6t} \tag{A.5}$$

or equivalently through the Green-Kubo relation:

$$D^0 = \frac{1}{3}\int_0^\infty \langle\mathbf{v}(t)\cdot\mathbf{v}^\dagger(0)\rangle \tag{A.6}$$

and thus the Einstein's relation, $D^0 = k_BT/\zeta^0$, is trivialy obtained.

A.2 Langevin equation for a brownian spherical tracer particle in the presence of other interacting particles

The previous discussion refers to the description of a Brownian particle in the absence of direct interactions with other Brownian particles (infinite dilution limit). In more realistic situations (that is, for finite concentrations) the effect of these interactions on the observables must be considered. For this, we may describe the motion of one of these particles, a tracer, with the following generalized Langevin equation [51, 53, 54]

$$m\frac{d\mathbf{v}}{dt}(t) = -\zeta^0\mathbf{v}(t) + \mathbf{f}^0(t) - \int_0^t dt^{'}\Delta\zeta(t-t^{'})\mathbf{v}(t^{'}) + \mathbf{F}(t) \tag{A.7}$$

where $\mathbf{F}(t)$ is an additional fluctuating force, whose origin lies in the spontaneous fluctuations of the force excerted on the tracer only due to the direct interactions with the other particles. In the time scale of our interest (diffusive regime), $\mathbf{F}(t)$ might be modeled as a stationary stocastic procces, not necessarily gaussian and certainly not white noise. Its self-correlation function is given by:

$$\langle\mathbf{F}(t)\cdot\mathbf{F}^\dagger(0)\rangle = \hat{\mathbf{I}}k_BT\Delta\zeta(t). \tag{A.8}$$

The memory function $\Delta\zeta(t)$ contains the friction contributions due to the direct interactions of the tracer with the rest of surrounding Brownian particles. Its own relaxation time is determined by the relaxation of this *cloud* of surrounding colloids. Let τ_I be the time in which one of these particles difusses the mean distance. In general $\tau_I \gg \tau_B$. Thus, in the diffusive regime ($t \gg \tau_B$) we might define a separation of time scales in reference to τ_I. Hereinafter we will refer to *long* times to the regime $t \gg \tau_I$, whereas we will refer to *short* times to the regime defined by $t \ll \tau_I$, but still $t \gg \tau_B$.

To illustrate this in more detail, let us consider both regimes for Eq. (A.7). In the *short* time limit, where the direct interactions effects have not manifested, we already know that

$$\langle(\Delta\mathbf{r}(t))^2\rangle \approx 6\frac{k_BT}{\zeta^0}t \qquad \tau_B \ll t \ll \tau_I \tag{A.9}$$

.

In the opposite limit ($t \gg \tau_I$) $\Delta\zeta(t)$ may be approximated essencially by a Dirac delta function, *i.e.*, its Markovian limit. This is equivalent to write Eq. (A.7) like Eq. (A.1) but with the purey hydrodynamic coefficient, ζ^0, replaced by an "effective" total friction coefficient given by $\zeta \equiv \zeta^0 + \Delta\zeta$
where $\Delta\zeta$ is given by:

$$\Delta\zeta \equiv \int_0^\infty \Delta\zeta(t)dt \tag{A.10}$$

Hence, in this time regime we may use again the results of the previous subsection to calculate the MSD, which now reads

$$\langle(\Delta\mathbf{r}(t))^2\rangle \approx 6\frac{k_BT}{\zeta^0+\Delta\zeta}t \qquad t \gg \tau_I \tag{A.11}$$

also, the long time diffusion coefficient (Eq. (A.5)) may be written as

$$D^L \equiv 6\frac{k_BT}{\zeta^0+\Delta\zeta}t \tag{A.12}$$

The full solution of this problem, namely, the complete determination of the time evolution of $\langle(\Delta\mathbf{r}(t))^2\rangle$ between these two limits might be obtained once the memory function, $\Delta\zeta(t)$ is determined. Assuming that this is possible, then we may use the exact relations

$$\langle(\Delta\mathbf{r}(t))^2\rangle = 2\int_0^t dt^{'}(t-t^{'})C(t^{'}) \tag{A.13}$$

where $C(t) \equiv \frac{1}{3}\langle\mathbf{v}(t)\cdot\mathbf{v}^{\dagger}(0)\rangle$. In terms of the corresponding Laplace transforms we may write

$$\begin{aligned}\tilde{C}(z) &= \frac{\frac{k_BT}{m}}{z+\frac{\zeta^0}{m}+\frac{\Delta\tilde{\zeta}(t)}{m}} \\ &\approx \frac{k_BT}{\zeta^0+\Delta\tilde{\zeta}(z)}\end{aligned} \tag{A.14}$$

where, in the second line of Eq. (A.14) we have considered the diffusive regime, $\zeta^0/m \gg z$. In summary, the Brownian motion of a tracer particle in the presence of another interacting particles is characterized once the memory function $\Delta\zeta(t)$ is determined.

A.3 Generalized Langevin Equation Formalism and $\Delta\zeta(t)$

According to the previous discussion, to characterize the Brownian motion of a tracer particle, which interacts with other Brownian particles the memory function $\Delta\zeta(t)$ must be determined. As discused by Medina-Noyola, this can be done within the Generalized Langevin Equation (EGL) formalism [33]. Under given specific approximations and assumptions, this approach allows to write $\Delta\zeta(t)$ in terms of the structural properties of a given system. A concrete result of this approach can be written as [33, 34]

$$\Delta\zeta(t) = \frac{\beta}{3} Tr\Big[\int d^3r \int d3r^{'} \left[\nabla\psi(r)\right] \langle \delta n(\mathbf{r};\mathbf{t})\delta n(\mathbf{r}^{'};0)\rangle \left[\nabla^{'}\psi(r^{'})\right]\Big] \tag{A.15}$$

where $\beta = (k_B T)^{-1}$ and $\psi(r)$ denotes the pair potential between the tracer particle and any other surrounding Brownian particle. The function $\langle \delta n(\mathbf{r};t))\delta n(\mathbf{r}^{'};0)\rangle$ (usually referred to as the van Hove function) contains the information concerning to the relaxation of the diffusive procces of the surrounding "cloud" of interacting particles. Within the EGL formalism, to determine $\Delta\zeta(t)$ using Eq. (A.15) we need to approximate in some way the van Hove function. For example, as showed in Ref. [34] one possibility leads to the result

$$\Delta\zeta(t) = \frac{k_B T n}{24\pi^3} \int d^3k \frac{[kh(k)]^2}{S(k)} \exp\left[\frac{-2D^0 k^2 t}{S(k)}\right] \tag{A.16}$$

where n denotes the bulk density and $S(k) = 1 + nh(k)$ [52, 55] is the structure factor. Notice that, even though several assumptions and approximations must be considered in order to obtain Eq. (A.15), we have not defined yet the pair potential $\psi(r)$. Furthermore, the application of Eq. (A.15) might involve additional approximations which may not be of dynamic character, for example, the independent determination of $S(k)$ for a given system.

A.4 Collective Dynamics

We have briefly discussed above the basic aspects concerning to the characterization of the individual Brownian motion of tracer particles within the Langevin equation formalism. For more details in Brownian motion theory we refer to the reader to Refs. [1, 42, 51, 52, 55]. As indicated on the introduction of this thesis, the main purposes of this work is to develop a theoretical approach able to describe both, self and collective dynamics of colloidal fluids with translational and orientational degrees of freedom. Recall that we want to addres an important issue in the context of Brownian fluids with orientational degrees of freedom, namely, the fundamental understanding of dynamically arrested states, a genuine collective phenomena.

Thus, it is necessary to consider a different type of physical observables characterizing simultaneously the self and collective dynamics and which are able to identify (from an experimental point of view) dynamically arrested states [9, 11].

A.4.1 Correlation Functions

Let us consider a system of N identical, spherical and interacting colloidal particles . The relevant dynamical variable of the system is the *so-called* microscopic density [54, 55] which is defined as

$$n(\mathbf{r};t) \equiv \frac{1}{\sqrt{N}} \sum_{n=1}^{N} \delta(\mathbf{r} - \mathbf{r}_n(t)) \tag{A.17}$$

where $\mathbf{r}$ is a fixed point in space and $\mathbf{r}_n(t)$ denotes the position vector of the nth-particle at the time t. Also, the corresponding current density is defined as

$$\mathbf{j}(\mathbf{r};t) \equiv \frac{1}{\sqrt{N}} \sum_{n=1}^{N} \mathbf{v}_n(t)\delta(\mathbf{r} - \mathbf{r}_n(t)) \tag{A.18}$$

where $\mathbf{v}_n(t) = d\mathbf{r}_n(t)/dt$ denote the velocity of the nth- particle. For completeness, we also define the self components

$$n_s(\mathbf{r},t) \equiv \delta(\mathbf{r}-\mathbf{r}_{tr}(t)) \tag{A.19}$$

with $\mathbf{r}_{tr}(t)$ denoting the position of a tracer particle. The van Hove correlation function, $G(\mathbf{r},\mathbf{r}^{'};t)$, is defined in therms of the fluctuations of $n(\mathbf{r},t)$ arround its equilibrium value as [54]

$$\begin{aligned} G(\mathbf{r},\mathbf{r}^{'};t) &\equiv V\left\langle \delta n(\mathbf{r},0)\delta n(\mathbf{r}^{'},t)\right\rangle && \text{(A.20)} \\ &= \frac{1}{n}\left\langle \sum_{n=1}^{N}\sum_{n'=1}^{N}\delta(\mathbf{r}-\mathbf{r}_n(t))\delta(\mathbf{r}-\mathbf{r}_{n'}(t))\right\rangle - n && \text{(A.21)} \end{aligned}$$

where we have used $\langle n(\mathbf{r},t)\rangle = \sqrt{N}/V$ and where the fluctuations of an arbitrarily dynamic variable, $A(\mathbf{r},t)$ are given by

$$\delta A(\mathbf{r},t) \equiv A(\mathbf{r},t) - \langle A(\mathbf{r},t)\rangle \tag{A.22}$$

In addition, the *self*-part of $G(\mathbf{r},\mathbf{r}';t)$: is defined as

$$\begin{aligned} G^{S}(\mathbf{r},\mathbf{r}^{'};t,t^{'}) &\equiv V\left\langle \delta n_s(\mathbf{r},0)\delta n_s(\mathbf{r}^{'},t)\right\rangle && \text{(A.23)} \\ &= V\left\langle \delta(\mathbf{r}-\mathbf{r}_1(0))\delta(\mathbf{r}^{'}-\mathbf{r}_1(t))\right\rangle - V^{-1} && \text{(A.24)} \end{aligned}$$

A.4.2 Correlation Functions in Fourier Space

The van Hove correlation functions play a essential role in the description of the dynamical properties of colloidal fluids because they provide all the relevant information needed to characterize self and collective dynamics. They are also physical quantities which are accesible through real experiments [9]. For this reason, it is useful to introduce the Fourier components of $G(\mathbf{r},\mathbf{r}';t)$ and $G^S(\mathbf{r},\mathbf{r}';t)$ usually refered to as the collective and self intermediate scattering functions, $F(k,t)$ and $F^S(k,t)$. For homogeneous systems, these functions may be writen as [54]

$$\begin{aligned} F(\mathbf{k},t) &= \left\langle \sum_{n,n^{'}} e^{i\mathbf{k}\cdot[\mathbf{r}_n(t)-\mathbf{r}_{n^{'}}(0)]}\right\rangle - n(2\pi)^3\delta(\mathbf{k}) && \text{(A.25)} \\ &= \left\langle n_{\mathbf{k}}^{*}(0)n_{\mathbf{k}}(t)\right\rangle - n(2\pi)^3\delta(\mathbf{k}), && \text{(A.26)} \end{aligned}$$

and

$$F^{s}(\mathbf{k},t) = \left\langle e^{i\mathbf{k}\cdot(\mathbf{r}_1(t)-\mathbf{r}_1(0))}\right\rangle \tag{A.27}$$

Clearly

$$n(\mathbf{k},t) \equiv \frac{1}{\sqrt{N}} \sum_{l}^{N} e^{i\mathbf{k}\cdot\mathbf{r}_l(t)} \tag{A.28}$$

Notice that the following continuity equation is clearly satisfied

$$\frac{\partial n(\mathbf{k},t)}{\partial t} = -i\mathbf{k}\cdot\mathbf{j}(\mathbf{r},t) \tag{A.29}$$

Finally, the self correlation function defined in Eq. (A.27) contains the necessary information to describe self difussion. From this quantity we may obtain properties [56] like the MSD or the time dependent difussion coefficient. For example we have

$$\frac{\langle(\Delta\mathbf{r}(t)^2)\rangle}{6} = -\frac{1}{2}\left[\frac{\partial^2 F_s(k,t)}{\partial k^2}\right]_{|k|=0} \tag{A.30}$$

Appendix B

SCGLE theory of the dynamics of simple brownian liquids

In this appendix, we briefly review the main feature of the equilibrium SCGLE theory of the dynamics of liquids formed by spherical particles. Let us start by considering a model colloidal suspension in the absence of hydrodynamic interactions, formed by N spherical Brownian particles which execute Brownian motion characterized by a short-time self-diffusion coefficient D_0, and which interact between them through a pair potential $u(r)$. The dynamics of this system is described in terms of the relaxation of the fluctuations $\delta n(\mathbf{r},t)$ of the microscopical local density (or concentration) $n(\mathbf{r},t) \equiv (1/\sqrt{N})\sum_{n=1}^{N}\delta(\mathbf{r}-\mathbf{r}_n(t))$ around its bulk equilibrium value $n^{eq} \equiv \langle n(\mathbf{r},t)\rangle$, where $\mathbf{r}_n(t)$ is the position of the particle n at time t. This relaxation can be analyzed by considering the intermediate scattering function (ISF) $F(k,t) \equiv \langle \delta n(\mathbf{k},t)\delta n(-\mathbf{k},0)\rangle$, which describes the average decay of the Fourier transform of $\delta n(\mathbf{r},t)$, defined as $\delta n(\mathbf{k},t) \equiv (1/N)\sum_{n=1}^{N}\exp[i\mathbf{k}\cdot\mathbf{r}_n(t)]$. $F(k,t)$ is commonly referred to as the intermediate scattering function. Also, it is possible to define the *self*-component of $F(k,t)$ as $F^S(k,t) \equiv \langle \exp[i\mathbf{k}\cdot\Delta\mathbf{R}(t)]\rangle$, where $\Delta\mathbf{R}(t)$ denotes the displacement of any of the N particles.

We now summarizing the four distinct fundamental elements of the spherical SCGLE theory of colloid dynamics, for the main details of the construction of this theory, the reader is referred to Refs. [17, 18]. The first of these elements consists of general and exact memory-function expressions for $F(k,t)$ and $F^S(k,t)$, derived within the generalized Langevin equation (GLE) formalism [33, 32], and written in the Laplace space as [17]

$$F(k,z) = \frac{S(k)}{z + \dfrac{k^2 D_0 S^{-1}(k)}{1+C(k,z)}}, \tag{B.1}$$

$$F^S(k,z) = \frac{1}{z + \dfrac{k^2 D_0}{1+C_S(k,z)}}, \tag{B.2}$$

where $S(k) = F(k,t=0)$ is the static structure factor and $C(k,z)$ and $C_S(k,z)$ are, the corresponding memory functions of $F(k,z)$ and $F^S(k,z)$.

The second element is an approximate relationship between the collective and self-dynamics, namely, the Vineyard-like approximation [17].

$$C(k,t) = C_S(k,t). \tag{B.3}$$

The third element consist of an independent approximate determination of the (self) memory function $C_S(k,t)$, which is proposed to be factorized as

$$C_S(k,t) = [\Delta\zeta^*(t)]\lambda(k) \tag{B.4}$$

where $\lambda(k)$ is a phenomenological interpolating function,

$$\lambda(k) \equiv [1 + (k/k_c)^2]^{-1}, \tag{B.5}$$

with k_c being an empirically-chosen cutoff wave-vector, roughly associated with the position k_{max} of the main peak of the static structure factor $S(k)$ [18]. The time-dependent friction function $\Delta\zeta^*(t)$ is the non-Markov contribution of the direct interactions to the friction coefficient of a tagged particle of the system, which is approximated by [33]

$$\Delta\zeta^*(t) = \frac{D_0}{3(2\pi)^3 n} \int d\mathbf{k} \left[\frac{k[S(k)-1]}{S(k)}\right]^2 F^S(k,t)F(k,t), \tag{B.6}$$

where $n \equiv N/V$.

Equations (B.1)-(B.6) constitute the simplified (spherical) version of the SCGLE theory. We emphasize that these equations can be numerically solved as soon as the structural static information contained in $S(k)$ is determined for a given system. As we have pointed out earlier, the main aim of this work is to generalize these equations to systems that also possess orientational degrees of freedom.

B.1 Long-time asymptotic stationary solutions: dynamical arrest theory

The solution of (B.1)-(B.6) provides the detailed time dependence of the ISFs $F(k,t)$ and $F^S(k,t)$, and allows us to discuss different regimes of the relaxation processes at specific points in the state space of a given system. It is also possible to consider more global properties, such as the dynamic arrest diagram, for which it is not necessary to solve the complete set of equations for the full time and wave-vector dependence of all the dynamic properties. For this one solves the so-called bifurcation equations, that is, the equations for the long-time stationary solutions of the full SCGLE theory. It is easy to show that such stationary solutions are given by [18]

$$\lim_{t\to\infty} F(k,t) = \frac{\lambda(k)S(k)}{\lambda(k)S(k) + k^2\gamma} S(k), \tag{B.7}$$

and

$$\lim_{t\to\infty} F^S(k,t) = \frac{\lambda(k)}{\lambda(k) + k^2\gamma}, \tag{B.8}$$

where the scalar nonergodicity parameter γ is the solution of the following equation

$$\frac{1}{\gamma} = \frac{1}{6\pi^2 n} \int_0^\infty dk k^4 \frac{[S(k)-1]^2\lambda^2(k)}{[\lambda(k)S(k) + k^2\gamma][\lambda(k) + k^2\gamma]}. \tag{B.9}$$

The physical meaning of γ can be recognized as the long-time asymptotic value of the MSD. For a state point of a given system (for which we must know $S(k)$), this parameter can be used as follows: in the arrested states γ is finite, representing, in fact, the localization length of the particles, whereas in the ergodic states it diverges.

Appendix C

Mean Spherical Approximation for the dipolar hard sphere fluid

Let us consider a model system consisting of N-identical hard spheres with diameter d and dipolar momentum $\boldsymbol{\mu}_n$, where $|\boldsymbol{\mu}_n| = \mu$ for all n. Thus, besides the hardcore interaction, a *pairwise* potential also exists, which characterizes the dipole-dipole interactions [1]. As discussed by M.S. Wertheim in Ref. [68], the direct correlation function of the system, denoted as $c(\mathbf{r},\boldsymbol{\mu},\boldsymbol{\mu}')$, can be determined using the *so-called* Ornstein-Zernike (OZ) equation [52, 55], which may be analytically solved appealing to the mean spherical approximation (MSA) [2]. Hence, as explained in Ref. [68], within the MSA, $c(\mathbf{r},\boldsymbol{\mu},\boldsymbol{\mu}')$ may be written as

$$c(\mathbf{r},\boldsymbol{\mu},\boldsymbol{\mu}') = c_{hs}(r) + c_{\Delta}(r)\Delta(\boldsymbol{\mu},\boldsymbol{\mu}') + c_D(r)D(\boldsymbol{\mu},\boldsymbol{\mu}') \tag{C.1}$$

where

$$\Delta(\boldsymbol{\mu},\boldsymbol{\mu}') = \boldsymbol{\mu}\cdot\boldsymbol{\mu}' \tag{C.2}$$

$$D(\boldsymbol{\mu},\boldsymbol{\mu}') = \frac{3(\boldsymbol{\mu}\cdot\mathbf{r})(\boldsymbol{\mu}'\cdot\mathbf{r})}{r^2} - (\boldsymbol{\mu}\cdot\boldsymbol{\mu}') \tag{C.3}$$

with $r = |\mathbf{r}|$. The r-dependent functions in Eq. (C.1) are thus given by [7, 68]

$$c_{hs}(r) = c_{PY}(r) \tag{C.4}$$

$$c_{\Delta}(r) = 2\kappa[c_{PY}(r;2\kappa\eta) - c_{PY}(r;-\kappa\eta)] \tag{C.5}$$

$$c_D(r) = c_D^0(r) - 3r^{-3}\int_0^r dr' r' c_D^0(r') \tag{C.6}$$

where

$$c_D^0(r) = \kappa[2c_{PY}(r;2\kappa\eta) + c_{PY}(r;-\kappa\eta)] \tag{C.7}$$

and where

$$c_{PY}(r) = \begin{cases} c_0(\eta) + c_1(\eta)(r/d) + c_3(\eta)(r/d)^3, & r < d \\ 0, & r > d, \end{cases} \tag{C.8}$$

---

[1] Such potential is explicity described by Eq. (3.1) in Chapter 3

[2] See Eq. (3.2)

with

$$c_0(\eta) = -(1+2\eta)^2/(1-\eta)^4 \tag{C.9}$$

$$c_1(\eta) = 6\eta(1+\eta/2)^2/(1-\eta)^4 \tag{C.10}$$

$$c_3(\eta) = \eta c(\eta)/2. \tag{C.11}$$

In turn, the cumulative parameter, $\kappa = \kappa(T,\eta)$, appearing in Eqs. (C.5)-(C.7) satisfies the following nonlinear equation

$$-c_0(2\kappa\eta) + c_0(-\kappa\eta) = 8\eta\beta\mu^2/d^3 \tag{C.12}$$

The reader should recognize Eqs. (C.8)-(C.11) as the well known result for the direct correlation function of the one component hard sphere fluid within the Percus-Yevick approximation [52, 55]. The two control parameters of the system appearing in these equations are the temperature, $T(\beta = 1/k_BT)$, and the packing fraction, $\eta = \pi n d^3/6$. Given that μ^2/d^3 represents the characteristic dipolar energy, the quantity $T^* = [\beta\mu^2/d^3]^{-1}$ is a scaled (dimensionless) temperature which describes the "*competition*" between the thermal energy and the dipolar energy.

Hence, using Eq. (C.1)-(C.12), the calculation of the spherical harmonics projections of $c(\mathbf{r},\boldsymbol{\mu},\boldsymbol{\mu}')$ given by

$$c_{lm;l'm'}(\mathbf{k}) = i^{l-l'}\int d\mathbf{r}\int\int d\boldsymbol{\mu}\, d\boldsymbol{\mu}'\, c(\mathbf{r},\boldsymbol{\mu},\boldsymbol{\mu}')\times e^{i\mathbf{k}\cdot\mathbf{r}}Y^*_{lm}(\boldsymbol{\mu})Y_{lm}(\boldsymbol{\mu}') \tag{C.13}$$

is straightforward.

As discussed in sec. 1.3 of Chapter 1, it is convenient to consider the k-frame [55, 57], where the components defined in eq. (C.13) become *diagonal* in m and m', *i.e.*, $c_{lm;l'm'}(k) \to c_{ll';m}\delta_{mm'}$. In addition, as discussed in Refs. [7, 57], within the MSA approximation for the dipolar hard sphere (DHS) fluid, these components are diagonal in l and l' too; and $c_{lm}(k) = 0$ for $l \geq 2$. The explicit analytical expressions for the resulting nonzero components $c_{00}(k)$, c_{10}(k) and $c_{11}(k)$ can be consulted, for example, in appendix E of Ref. [7]. However, the reader should be careful in noticing that those expressions clearly contain typographical errors. For this reason, in what follows we provide the correct expressions to compute the functions $c_{00}(k)$, c_{10}(k) and $c_{11}(k)$. Such expressions reads

$$\begin{aligned} c_{00}(y) = 16\pi^2 d^3 y^{-6}\Big[&\{24c_3 - 2c_1y^2\} + \{-24c_3y + (c_{PY} + 2c_1 + 4c_3)y^3\}\sin y \\ &+\{-24c_3 + (2c_1 + 12c_3)y^2 - (c_{PY} + c_1 + c_3)y^4\}\cos y\Big] \end{aligned} \tag{C.14}$$

$$\begin{aligned} c_{10}(y) &= 16\pi^2 d^3 y^{-6}\Big[\{8(c_\Delta^{(3)}+4c_D^{(3)})-\frac{2}{3}(c_\Delta^{(1)}+8c_D^{(1)})y^2\} \\ &+ \{-8(c_\Delta^{(3)}+4c_D^{(3)})y+\frac{1}{3}\Big(c_\Delta^{(0)}+2c_\Delta^{(1)}+4c_\Delta^{(3)}+10c_D^{(1)}+14c_D^{(3)}-2\frac{\beta\mu^2}{d^3}\Big)y^3\}\sin y \\ &+ \{-8(c_\Delta^{(3)}+4c_D^{(3)})+\Big(\frac{2}{3}c_\Delta^{(1)}+4c_\Delta^{(3)}+\frac{16}{3}c_D^{(1)}+16c_D^{(3)}\Big)y^2 \\ &- \frac{1}{3}\Big(c_\Delta^{(0)}+c_\Delta^{(1)}+c_\Delta^{(3)}+2c_D^{(1)}+2c_D^{(3)}-2\frac{\beta\mu^2}{d^3}\Big)y^4\}\cos y\Big] \end{aligned} \tag{C.15}$$

$$\begin{aligned} c_{11}(y) &= 16\pi^2 d^3 y^{-6}\Big[\{8(c_\Delta^{(3)}-2c_D^{(3)})-\frac{2}{3}(c_\Delta^{(1)}-4c_D^{(1)})y^2\} \\ &+ \{-8(c_\Delta^{(3)}-2c_D^{(3)})y+\frac{1}{3}\Big(c_\Delta^{(0)}+2c_\Delta^{(1)}+4c_\Delta^{(3)}-5c_D^{(1)}-7c_D^{(3)}+\frac{\beta\mu^2}{d^3}\Big)y^3\}\sin y \\ &+ \{-8(c_\Delta^{(3)}-2c_D^{(3)})+\Big(\frac{2}{3}c_\Delta^{(1)}+4c_\Delta^{(3)}-\frac{8}{3}c_D^{(1)}-8c_D^{(3)}\Big)y^2 \\ &- \frac{1}{3}\Big(c_\Delta^{(0)}+c_\Delta^{(1)}+c_\Delta^{(3)}-c_D^{(1)}-c_D^{(3)}+\frac{\beta\mu^2}{d^3}\Big)y^4\}\cos y\Big] \end{aligned} \tag{C.16}$$

where $y = kd$ is a dimensionless wave number and with

$$c_\Delta^{(\nu)} = 2\kappa\big[c_\nu(2\kappa\eta)-c_\nu(-\kappa\eta)\big]; \quad \nu = 0,1,3 \tag{C.17}$$

$$c_D^{(1)} = \frac{1}{4}\kappa[2c_1(2\kappa\eta)+c_1(-\kappa\eta)] \tag{C.18}$$

$$c_D^{(3)} = \frac{1}{2}\kappa[2c_3(2\kappa\eta)+c_3(-\kappa\eta)] \tag{C.19}$$

Finally, using the OZ equation [69, 70]

$$S_{lm}(k) = \Big[1-\frac{n}{4\pi}c_{lm}(k)\Big]^{-1} \tag{C.20}$$

the desired correlators $S_{00}(k), S_{10}(k)$ and $S_{11}(k)$ may be obtained.

Bibliography

[1] J. K. G. Dhont, *An Introduction to Dynamics of Colloids*. Elsevier, First Edition (1996).

[2] *Soft Matter, Volume 2: Complex Colloidal Suspensions*, edited by G. Gompper and M. Shick. Wiley (2006).

[3] Kazem V. Edmond, Mark T. Elsesser, Gary L. Hunter, David J. Pine and Eric R. Weeks, *PNAS* **109**(44), 17891-17896. doi/10.1073/pnas.1203328109

[4] G. Yatsenko and K. S. Schweizer, *Langmuir* 2008, **24**, 7474-7484.

[5] Zhongyu Zheng, Feng Wang, and Yilong Ha, *Phys. Rev. Lett.* **107**, 065702 (2011).

[6] P. Pfleiderer, K. Milinkovic and T. Schilling, *Europhys. Lett.* **84** (2008) 16003.

[7] R. Schilling and T. Scheidsteger, *Phys. Rev. E* **56**, No.3, 2932 (1997).

[8] C. de Michele, R. Schilling and F. Sciortino, *Phys. Rev. Lett.* **98**, 265702 (2007).

[9] W. van Megen, T. C. Mortensen, S. R. Williams and J. Müller, *Phys. Rev. E* **58**, No.5, 6073, (1998).

[10] P. N. Pusey in *Liquids, Freezing and Glass Transition*, edited by J.P. Hansen, D. Levesque, and J. Zinn-Justin. Elsevier, Amsterdam, (1991).

[11] K.N. Pham, A.M. Puertas, J. Bergenholtz, S.U. Egelhaaf, A. Moussaid, P.N. Pusey, A.B. Schofield, M.E. Cates, M. Fuchs and W.C.K. Poon, *Science*, **296** (2002),104.

[12] P. G. Debenedetti and F. H. Stillinger, Nature **410**, 359 (2001).

[13] E. Zaccarelli, *J. Phys.: Cond. Matter* **19**, 323101 (2005).

[14] W. Götze, in Liquids, Freezing and the Glass Transition, edited by J. P. Hansen, D. Levesque and J. Zinn-Justin. North-Holland, Amsterdam, (1991) p. 287.

[15] W. Götze and L. Sjögren, *Rep. Prog. Phys.* **55**, 241 (1992).

[16] P.E. Ramírez-González, R. Juárez Maldonado, L. Yeomans-Reyna, M. A. Chávez-Rojo, M. Chávez-Páez, A. Vizcarra-Rendón and M. Medina Noyola, *Rev. Mex. Fís.* **53**, 327 (2007).

[17] R. Juárez-Maldonado, M.A. Chávez-Rojo, P.E. Ramírez-González, L. Yeomans-Reyna and M. Medina-Noyola, *Phys. Rev. E* **76**, 062502 (2007).

[18] L. Yeomans-Reyna, M.A. Chávez-Rojo, P. E. Ramírez-González, R. Juárez-Maldonado, M. Chávez-Páez and M. Medina-Noyola, *Phys. Rev. E* **76**, 041504 (2007).

[19] R. Juárez-Maldonado and M. Medina-Noyola, *Phys. Rev. E* **77**, 051503 (2008).

[20] W. Götze, A. P. Singh and Th. Voigtmann, *Phys. Rev. E* **61**,6, 6934, (2000).

[21] S. -H. Chong and W. Götze, *Phys. Rev. E* **65**, 051201 (2002).

[22] T. Franosch, M. Fuchs, W. Götze, M. R. Mayr, and A. P. Singh, *Phys. Rev. E* **56**, 5, 5659 (1997).

[23] S. -H. Chong and W. Götze, *Phys. Rev. E* **65**, 041503 (2002).

[24] L. Fabbian, A. Latz, R. Schilling, F. Sciortino, P. Tartaglia and Theis. C, *Phys. Rev. E* **60**, No.5, 5768 (1999).

[25] M. Letz, R. Schilling and A. Latz, *Phys. Rev. E* **62**, No.4, 5173 (2000).

[26] T. Theenhaus, R. Schilling, A. Latz and M. Letz, *Phys. Rev. E* **64**, 051505, (2001).

[27] M. Hernández-Contreras and M. Medina-Noyola, *PhD thesis, IFUASLP-UASLP* (1995).

[28] M. Hernández-Contreras, M. Medina-Noyola and A. Vizcarra-Rendón, *Physica A*, **234** (1996), 271-310.

[29] M. Hernández-Contreras, P. González-Mozuelos, O. Alarcón-Waess and H. Ruiz-Estrada *Phys. Rev. E* **57**, 1817 (1998)

[30] M. Hernández-Contreras and M. Medina-Noyola, *Phys. Rev. E* **54**, No.6, 6573 (1996).

[31] M. Hernández-Contreras and M. Medina-Noyola, *Phys. Rev. E* **53**, No.5, R4306 (1996).

[32] M- Medina-Noyola and J.L- Del Río-Correa, *Physica* **146**A, (1987), 483.

[33] M. Medina-Noyola, *Faraday Discuss. Chem. Soc.* (1987), **83**, 21-31.

[34] M. Medina-Noyola, Phys. Rev. Lett. **60**, 26, 2705 (1988).

[35] P.F. Zubieta-Rico, O. Alarcón Waess and M. Medina-Noyola, *Master degree thesis, IFUASLP-UASLP* (1995).

[36] L. F. Elizondo-Aguilera, P. F. Zubieta-Rico, H. Ruiz-Estrada and O. Alarcón-Waess, *Phys. Rev. E* **90**, 052301 (2014).

[37] P. E. Ramírez-González and M. Medina-Noyola, *Phys. Rev. E* **82**, 061503 (2010).

[38] P. E. Ramírez-González and M. Medina-Noyola, *Phys. Rev. E* **82**, 061504 (2010).

[39] L. E. Sánchez-Díaz, P. E. Ramírez-González and M. Medina-Noyola, *Phys. Rev. E* **87**, 052306 (2013).

[40] L. F. Cugliandolo and J. Kurchan, *Phys. Rev. Lett.* **71**, 173 (1993).

[41] E. Cortés-Morales, L.F. Elizondo-Aguilera, and M. Medina-Noyola, work under progress

[42] J. Keizer, *Statistical Thermodynamics of Nonequilibrium Processes*. Springer-Verlag, New York Inc. (1987)

[43] A. Imhof and J.K.G. Dhont, *Phys. Rev. Lett.* **75**, 1662 (1995).

[44] S. J. Woltman, G. D. Jay and G. P. Crawford, *Nature Materials*, **6** 929-938 (2007).

[45] J. A. Moreno-Razo, , E. J. Sambriski, N. L. Abbott, J. P. Hernández-Ortiz and J. J. de Pablo, *Nature* **485**, 86-89 (2012).

[46] A. D. Rey, *Soft Matter*, 2010, **6**, 3402-3429

[47] B. Kim, E. J. Jeong, J. W. Chung, S. Seo, B. Koo and J. Kim, *Nature Materials*, **12** 659-664 (2013)

[48] Kyongok Kang and Jan K. G. Dhont, *Soft Matter*, (2013), **10**, 1987.

[49] Kyongok Kang and Jan K. G. Dhont, *Soft Matter*, (2010), **6**, 273.

[50] D. Klemm, F. Kramer, S. Moritz, T. Lindstrom, M. Ankerfors, D. Gray, and A. Dorris, *Angew Chem Int Ed Engl.* (2011) Jun 6;50(24):5438-66

[51] D.S. Lemons and A. Gythiel, *Am. J. Phys.* **65** (11) (1997)

[52] D. McQuarrie, *Statistical Mechanics*, First Edition, Harper-Row, London (1976).

[53] S. Chandrasekhar, *Rev. Mod. Phys.* **15** (1943).

[54] J.P. Boon and S. Yip, *Molecular Hydrodynamics*, McGraw-Hill, New York, (1980).

[55] J.P. Hansen y I.R. McDonald, *Theory of simple liquids*, Third Edition, Academic Press (2006).

[56] G. Nägele, M. Medina-Noyola, R. Klein and J. L. Arauz-Lara, *Physica A*, **149**, 123 (1988).

[57] C. G. Gray and K. E. Gubbins, *Theory of Molecular Fluids*, Clarendon, Oxford, Vol.1 (1984)

[58] W. Hess and R. Klein, *Adv. Phys.*, (1983), **32**, 173.

[59] M. Hillert, *Phase Equilibria, Phase Diagrams and Phase Transformations*, Cambridge University Press, (2008).

[60] H.A.J. Oonk and M.T. Calvet, *Equilibrium Between Phases of Matter Phenomenology and Thermodynamics*, Springer (2008).

[61] P. Papon, J. Leblond and P.H.E. Meijer, *The Physics of Phase Transitions : Concepts and Applications*, Spinger (2006).

[62] J. Willard Gibbs, *Elementary Principles in Statistical Mechanics*, Dover (1960).

[63] H. B. Callen, *Thermodynamics and an Introduction to Thermostatistics*, Second Edition, John Wiley and Sons, Inc.(1985).

[64] D. L. Goodstein, *States of Matter*, Dover (1985).

[65] S. R. de Groot and P. Mazur *Non-equlibrium Thermodynamics*, Dover, (1984).

[66] G. Lebon, D. Jou, and J. Casas-Vázquez, *Understanding Non-equilibrium Thermodynamics Foundations, Applications, Frontiers*, Springer-Verlag (2008).

[67] R. Wittkowski and H. Löwen, *Phys. Rev. E*, **85**, 021406 (2012).

[68] M. S. Wertheim, *J. Chem. Phys.* **55**, 4291 (1971).

[69] L. Blum and J. Torruella, *J. Chem. Phys.* **56**, 303 (1972).

[70] L. Blum, *J. Chem. Phys.* **57**, 1862 (1972).

[71] B. Bagchi and A. Chandra, *Adv. in Chem. Phys.* Vol. **LXXX**. Edited by I. Prigogine and S.A. Rice. John Wiley (1991).

[72] J. M. Caillol, *J. Chem. Phys.* **98**, 9835 (1993).

[73] P.I.C. Teixeira, J.M. Tavares and M.M. Telo da Gama , *J. Phys. Condens. Matter* **12**, R411, (2000).

[74] L. Rovigatti, J. Russo, F. Sciortino , *Soft Matter*, (2012), **8**, 6310.

[75] C. de Dominicis and I. Giardina, *Random Fields and Spin Glasses: A Field Theory Approach*, Cambridge University Press (2006).

[76] S. F. Edwards and P.W. Anderson, *J. Phys. F: Metal Phys.* **5**, 965 (1975).

[77] E. A. Goremychkin, R. Osborn, B. D. Rainford, R. T. Macaluso, D. T. Adroja and M. Koza, *Nature Physics*, **4**, 766-770 (2008).

[78] R. Mathieu, A. Asamitsu, Y. Kaneko, J. P. He, and Y. Tokura, *Phys. Rev. B* **72**, 014436 (2005).

[79] R. F. Wang, *Nature*, **439**, 303-306 (2006).

[80] A. Biltmo and P. Henelius, *Europhys. Lett.*, **87** (2009) 27007.

[81] A. Biltmo and P. Henelius, *Nature Comm.*, 3 857-(2012).

[82] Wenhao Wu, B. Ellman and T.F. Rosenbaum, *Phys. Rev. Lett.* **67**, No. 15, 2076 (1991).

[83] M. J. P. Gingras and P. Henelius, *Journal of Physics: Conference Series* **320** (2011) 012001.

[84] P. B. Chakraborty, P. Henelius, H. Kjønsberg, A. W. Sandvik, and S. M. Girvin, *Phys. Rev. B* **70**, 144411, (2004).

[85] J. A. Quilliam, S. Meng, C. G. A. Mugford, and J. B. Kycia, *Phys. Rev. Lett.* **101**, 187204 (2008).

[86] L. López-Flores. P. Mendoza-Méndez, L.E. Sánchez-Díaz, L. Yeomans-Reyna, A. Vizcarra-Rendón, G. Pérez-Ángel, M. Chávez-Páez and M. Medina-Noyola, *Europhys. Lett.* **99**, 46001 (2012).

[87] L. López-Flores, L. L. Yeomans-Reyna, M. Chávez-Páez, and M. Medina-Noyola, *J. Phys.: Condens. Matter*, **24**, 375107 (2012).

[88] L. López-Flores, H. Ruiz-Estrada, M. Chávez-Páez, and M. Medina-Noyola, *Phys. Rev. E* **88**, 042301 (2013).

[89] P. Mendoza-Méndez, L. López-Flores, A. Vizcarra-Rendón, L. E. Sánchez-Díaz, and M. Medina-Noyola, *Physica A* **394**1 (2014).

[90] G. Pérez-Ángel, L.E. Sánchez-Díaz, P.E. Ramírez-González, R. Juárez-Maldonado, A. Vizcarra-Rendón and M. Medina-Noyola, *Phys. Rev. E* **83**, 060501(R) (2011).